→ 6th ESA ADVANCED TRAINING COURSE ON LAND REMOTE SENSING

MULTITEMPORAL ANALYSIS

Lorenzo Bruzzone

E-mail: lorenzo.bruzzone@ing.unitn.it

Web page: http://rslab.disi.unitn.it

14–18 September 2015 | University of Agronomic Science and Veterinary Medicine Bucharest | Bucharest, Romania

Outline

1. Current trends and background on multitemporal images
2. Change detection in multispectral and SAR images
3. Change detection in VHR multispectral images
4. Change detection in VHR SAR images
5. Change detection in hyperspectral images
6. Change detection in multisensor/multisource images
7. Conclusion

1. Current Trends and Background on Multitemporal Images

Multitemporal Images

In the last ten years we had a significant increase in the interest on topics related to the time series and the analysis of multitemporal data:

- ✓ Sharp increase in the number of papers published on the major remote sensing journals (e.g., IEEE Transactions on Geoscience and Remote Sensing, IEEE Geoscience and Remote Sensing Letters, IEEE Journal on Selected Topics in Applied Earth Observation and Remote Sensing, Remote Sensing of Environment, International Journal of Remote Sensing).
- ✓ Increased number of related sessions in international conferences.
- ✓ Increased number of projects related to multitemporal images and data.

Multitemporal Images

The increased interest in multitemporal data analysis is due to many issues:

- ✓ Increased number of satellites with increased revisitation time that allow the acquisition of either long time series or frequent bitemporal images.
- ✓ New policy for data distribution of archive data that makes it possible a retrospective analysis on large scale (e.g. the Landsat Thematic Mapper archive).
- ✓ New policies for the distribution of new satellites data (e.g. ESA Sentinel).

Multitemporal Images: Change Detection

- ✓ Change detection (CD): process that analyzes multitemporal remote sensing images acquired on the same geographical area for identifying changes occurred between the considered acquisition dates.

- ✓ We can define different change detection problems:

    - Binary change detection.
    - Multiclass change detection.
    - Change detection in long time series of images.

Taxonomy of CD Problems

1. Binary change detection

- ✓ Goal: production of binary maps in which changed and unchanged areas are separated;
- ✓ Number of images: 2 (or pairs of images extracted from a series);
- ✓ Application domain: detection of abrupt (step) changes.

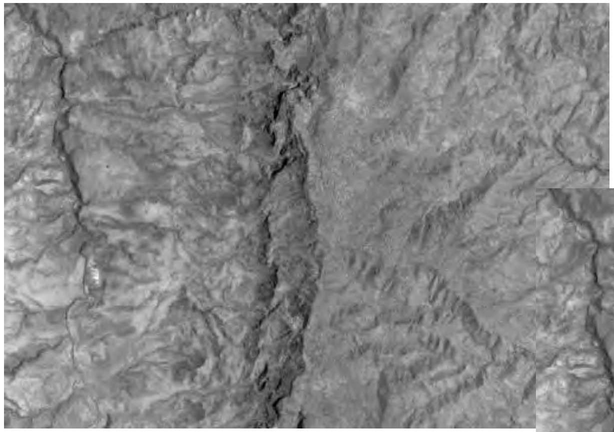

Mexico, April 2000

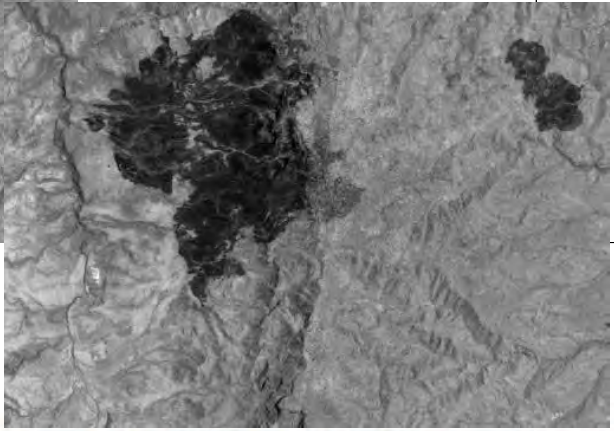

Mexico, May 2002

Map of burned areas

Taxonomy of CD Problems

2. Multiclass change detection

- ✓ Goal: generation of a change-detection map in which land-cover transitions are explicitly identified;
- ✓ Number of images: 2 (or pairs of images extracted from a series);
- ✓ Application domain: updating thematic maps, detection of multiple changes.

May 1995 (Landsat)

July 1995 (Landsat)

Thematic Map

- URBAN / URBAN
- BARE SOIL / SUGAR BEET
- WHEAT / BARE SOIL
- BARE SOIL / CORN
- BARE SOIL / SOYBEAN

Taxonomy of CD Problems

3. Change detection in long time series of images

- ✓ Goal: detection of changes associated with modifications of the behavior of the temporal signature of a land cover between two time series (detection of long term changes);
- ✓ Number of images: 2 time series made up on n images (n>>2);
- ✓ Application domain: monitoring seasonal/annual changes.

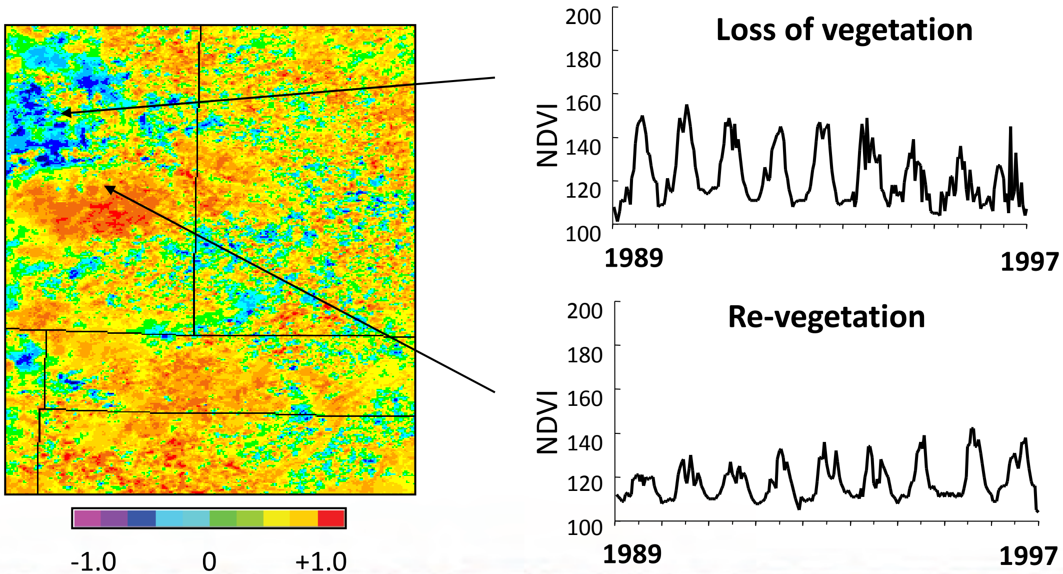

Change Detection Architecture

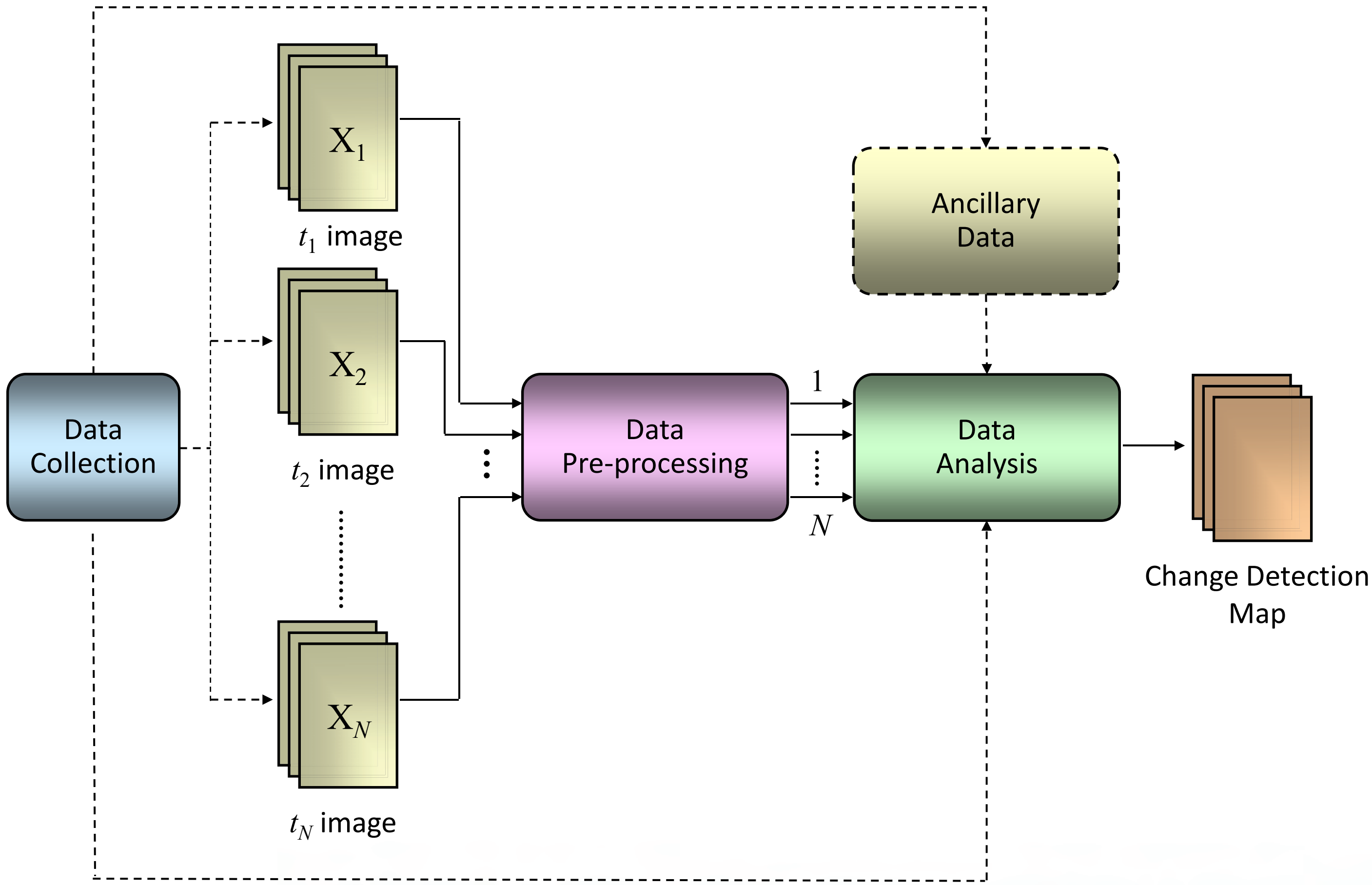

Change Detection: Sensors and Satellites

- ✓ Geometrical resolution: the geometrical detail required from the application is of major importance for the choice of the sensor and of both the pre-processing and data analysis algorithms.

- ✓ Spectral resolution: the complexity of the addressed problem and the end-user's requirements involve constraints on the choice of the kind of sensor (active or passive) and on the necessary spectral resolution.

- ✓ Acquisition frequency: high acquisition frequency may result in a high probability to include in the analysis data taken from different sensors (e.g. different satellites, in-situ sensor networks, etc.) with important consequences in the data analysis phase.

- ✓ Meteorological conditions: the constraints on the robustness of the system to clouds or atmospheric conditions (e.g. related to the latitude of the investigated area) result in constraints for the choice of both the sensor and the satellite.

Change Detection: Application Requirements

- ✓ Ground reference data ("ground truth"): it is important to understand if it is possible to collect ground truth data for the training of the processing algorithms or if the system should be completely unsupervised.

- ✓ Prior information: it is important to collect all the prior information available on the application in order to translate it in possible useful constraints in the phase of design of algorithms.

- ✓ Ancillary data: it is important to identify possible ancillary data that can be used in the development of the system according to a multisource processing architecture.

Change Detection: User Needs and Requirements

- ✓ User expectation: given an application, it is important to properly understand the final goal of the users. Different specific goals result in the choice of different processing strategies and algorithms.
- ✓ Cost: the economical cost of the development of the architecture and of the operational use of the system should be properly understood.
- ✓ Processing time: it is important to identify the requirements (if any) related to the expected processing time for the developed service.

2. Change Detection in Multispectral and SAR Images

Change Detection Architecture

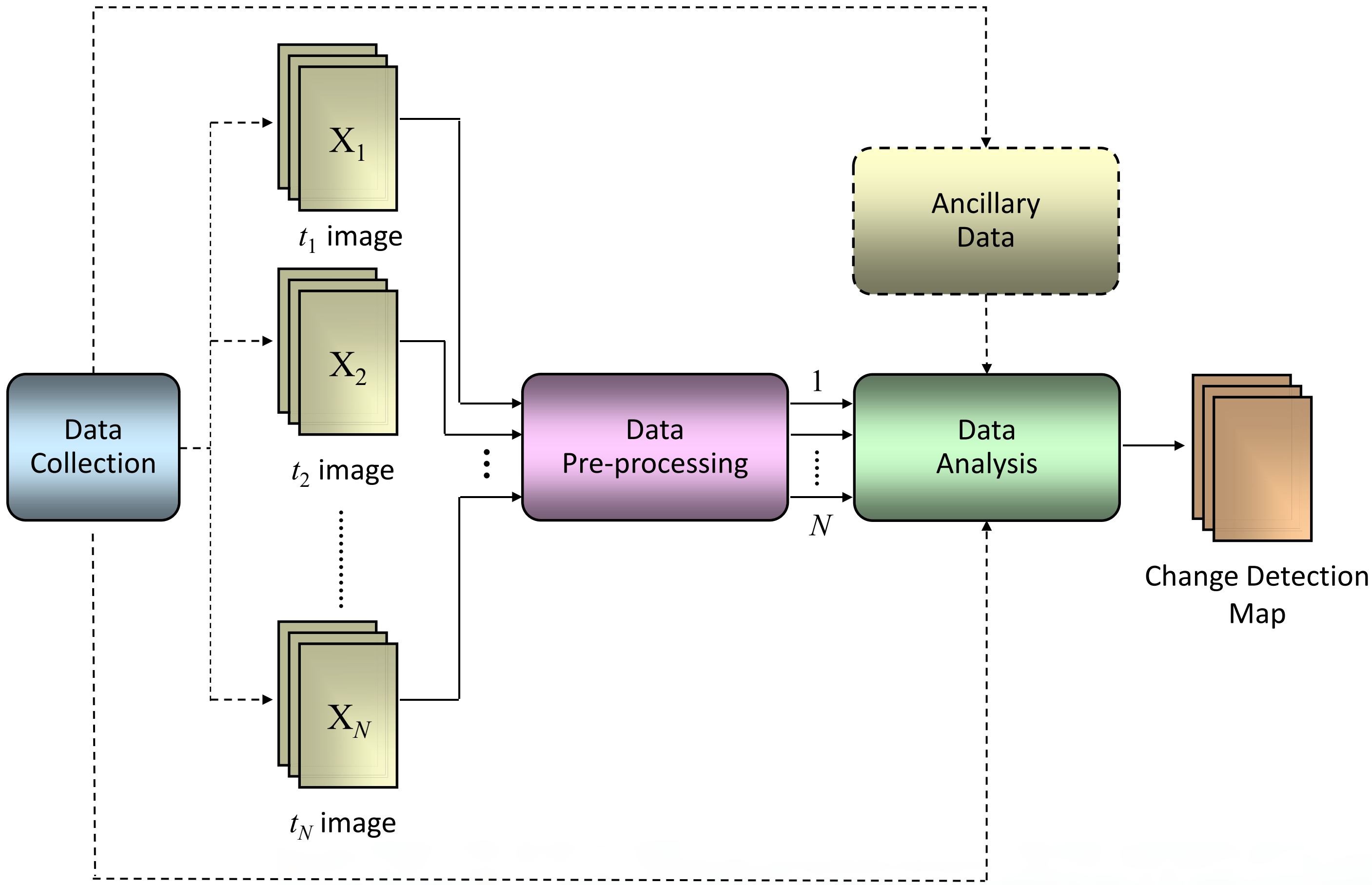

Data Pre-processing: Multispectral Images

Very important with optical images

Mandatory in all change-detection techniques

Depends on the specific sensor considered and on the quality of the considered images

Depends on the requested acquisition frequency and data availability (careful application, see information theory!)

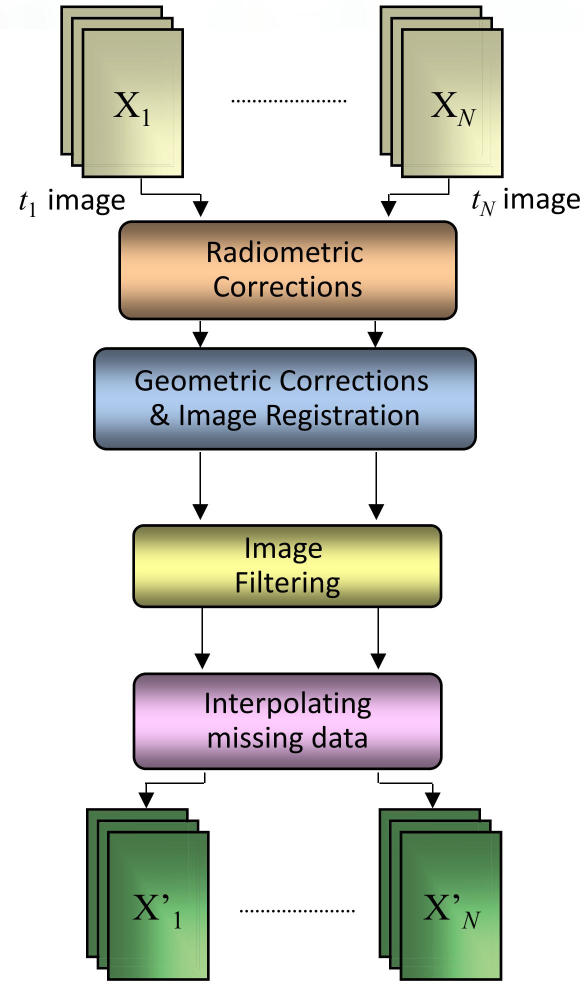

Data Pre-processing: Radiometric Corrections

Differences in light and atmospheric conditions between the two acquisition times can be mitigated by applying radiometric calibration to the images. Two different approaches can be applied:

- ✓ Absolute calibration: digital numbers are transformed into the corresponding ground reflectance values (radiometric transfer models, regression algorithms applied to ground-reflectance measurements collected during the data acquisition phase).

- ✓ Relative calibration: modification of the histograms, so that the same gray-levels values in the two images can represent the same reflectance values, whatever the reflectance values on the ground may be (histogram matching).

The choice of one of the two approaches depends on the particular application considered and on the specific information available.

Data Pre-processing: Image Registration

Generally it is not possible to obtain a perfect alignment between multitemporal images. This is mainly due to local defects in the geometries of the images.

Residual misregistration results in a very critical source of noise, which is called "registration noise"

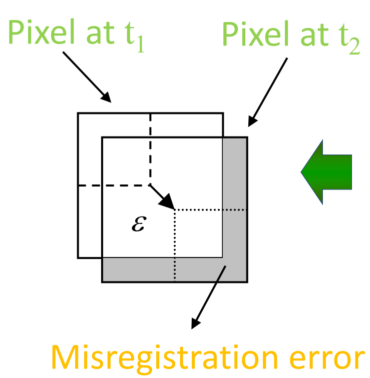

Generic effect of misregistration

Error in area as a function of the displacement in high resolution sensors

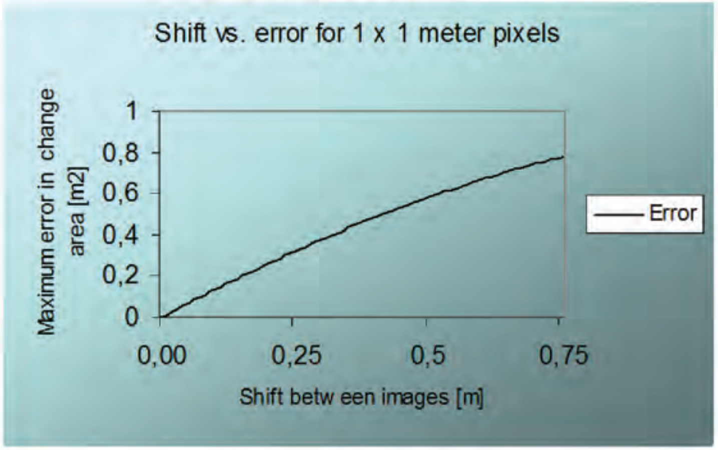

Data Pre-processing: Registration Noise Effects

Elba Island, Landsat-TM4

August 1992

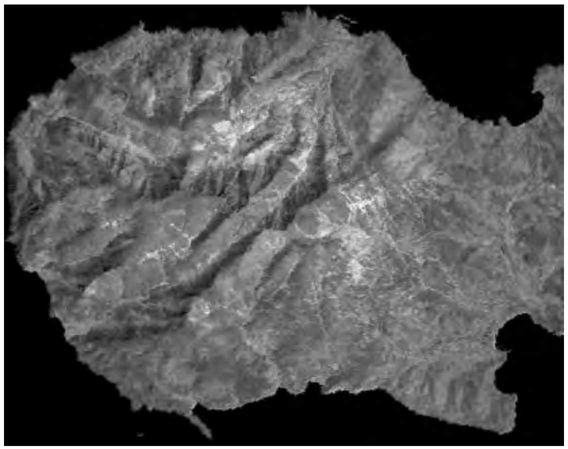

September 1994

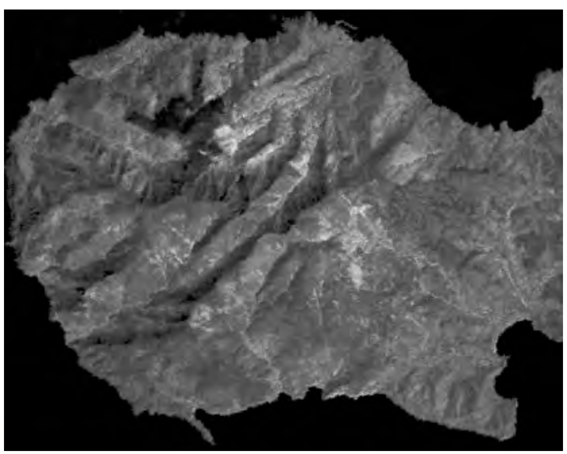

t_1 image

t_2 image

Change-detection map

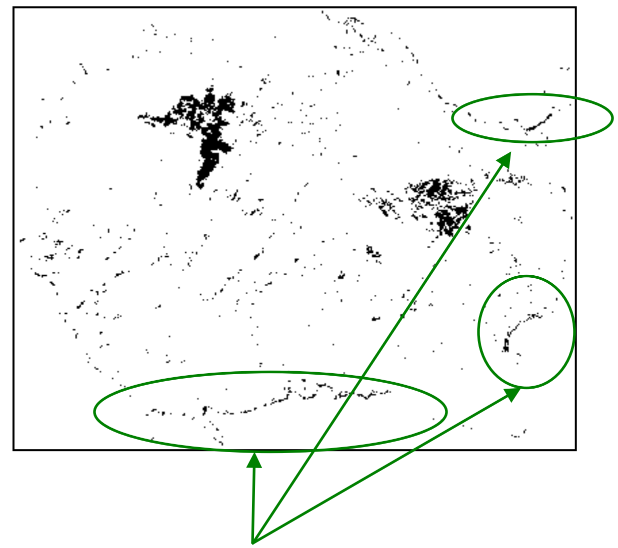

Registration noise

Change Detection Architecture

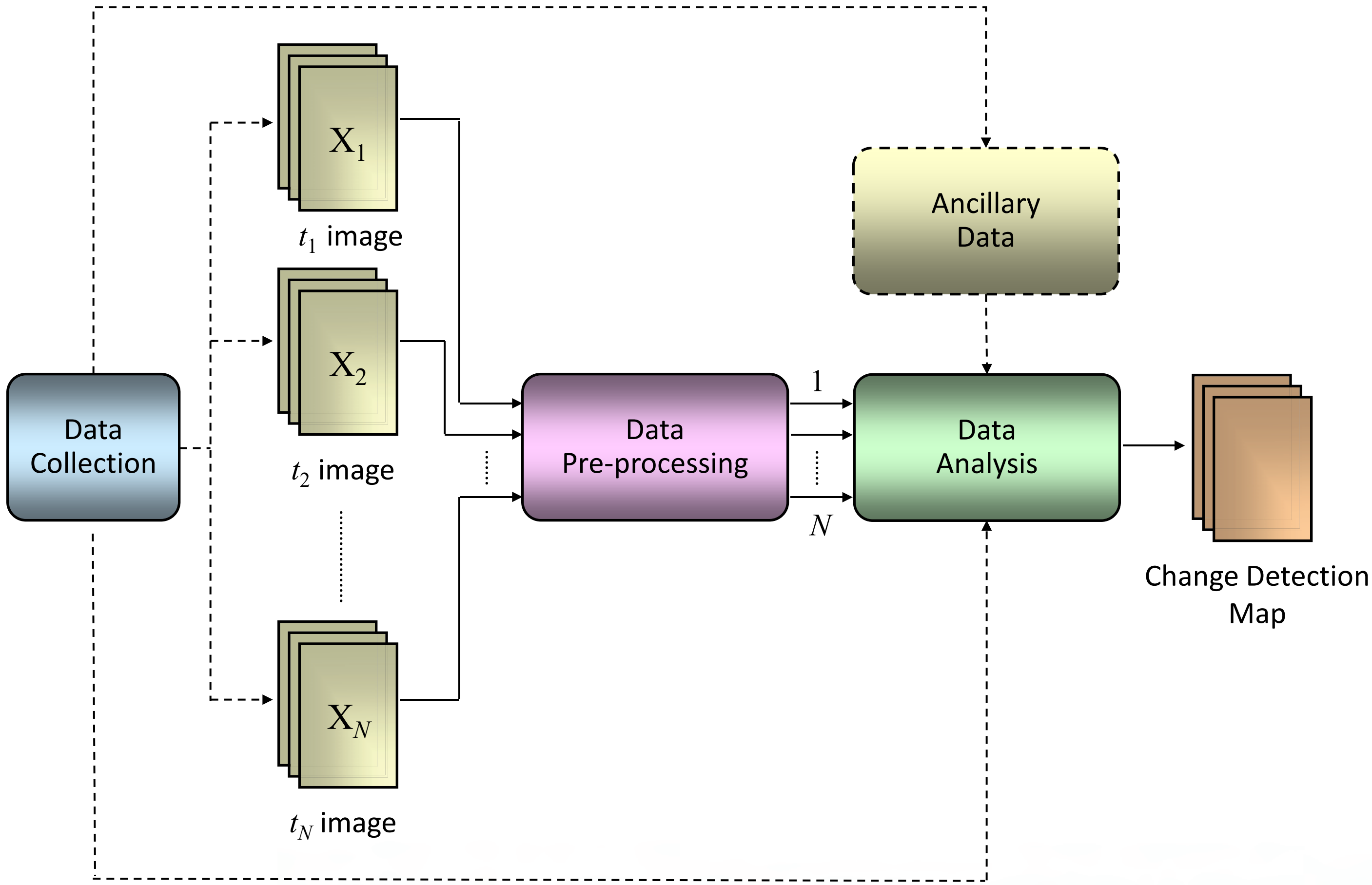

Binary Change Detection in Remote Sensing

Binary change detection in remote-sensing images is characterized by several peculiar factors that render ineffective some of the multitemporal image analysis techniques typically used in other application domains. Some of these factors are:

- ✓ Differences in light conditions, sensor calibration, and ground moisture at the two acquisition dates considered;
- ✓ Absence of a reference background;
- ✓ Lack of a priori information about the shapes of changed areas;
- ✓ Non-perfect alignment (registration noise) between the two considered images;
- ✓ Different acquisition conditions of multitemporal images (view angle, shadows, etc.).

Binary CD in Multispectral Images: Typical Architecture

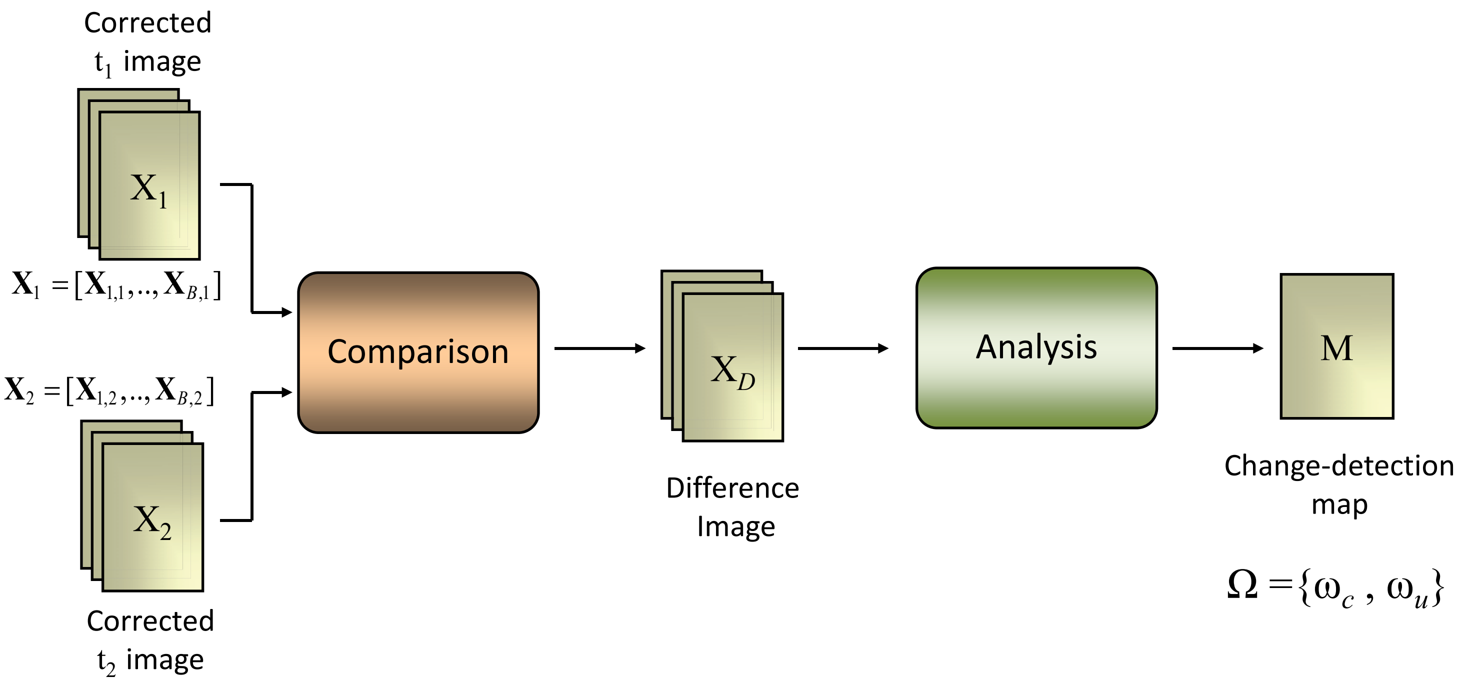

CD in Multispectral Images: Comparison Operators

Technique	Feature vector $\mathbf{f}_k$ at the time t_k	Computation of X_D
Univariate image differencing	$\mathbf{f}_k = X_k^b$	$X_D = \mathbf{f}_1 - \mathbf{f}_2 + C$
Vegetation index differencing	$\mathbf{f}_k = V_k$	$X_D = \mathbf{f}_1 - \mathbf{f}_2 + C$
Change vector analysis	$\mathbf{f}_k = [X_k^1, .., X_k^m]$	$X_D = \left\| \mathbf{f}_1 - \mathbf{f}_2 \right\|$
Regression	$\mathbf{f}_1 = X_1^b$ and $\mathbf{f}_2 = \hat{X}_2^b$	$X_D = \mathbf{f}_1 - \mathbf{f}_2 + C$
Principal component Analysis	$\mathbf{f}_k = [P_k^1, .., P_k^m]$	$X_D = \left\| \mathbf{f}_1 - \mathbf{f}_2 \right\|$

b: variable associated with the spectral channel
k: variable associated with the acquisition date

Change Vector Analysis (CVA)

Assumption: only 2 spectral channels are considered for each date.

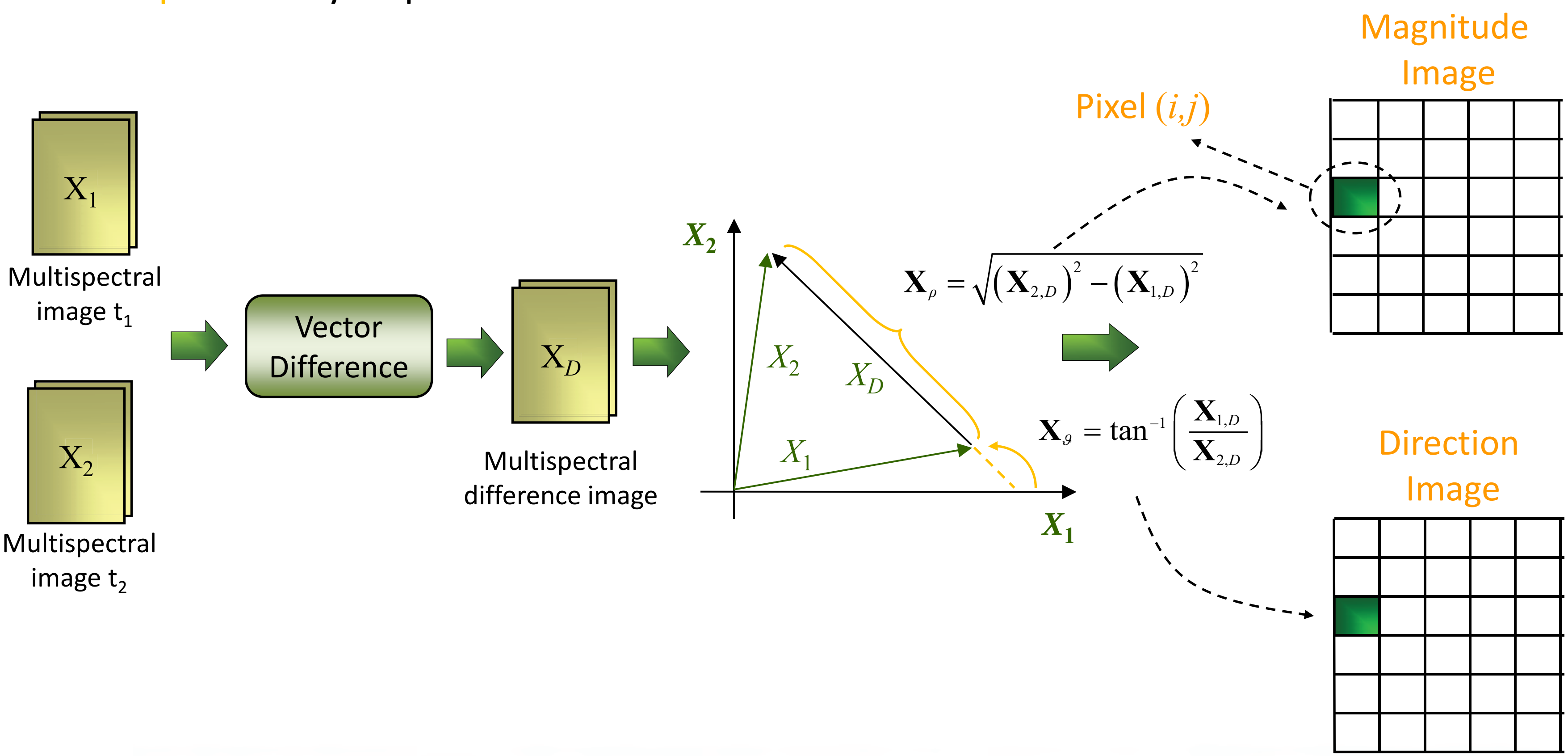

Polar Change Vector Analysis

Polar Domain

$$D = \{\rho, \vartheta : 0 \le \rho < \rho_{max} \ \text{ and } \ 0 \le \vartheta < 2\pi\}$$

ρ -> Random variable associate to magnitude image X_ρ

ϑ -> Random variable associate to direction image X_ϑ

Circle of unchanged pixels

$$C_n = \{\rho, \vartheta : 0 \le \rho < T \ \text{ and } \ 0 \le \vartheta < 2\pi\}$$

Annulus of changed pixels

$$A_c = \{\rho, \vartheta : T \le \rho \le \rho_{max} \ \text{ and } \ 0 \le \vartheta < 2\pi\}$$

Sector of changed pixels

$$S_k = \{\rho, \vartheta : \rho \ge T \ \text{ and } \ \vartheta_{k_1} \le \vartheta < \vartheta_{k_2}, \ 0 \le \vartheta_{k_1} < \vartheta_{k_2} < 2\pi\}$$

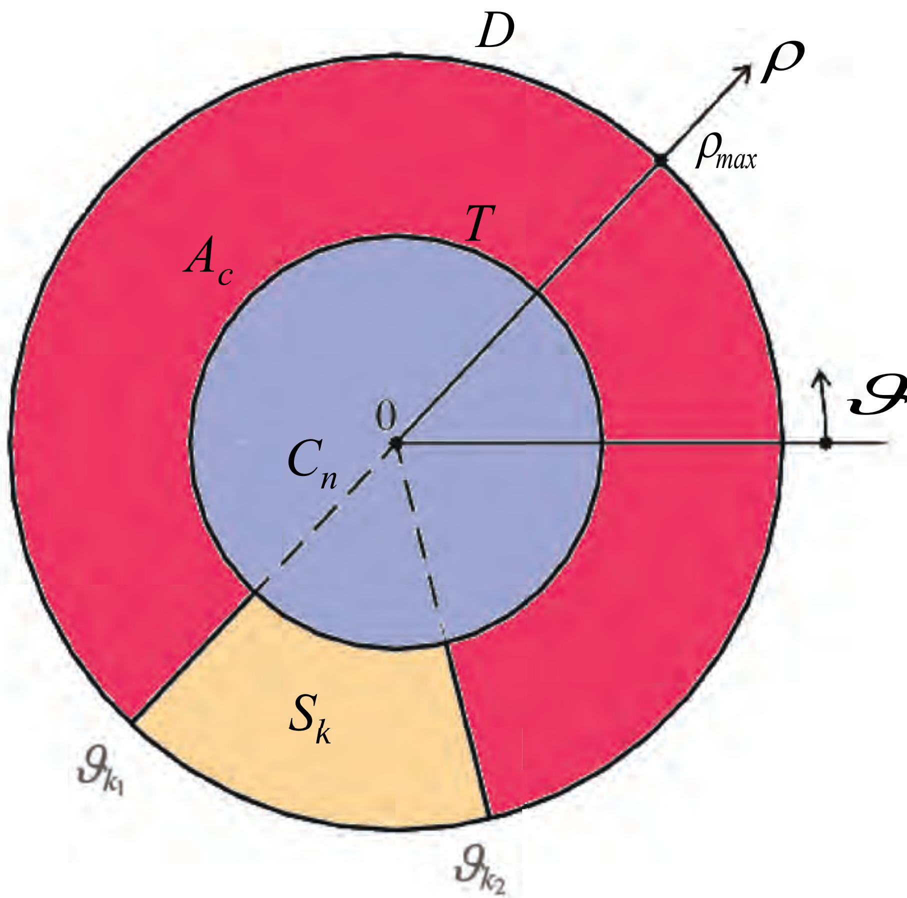

Polar Change Vector Analysis: Example

Study area: Lake Mulargia, Sardinia Island (Italy).

Multitemporal data set: a portion of 412×300 pixels of two images acquired by the TM sensor of Landsat-5 satellite in September 1995 and July 1996.

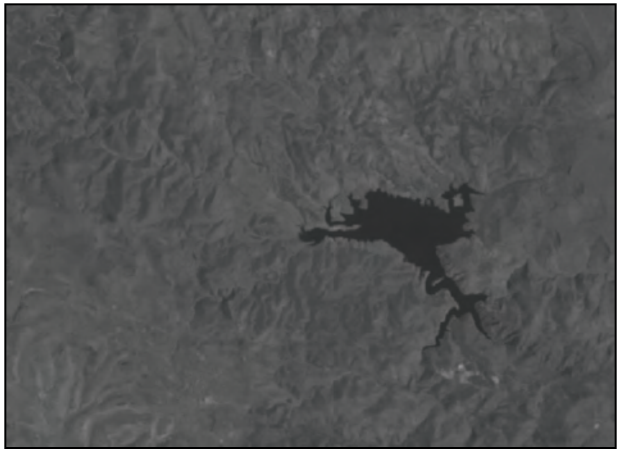

Before Change

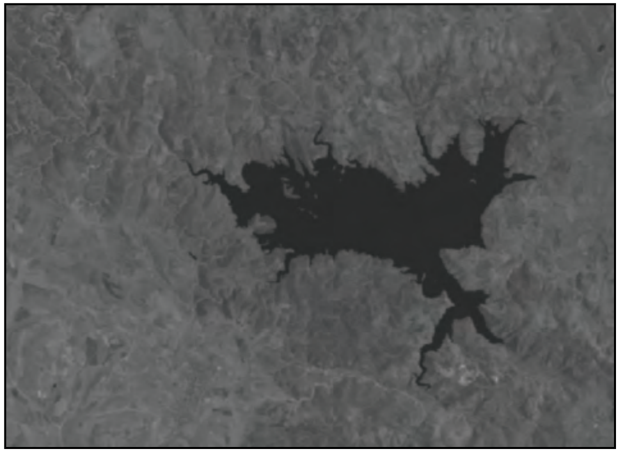

After Change

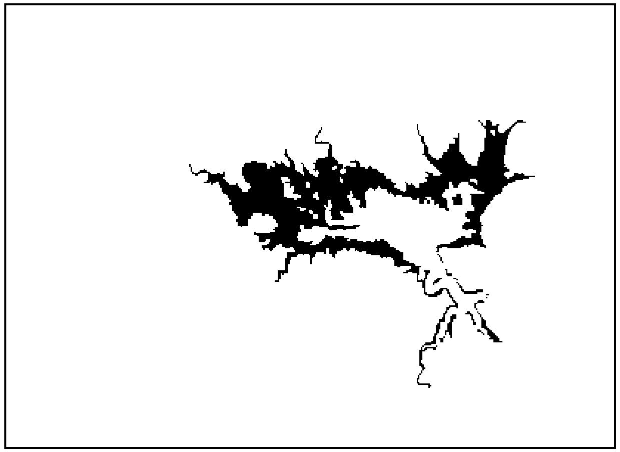

Reference Map

Polar Change Vector Analysis: Example

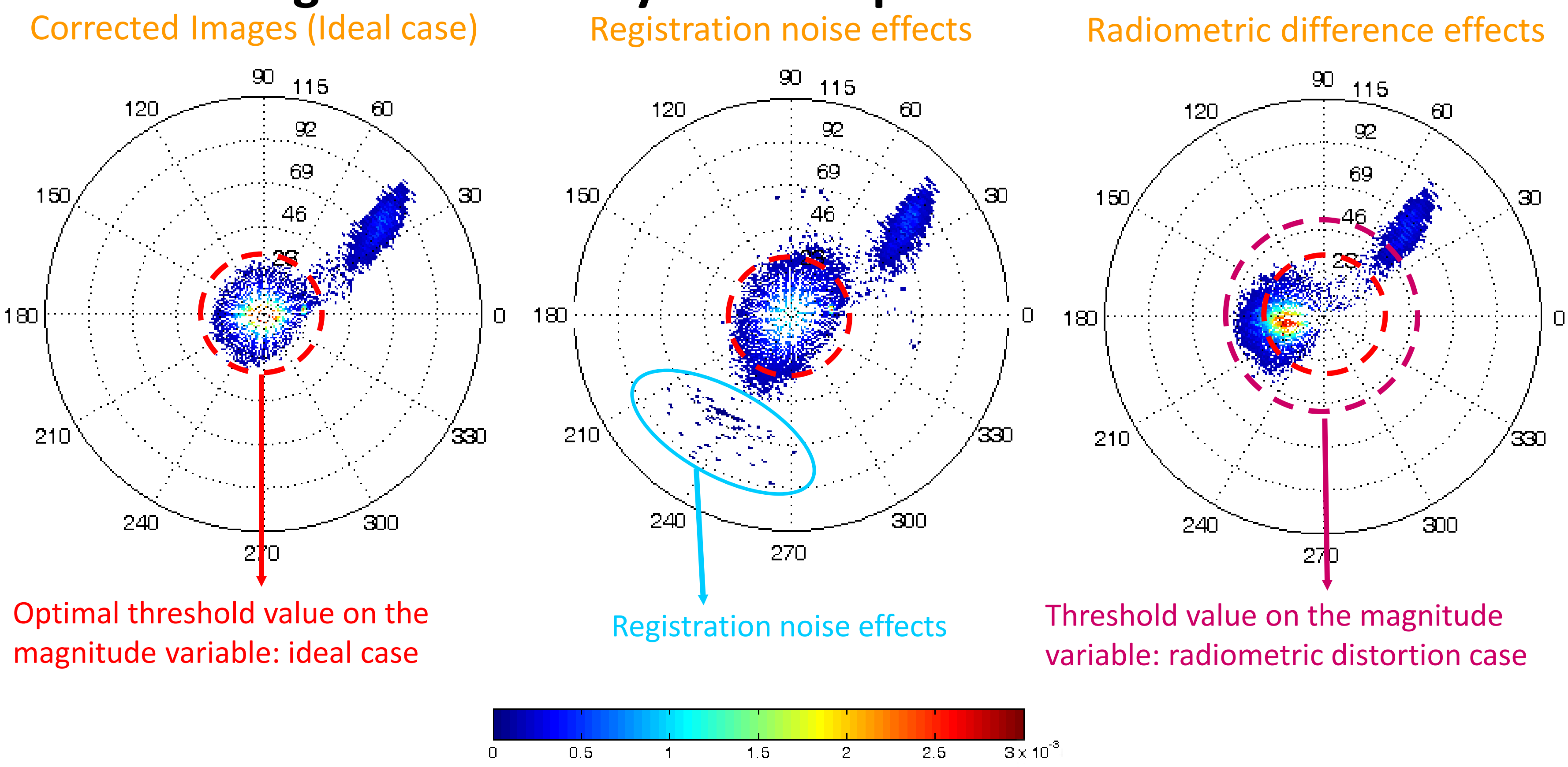

[1] F. Bovolo, L. Bruzzone, A Theoretical Framework for Unsupervised Change Detection Based on Change Vector Analysis in Polar Domain, *IEEE Transactions on Geoscience and Remote* Sensing, Vol. 45, No.1, 2007, pp.218-236.

Polar Change Vector Analysis: Example

Study area: Lake Mulargia, Sardinia Island (Italy).

Multitemporal data set: a portion of 412×300 pixels of two images acquired by the TM sensor of Landsat-5 satellite in September 1995 and July 1996.

Changes: 1 natural change, 1 simulated change.

September 1995 | July 1996

Polar Change Vector Analysis: Example

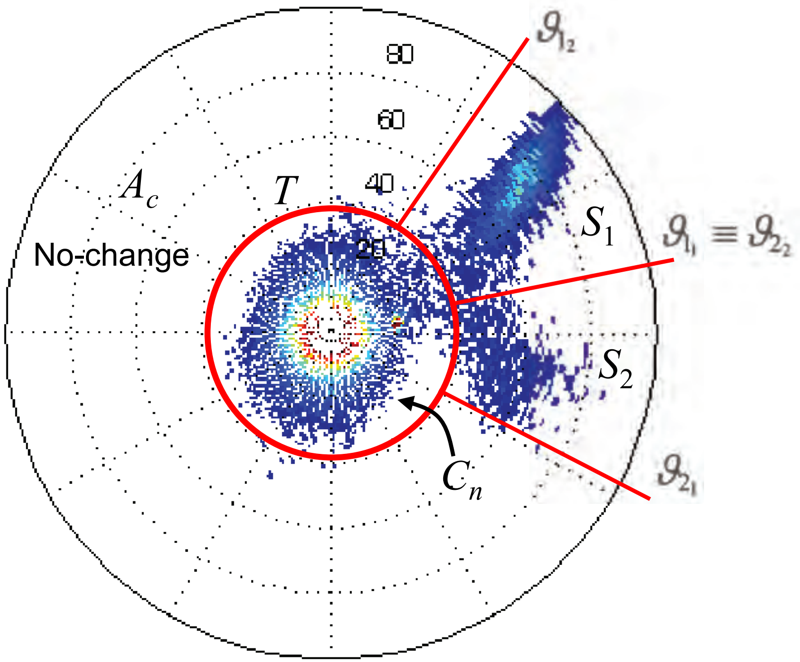

[2] F. Bovolo, S. Marchesi, L. Bruzzone, "A Framework for automatic and unsupervised detection of multiple changes in multitemporal images," IEEE Transactions on Geoscience and Remote Sensing, Vol. 50, No. 6, pp. 2196–2212, 2012.

Compressed Change Vector Analysis (C^2VA)

- ✓ CVA in 2 dimensions permits to easily visualize the change information in polar coordinates, but may results in the loss of information due to spectral channel selection.

- ✓ CVA may be applied on $B > 2$ spectral channels in hyperspherical coordinates. However, when B is greater than 3 it is impossible to visualize the data in the polar domain.

- ✓ Compressed CVA (C^2VA) can overcome the abovementioned limit of polar CVA [3].

[3] F. Bovolo, S. Marchesi, L. Bruzzone, "A Framework for Automatic and Unsupervised Detection of Multiple Changes in Multitemporal Images," IEEE Transactions on Geoscience and Remote Sensing, Vol. 50, No. 6, pp. 2196-2212, 2012.

Compressed Change Vector Analysis (C²VA)

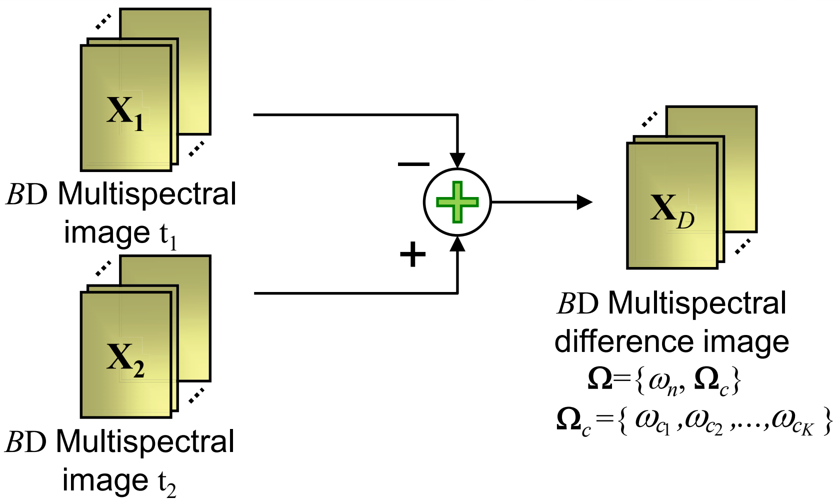

Magnitude: the length of the multispectral difference vector ($\mathbf{X}_D$).

$$\mathbf{X}_\rho = \sqrt{\sum_{b=1}^{B} \mathbf{X}_{b,D}^2} = \sqrt{\sum_{b=1}^{B} \left(\mathbf{X}_{b,2} - \mathbf{X}_{b,1}\right)^2}$$

bth spectral band of X_1

Direction: the angle between the multispectral difference vector ($\mathbf{X}_D$) and a reference vector ($\mathbf{X}_{ref}$) in a *BD* space.

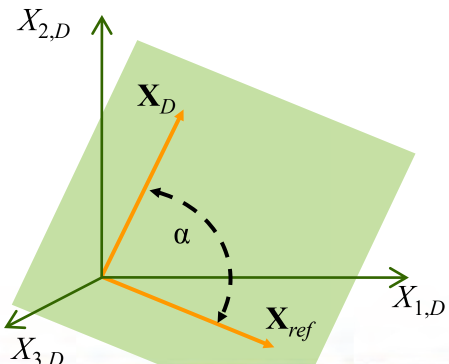

$$\mathbf{X}_\alpha = \arccos\left(\sum_{b=1}^{B} \left(\mathbf{X}_{b,D}\mathbf{X}_{b,ref}\right) \Big/ \sqrt{\sum_{b=1}^{B} \mathbf{X}_{b,D}^2 \sum_{b=1}^{B} \mathbf{X}_{b,ref}^2} \right)$$

$$\alpha \in [0, \pi]$$

BD unit vector

$$\mathbf{X}_{ref} = \left[\frac{\sqrt{B}}{B}, \ldots, \frac{\sqrt{B}}{B} \right]$$

Compressed Change Vector Analysis (C²VA)

Definitions

1. *Compressed CVA (C²VA) Domain*

$$C^2VA = \{\rho, \alpha : 0 \le \rho < \rho_{max} \text{ and } 0 \le \alpha < \pi\}$$

$$\rho_{max} = max\left\{\sqrt{\sum_{b=1}^{B} X_{b,D}^2}\right\}$$

α -> Random variable associate to direction image $\mathbf{X}_\alpha$

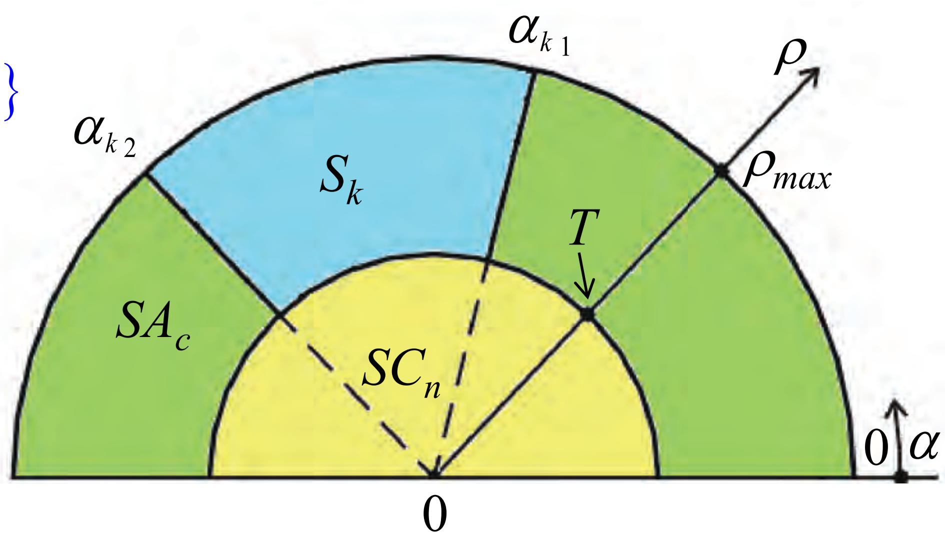

2. *Semi-Circle of unchanged pixels*

$$SC_n = \{\rho, \alpha : 0 \le \rho < T \text{ and } 0 \le \alpha < \pi\}$$

3. *Semi-Annulus of changed pixels*

$$SA_c = \{\rho, \alpha : T \le \rho \le \rho_{max} \text{ and } 0 \le \alpha < \pi\}$$

4. *Annular sector of the k-th kind of change*

$$S_k = \{\rho, \alpha : \rho \ge T \text{ and } \alpha_{k1} \le \alpha < \alpha_{k2},\ 0 \le \alpha_{k1} < \alpha_{k2} < \pi\}$$

C²VA: Example

Study area: Lake Mulargia, Sardinia Island (Italy).

Multitemporal data set: a portion of 412×300 pixels of two images acquired by the TM sensor of Landsat-5 satellite in September 1995 and July 1996.

Changes: 2 natural changes, 1 simulated change

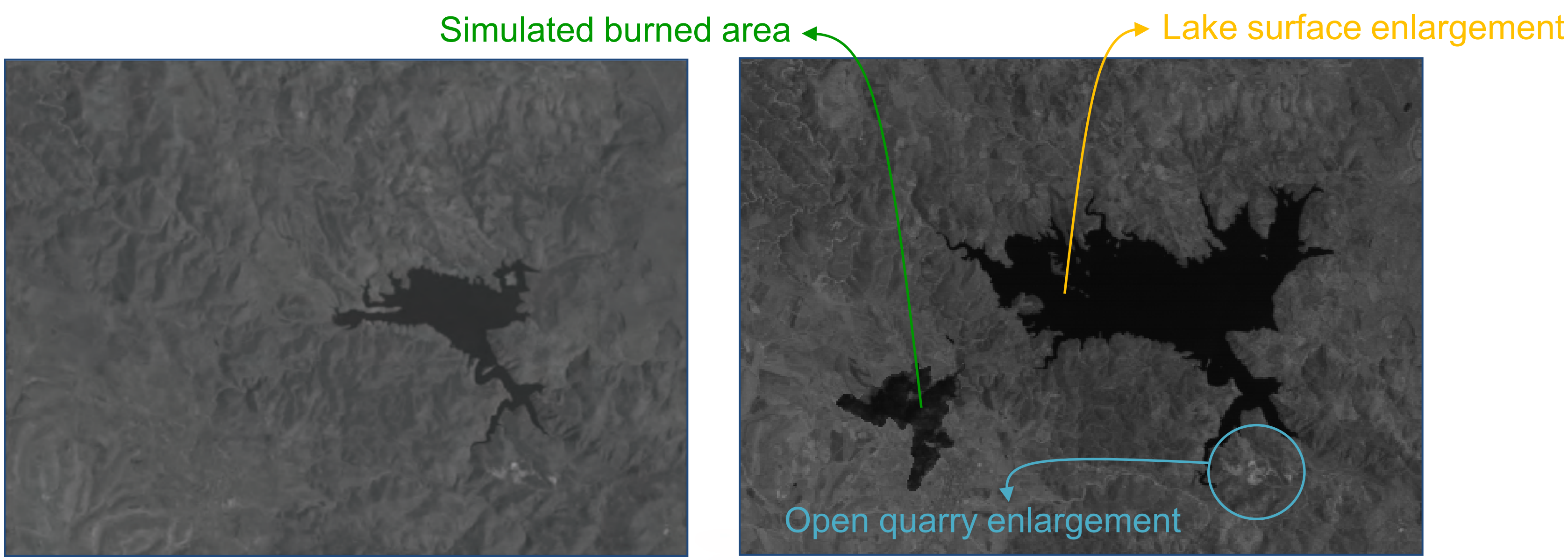

September 1995 July 1996

C^{2}VA: Example

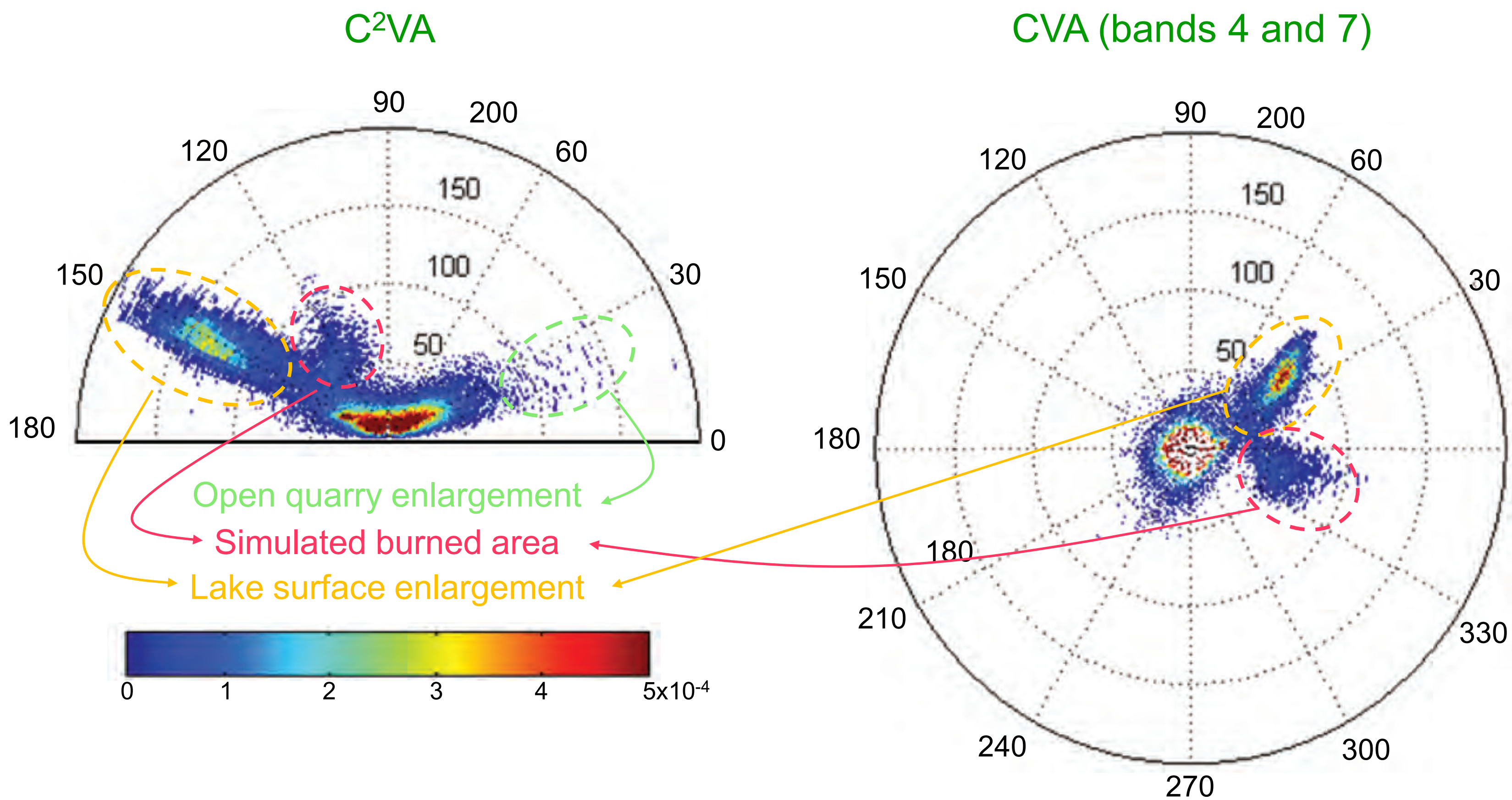

Data Pre-processing: SAR Images

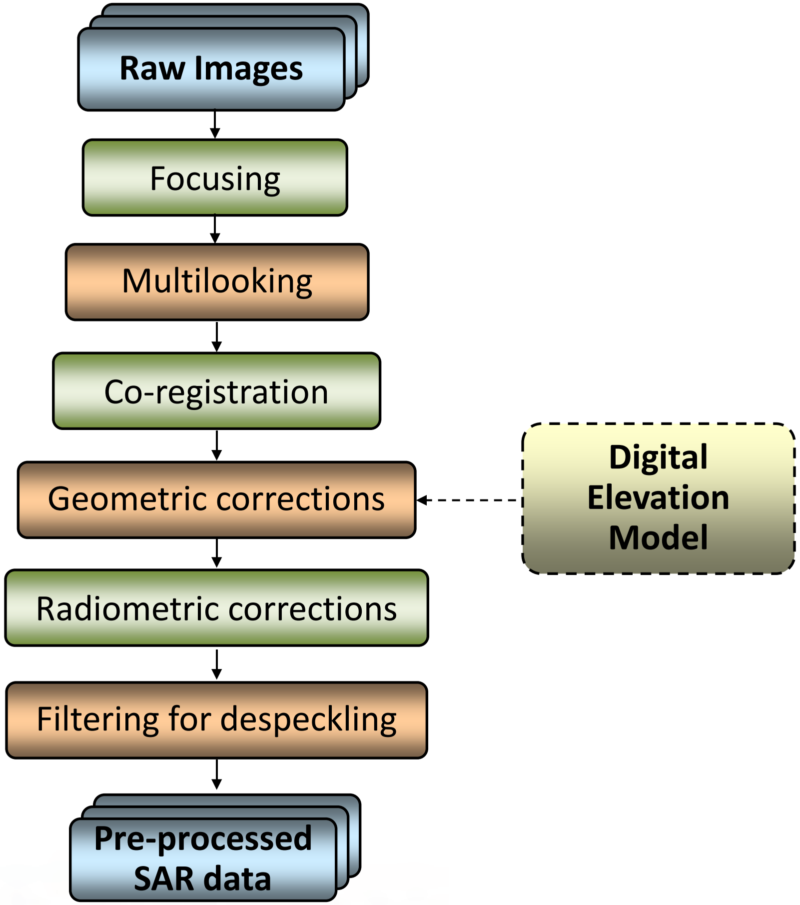

Binary CD in SAR: Typical Architecture

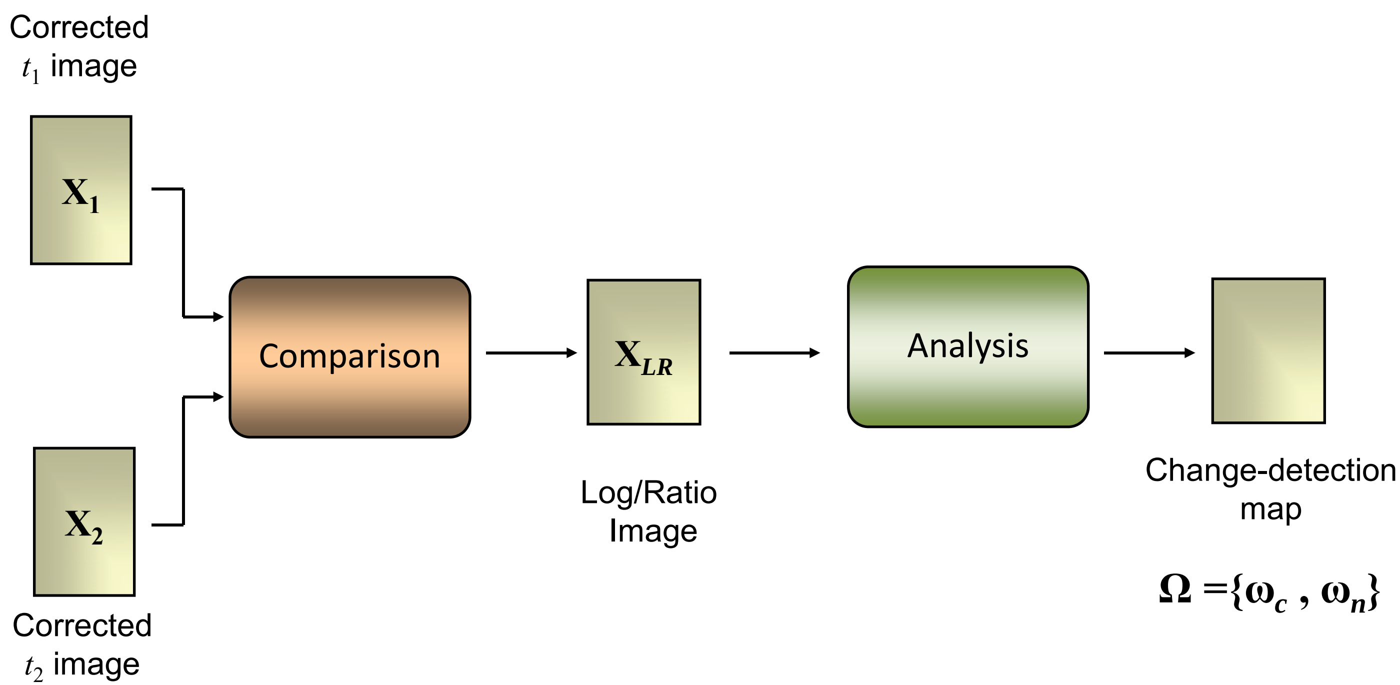

Binary CD in SAR: Comparison Operators

Technique	Feature vector $\boldsymbol{f}_k$ at the time t_k	Computation of X_D
Image rationing	$\boldsymbol{f}_k = X_k^b$	$X_D = \boldsymbol{f}_2 / \boldsymbol{f}_1$
Kullback-Leibler distance (Similarity measures)	$\boldsymbol{f}_k = [p(X_k)]$	$KL(X_2 \| X_1) = \int \log(f_1/f_2) f_1$
Difference of scattering matrix element products	$\boldsymbol{f}_k = [S_{HH} S_{VV}^*]$	$X_D = \boldsymbol{f}_1 - \boldsymbol{f}_2$
Difference of scattering matrix amplitude correlation coefficients	$\boldsymbol{f}_k = \left[\frac{S_{HH} S_{VV}^*}{\sqrt{\|S_{HH}\|^2 \|S_{VV}\|^2}} \right]$	$X_D = \boldsymbol{f}_1 - \boldsymbol{f}_2$

k: variable associated with the acquisition date

Binary CD in SAR: Comparison Operators

Difference operator:

Mean intensities of X_1 and X_2 in an homogeneous area

Equivalent number of looks

$$P(X_D|\bar{I}_1,\bar{I}_2)=\frac{L^L}{(L-1)!}\frac{1}{(\bar{I}_1+\bar{I}_2)^L}\exp\left(-\frac{LX_D}{\bar{I}_2}\right)\sum_{j=0}^{L-1}\frac{(L-1+j)\ !}{j\ !\ (L-1-j)\ !}X_D^{\ L-1-j}\left[\frac{\bar{I}_1\bar{I}_2}{L(\bar{I}_1+\bar{I}_2)}\right]^j$$

The statistical distribution of the difference image depends on both:

- ✓ the relative change between the intensity values in the two images;
- ✓ a reference intensity value.

This leads to a higher change-detection error for changes occurred in high intensity regions of the image than in low intensity regions (i.e., changes are detected in a different way in dark and bright regions).

Binary CD in SAR: Comparison Operators

Ratio operator:

- ✓ reduces the multiplicative distortions common to the two considered images due to speckle noise;
- ✓ makes the distribution of the ratio image depending only on the relative changes between images.

Equivalent number of looks

Mean intensities

$$P(X_R \mid \bar{I}_1, \bar{I}_2) = \left(\frac{\bar{I}_2}{\bar{I}_1}\right)^L \frac{(2L-1)!}{(L-1)!^2} \frac{X_R^{\,L-1}}{\left[\bar{I}_2/\bar{I}_1 + X_R\right]^{2L}}$$

Log-ratio operator ($\mathbf{X}_{LR}$):

- ✓ produces more symmetrical statistical distribution of the classes of changed and unchanged pixels;
- ✓ transforms the residual multiplicative noise model into an additive noise model.

Example: Change Detection in SAR Images

ERS-2, Pre-event Image

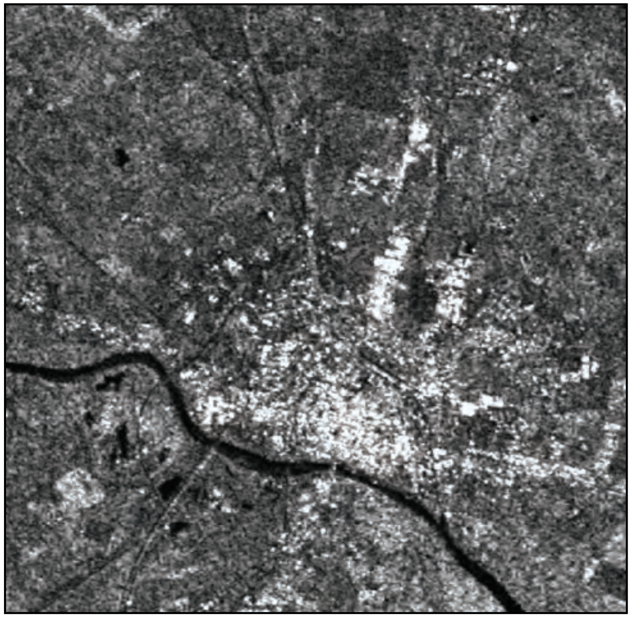

ERS-2, Post-event Image

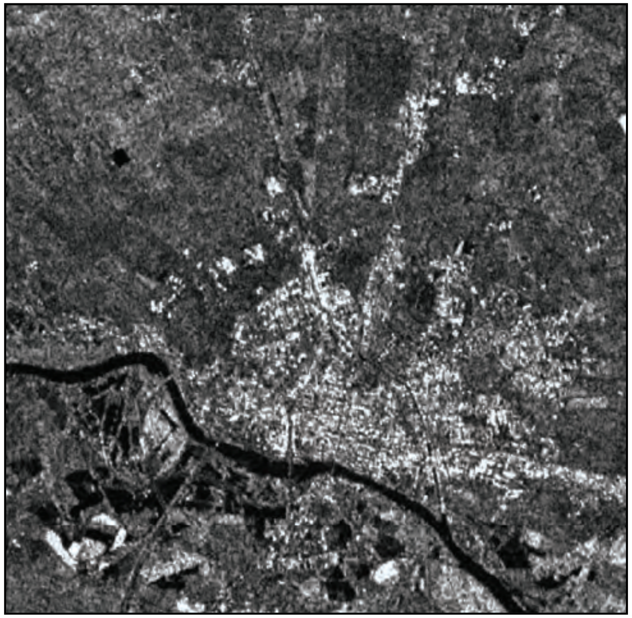

Change Detection Map
(Flooded Area)

ERS-2 SAR images of a flood in the City of Pavia, Italy

→ 6th ESA ADVANCED TRAINING COURSE ON LAND REMOTE SENSING

3. Change Detection in Very High Resolution Multispectral Images

Optical satellite Missions

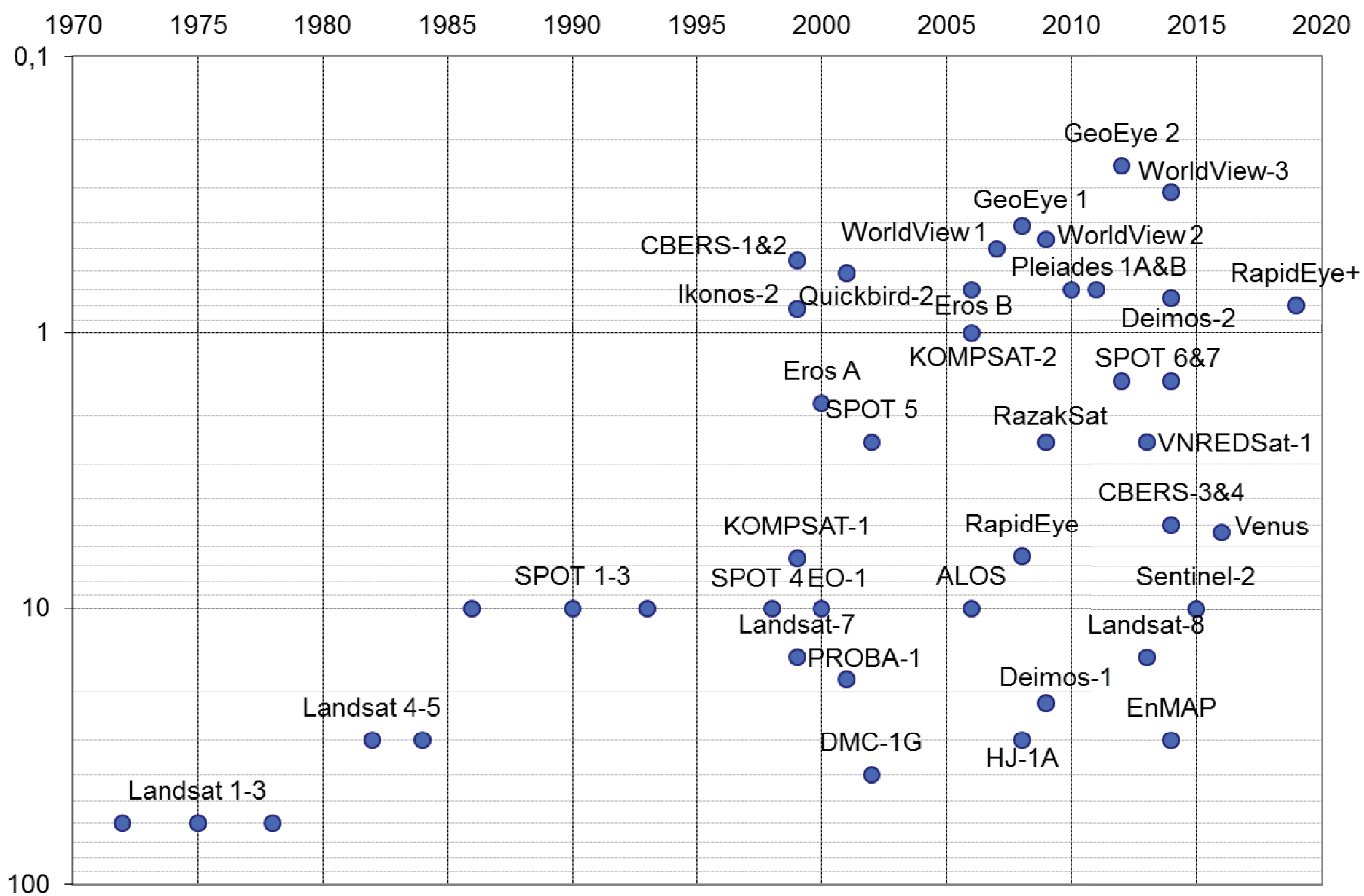

CD in Multitemporal VHR MS images

July 2006

October 2005

Quickbird images of the city of Trento (Italy)

CD in Multitemporal VHR MS images

October 2005

July 2006

Quickbird images of the city of Trento (Italy)

CD in Multitemporal VHR MS images

October 2005

July 2006

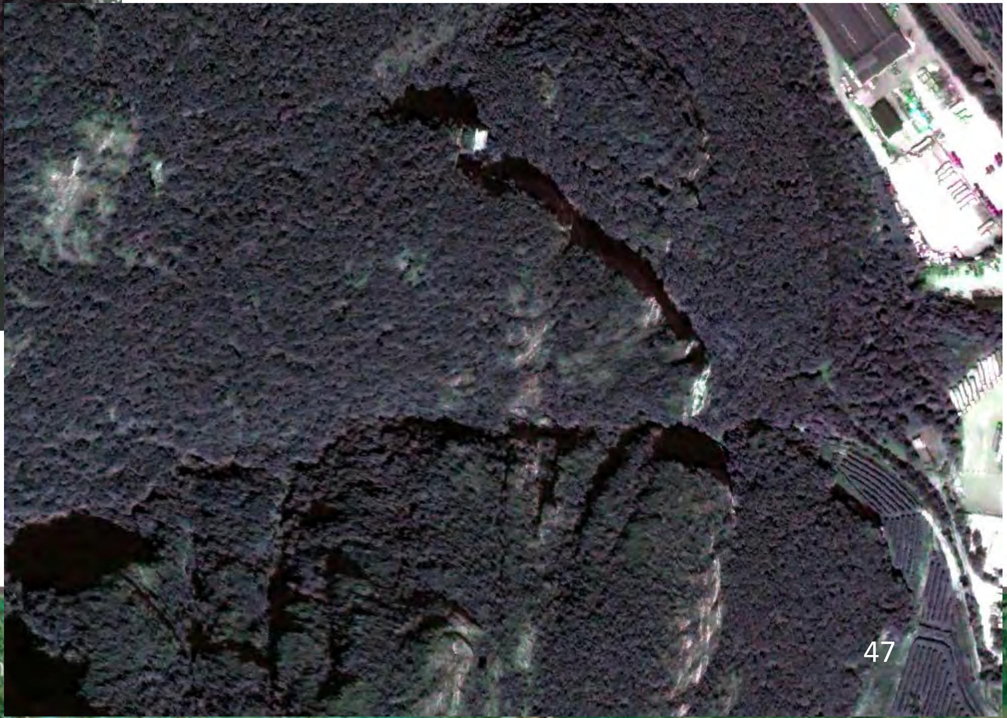

Quickbird images of
the city of Trento (Italy)

Unsupervised CD: Typical Architecture

Comparison Operators:

- Difference
- Vector difference
- Ratio
- Log-ratio

Difference, Vector difference: Optical Images

Ratio, Log-ratio: Synthetic Aperture Radar (SAR) Images

Corrected t_1 image

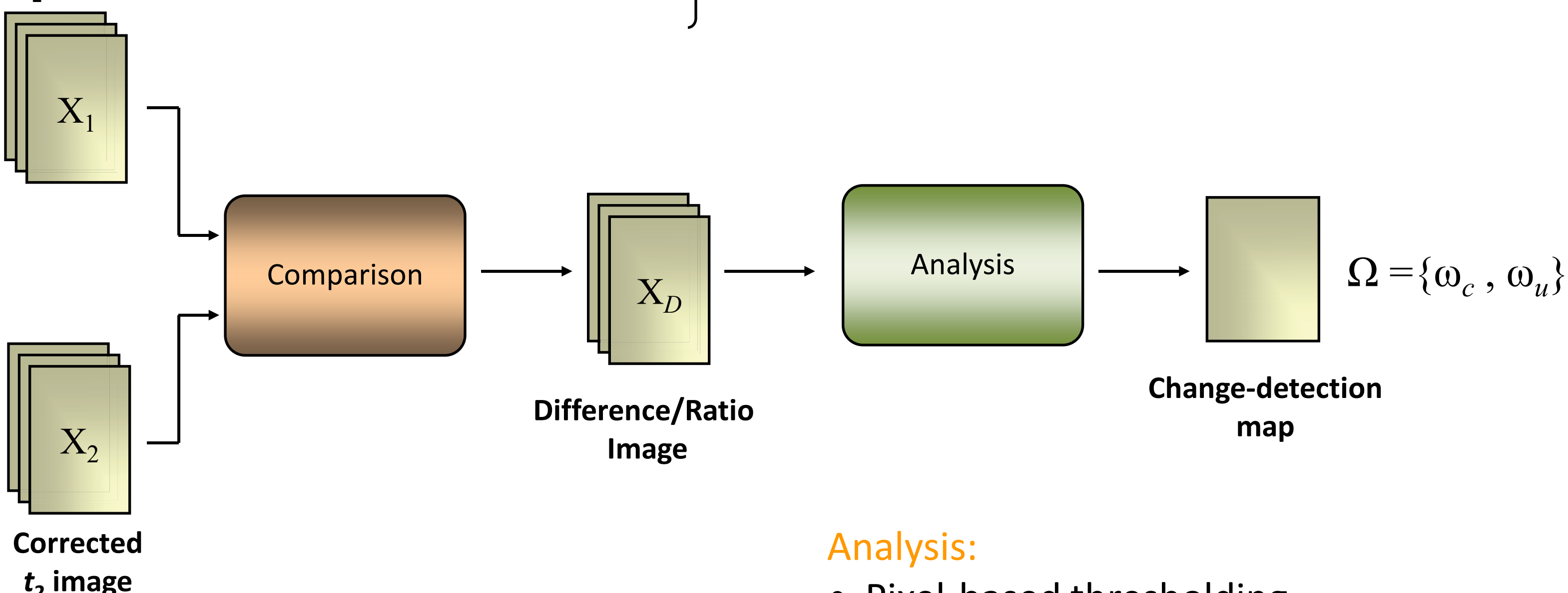

Analysis:

- Pixel-based thresholding
- Context-based approaches

CD in Multitemporal VHR Images: Example

Quickbird, October 2004 (true color composition)

Quickbird, July 2006 true color composition

Magnitude Difference Image

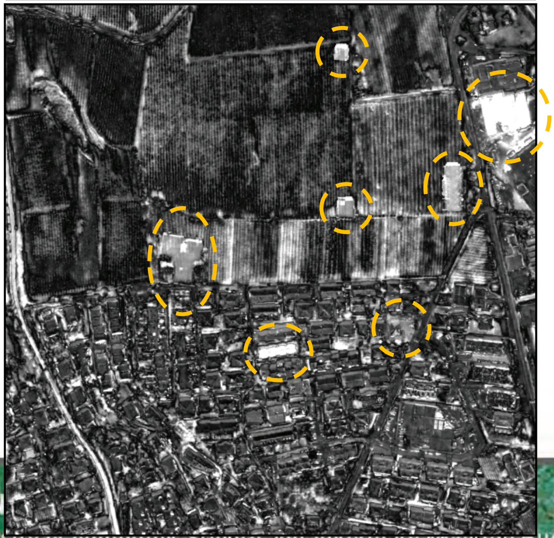

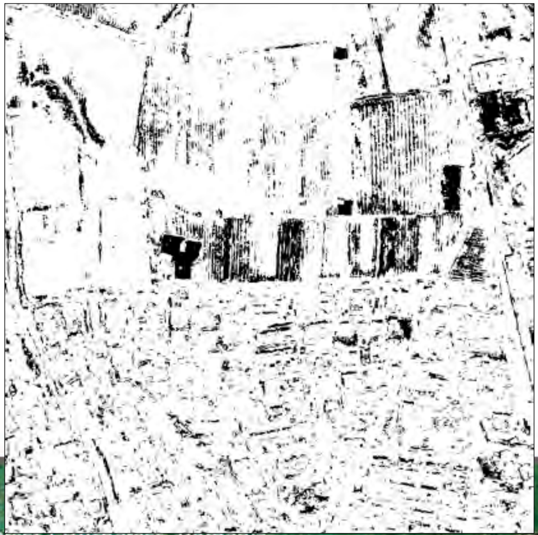

Pixel-Based Change Detection Map

CD in Multitemporal VHR images

Change detection in VHR Images should exploit a top-down approach to the definition of the processing architecture. This approach should [4]:

- ✓ explicitly model the presence of different radiometric changes on the basis of the properties of the considered images;
- ✓ extract the semantic meaning of changes;
- ✓ identify changes of interest with strategies designed on the basis of the specific application;
- ✓ exploit the intrinsic multiscale properties of the objects and the high spatial correlation between pixels in a neighborhood.

[4] L. Bruzzone, F. Bovolo, "A Conceptual Framework for Change Detection in Very High Resolution Remote Sensing Images," *Proceedings of IEEE*, Vol. 101, pp. 609-630, 2013.

CD in VHR MS Images: Architecture Design

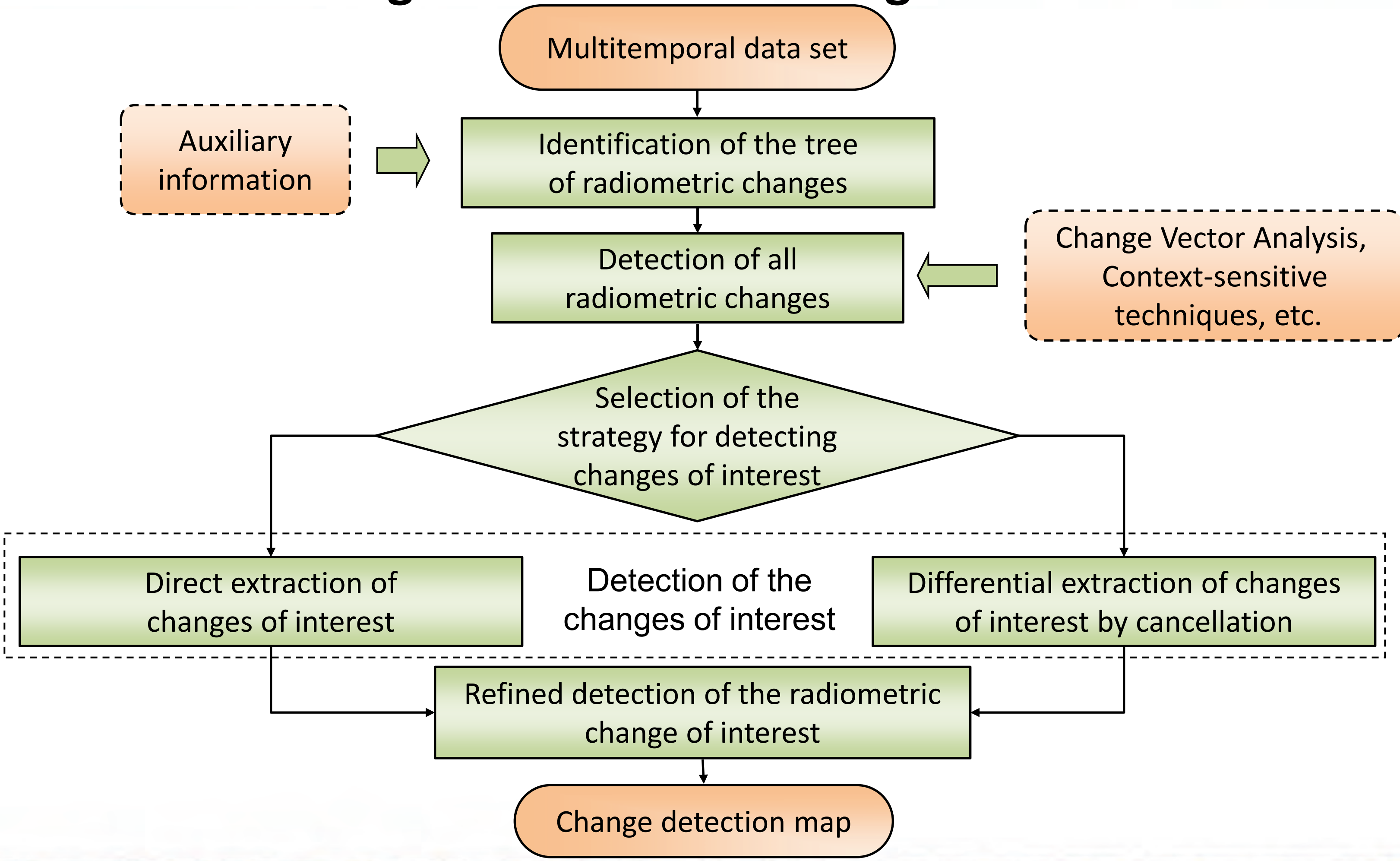

Identification of the Tree of Radiometric Changes

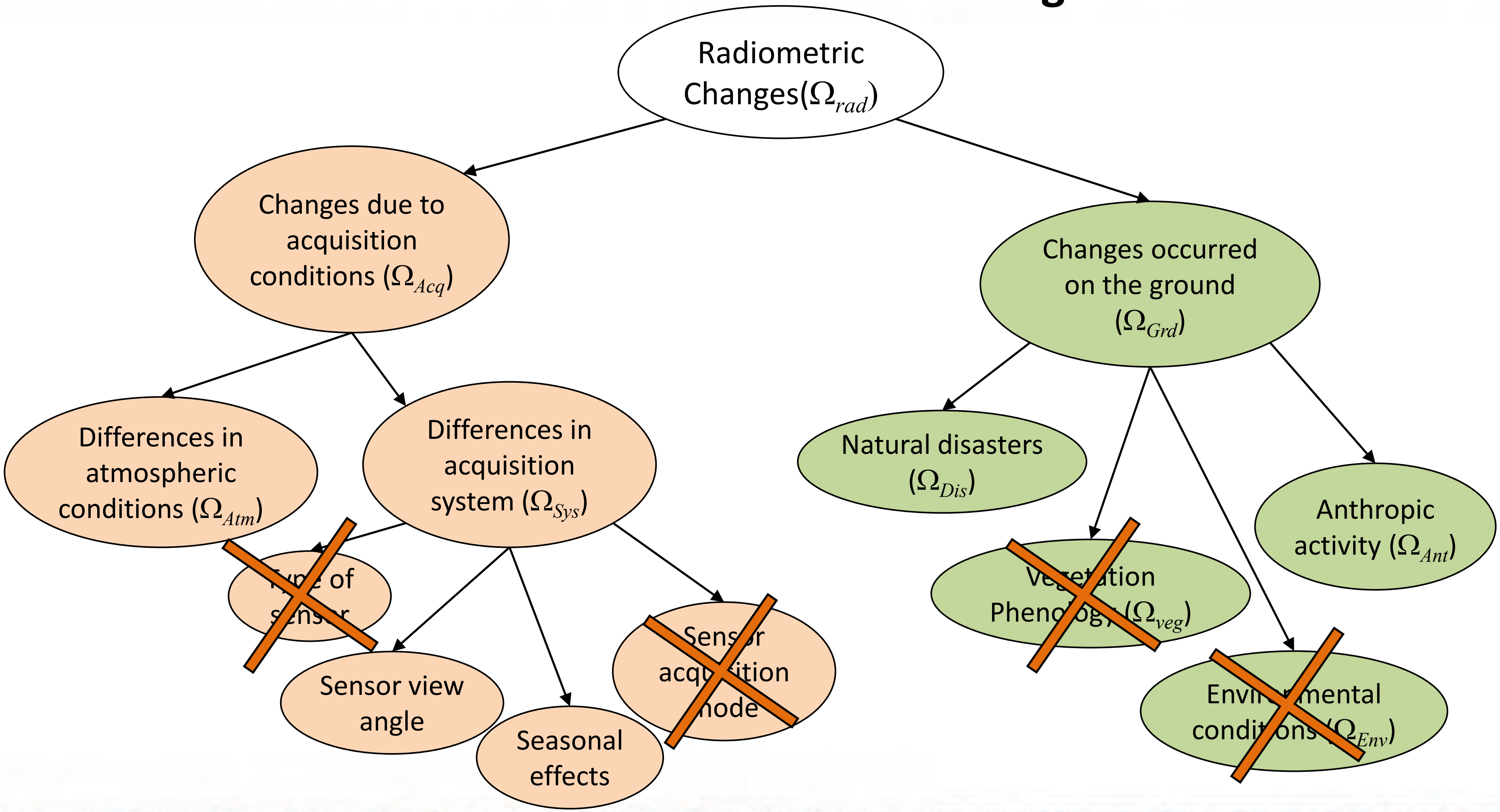

Detection of Changes of Interest

Direct detection

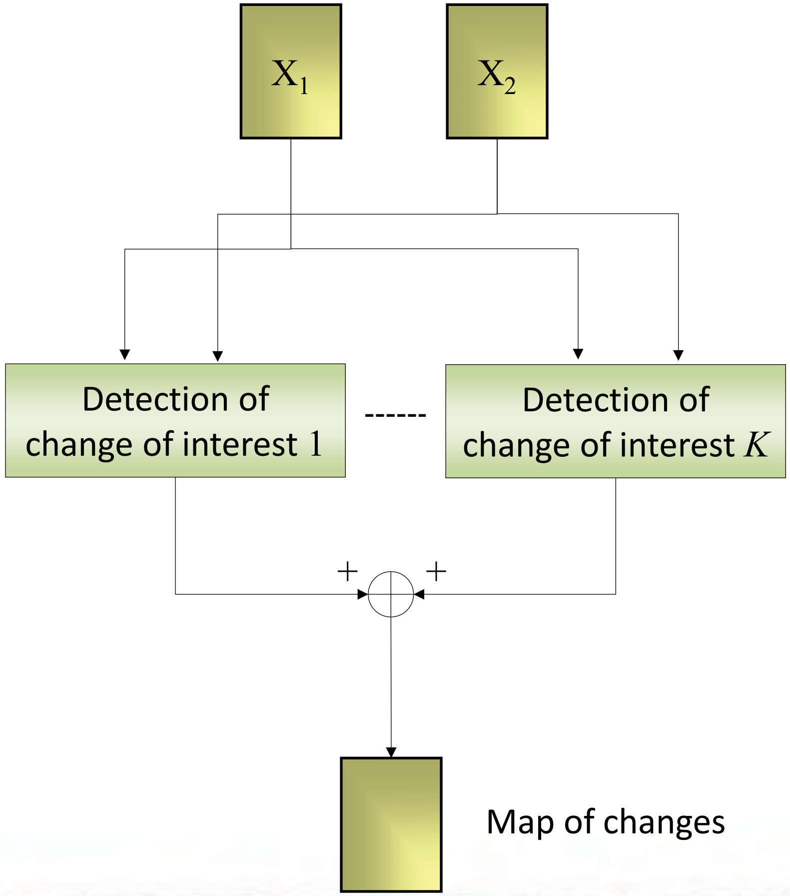

Differential detection by cancellation

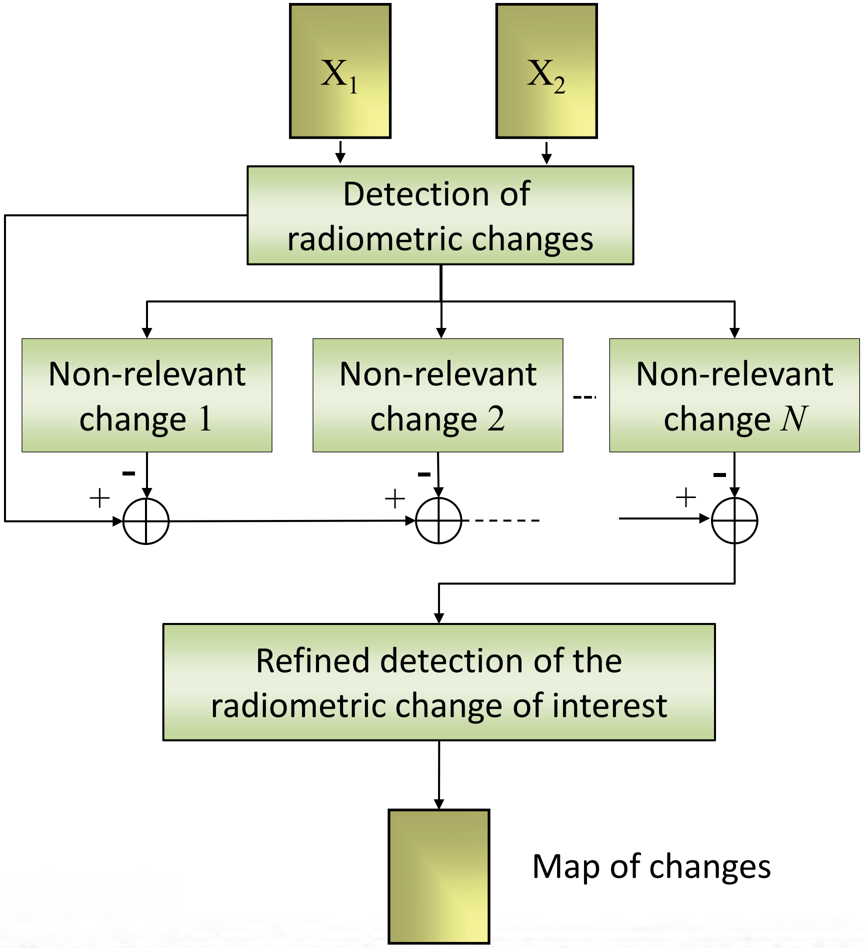

Multilevel Approach: Semantic of Changes

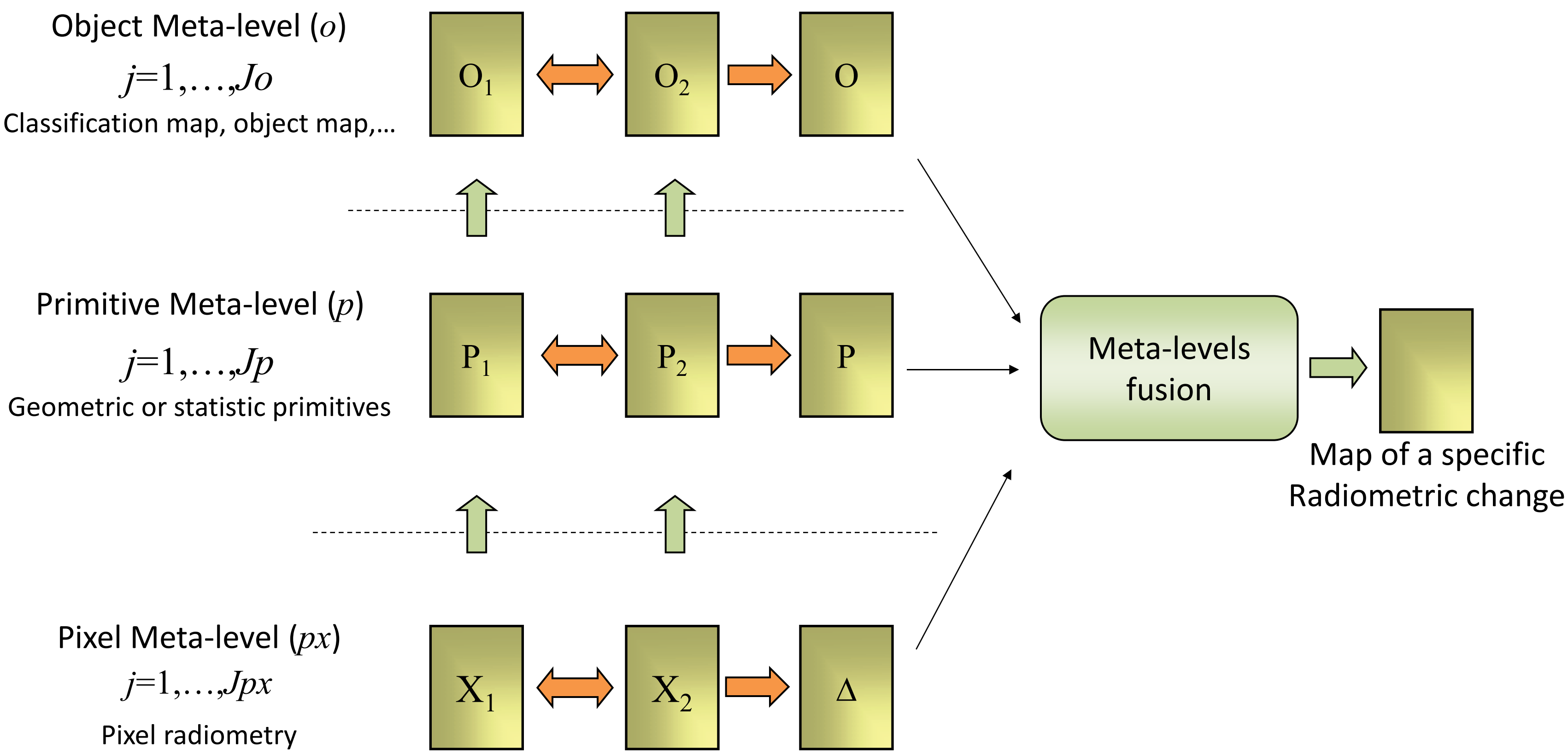

[5] L. Bruzzone, F. Bovolo "A Conceptual Framework for Change Detection in Very High Resolution Remote Sensing Images," Proceedings of *IEEE*, Vol. 101, pp. 609-630, 2013.

Example: CD in VHR Optical Images

Study area: South part of Trento (Italy).

Multitemporal data set: portion (380×430 pixels) of two images acquired by the Quickbird satellite in October 2004 and July 2006.

Causes of Change: changes on the ground, seasonal changes, registration noise.

CD in VHR MS Images: Architecture Design

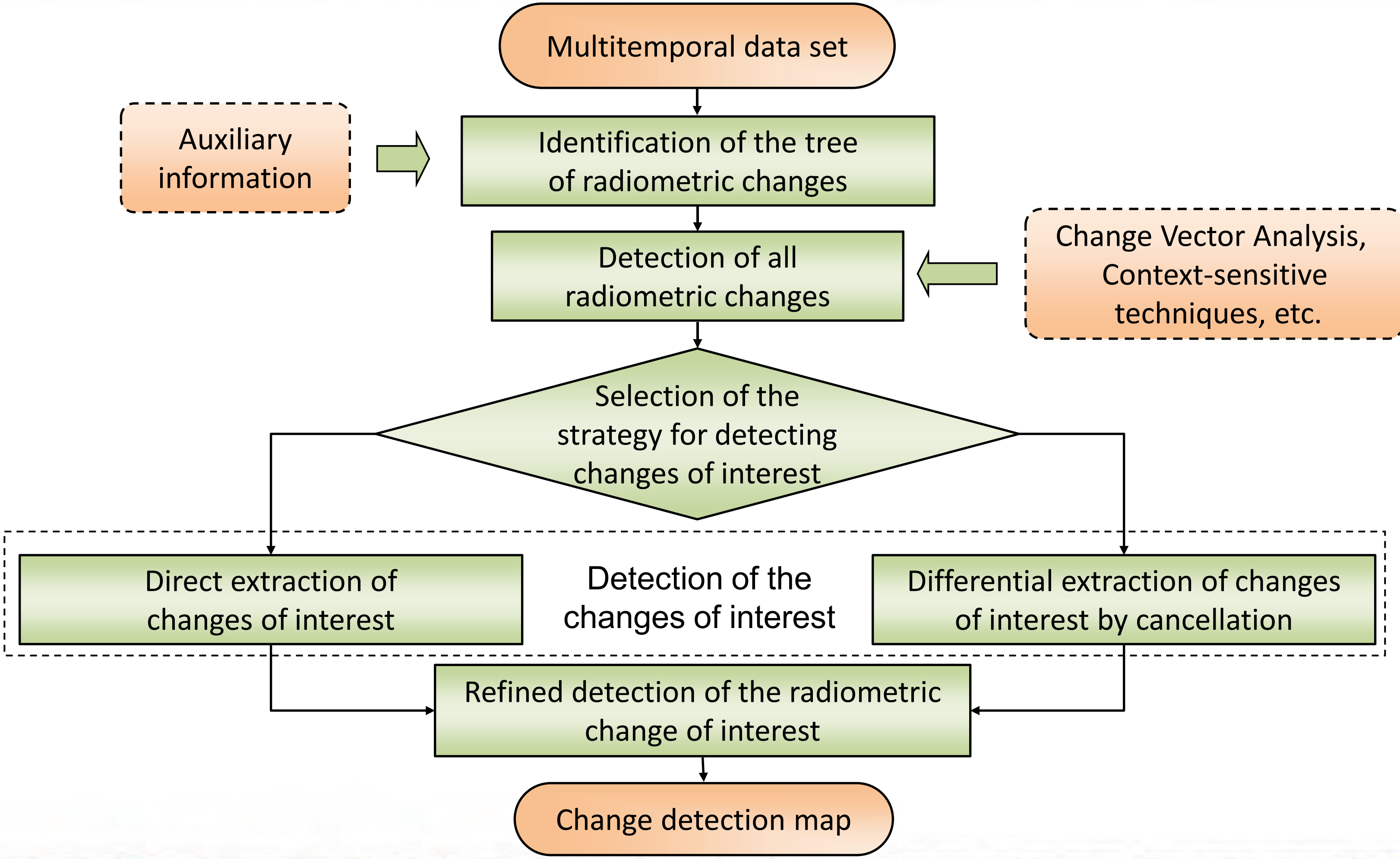

Identification of the Tree of Radiometric Changes

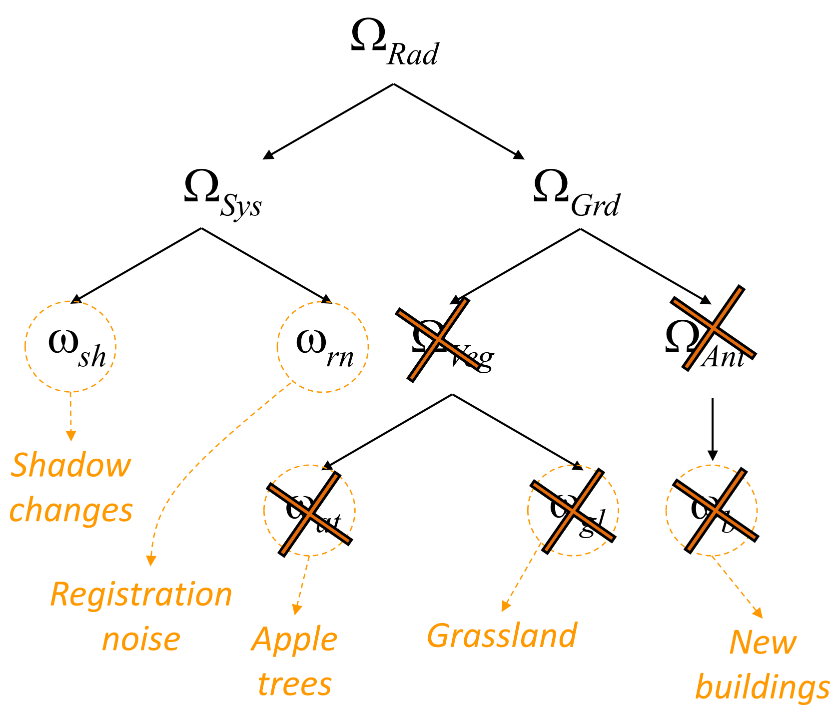

Changes Tree and Detection Strategy

Identification of the tree of radiometric changes

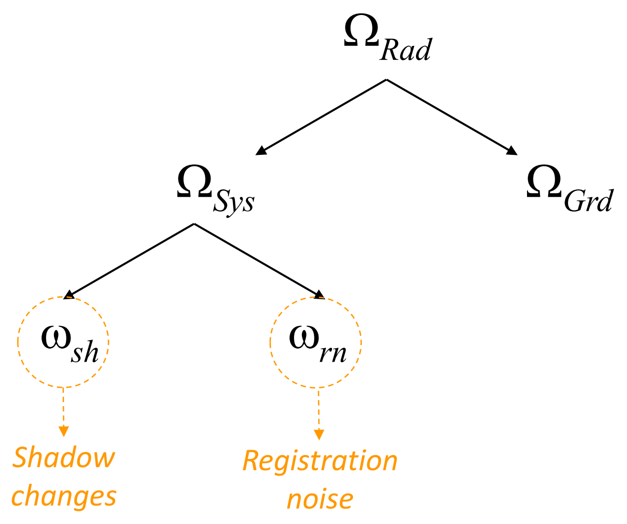

Differential detection by cancellation

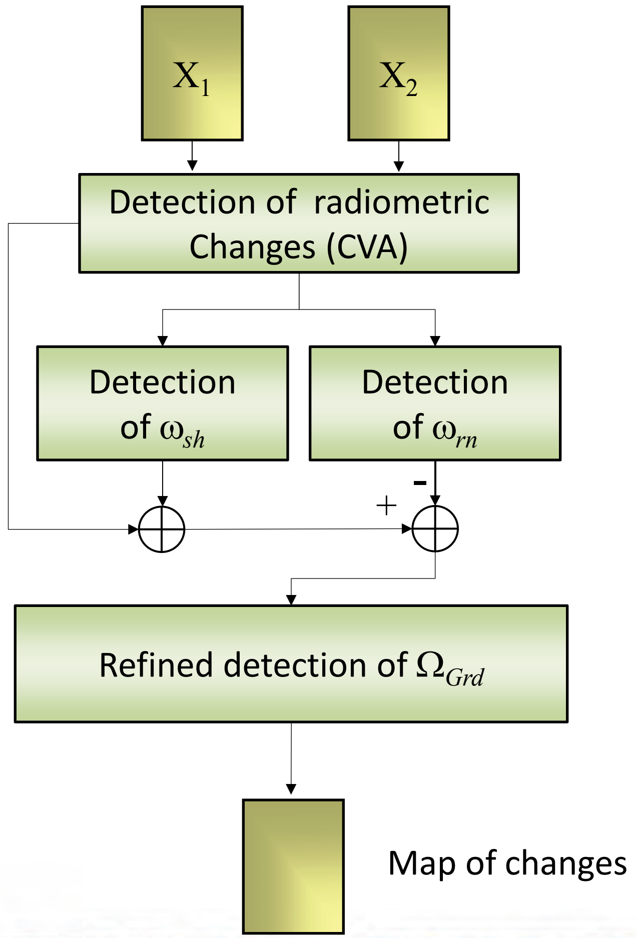

Multilevel Representation of Radiometric Changes

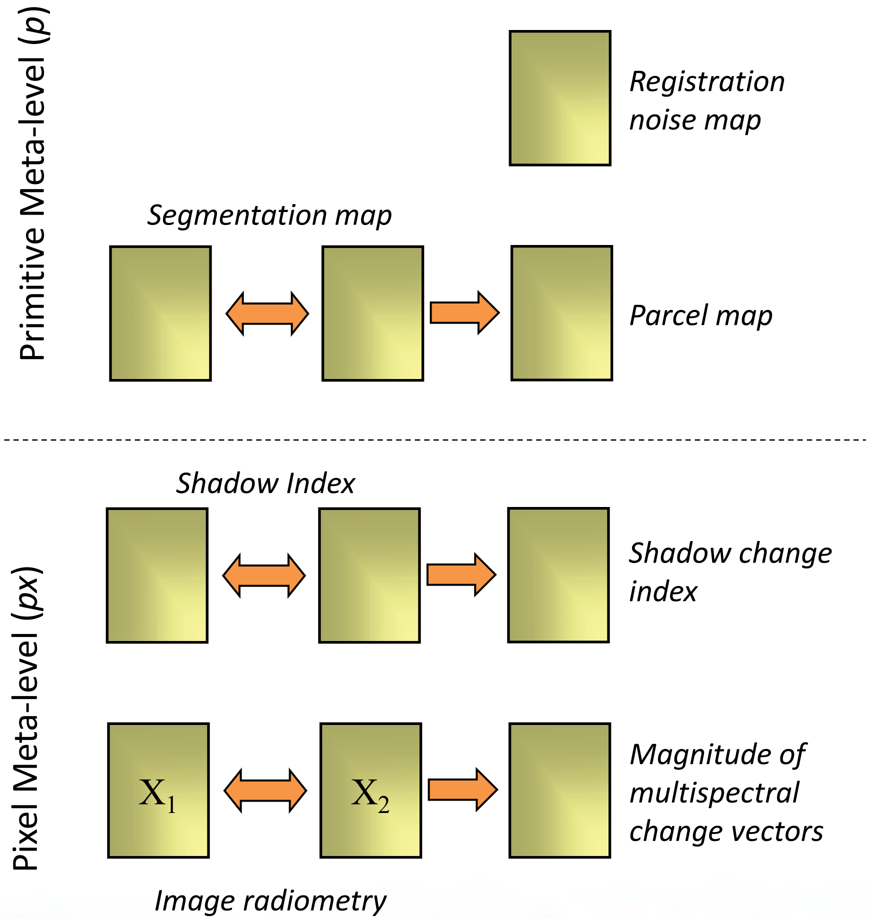

[6] S. Marchesi, F. Bovolo, L. Bruzzone, “A Context-Sensitive Technique Robust to Registration Noise for Change Detection in VHR Multispectral Images”, *IEEE Transactions on Image Processing*, Vol. 19, pp. 1877-1889, 2010.

[7] F. Bovolo, “A Multilevel Parcel-Based Approach to Change Detection in Very High Resolution Multitemporal Images,” IEEE Geoscience and Remote Sensing Letters, Vol. 6, No. 1, pp. 33-37, January 2009.

[8] V. J. D. Tsai, "A comparative study on shadow compensation of color aerial images in invariant color models," IEEE Trans. Geosci. Remote Sens., vol. 44, pp. 1661-1671, 2006.

[9] L. Bruzzone and D. Fernández-Prieto, "Automatic Analysis of the Difference Image for Unsupervised Change detection," IEEE Trans. Geosci. Rem. Sens., vol. 38, pp. 1170-1182, 2000.

Example: CD Architecture

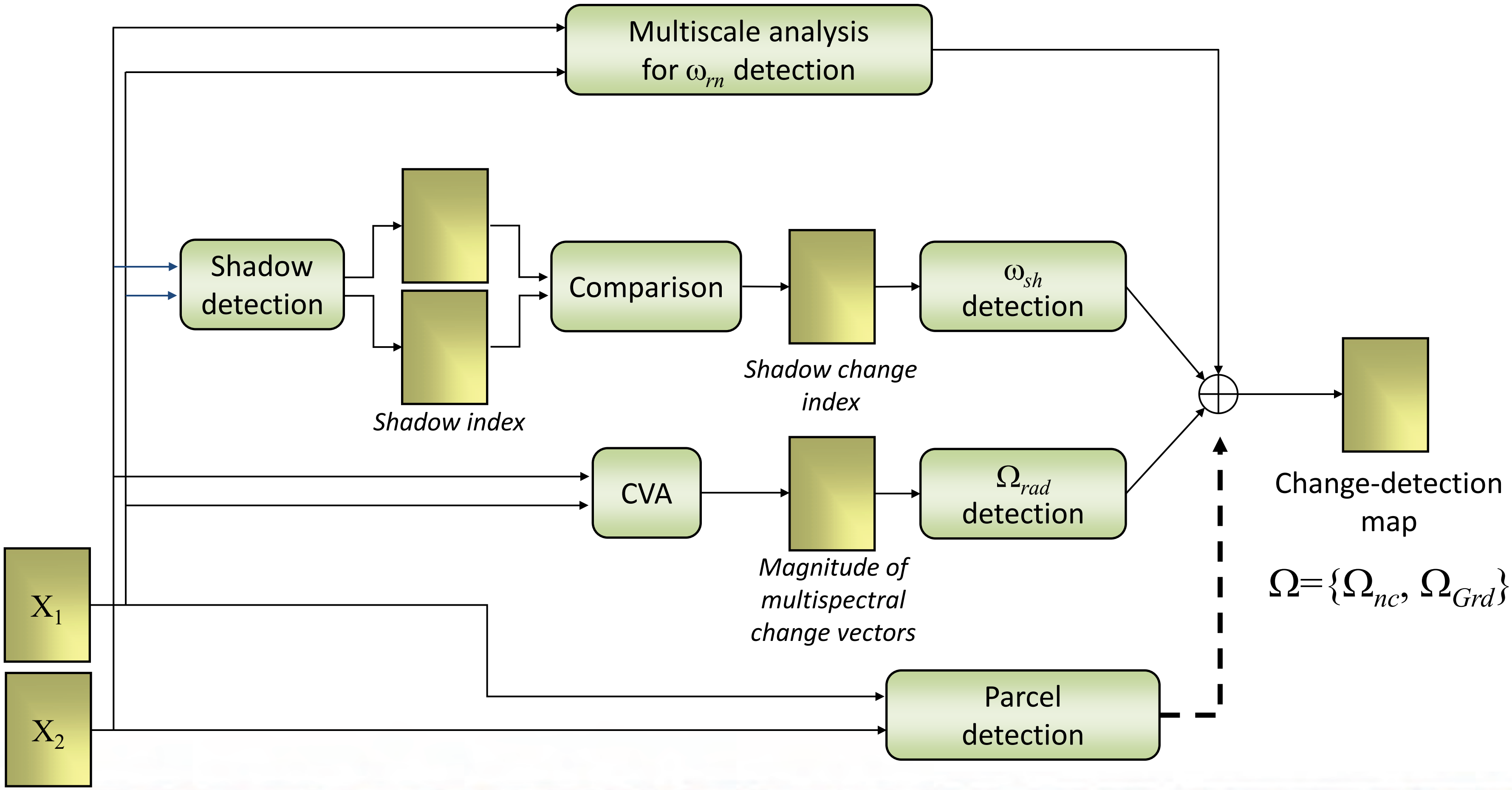

Example: Qualitative Results


October 2005


July 2006


Reference Map

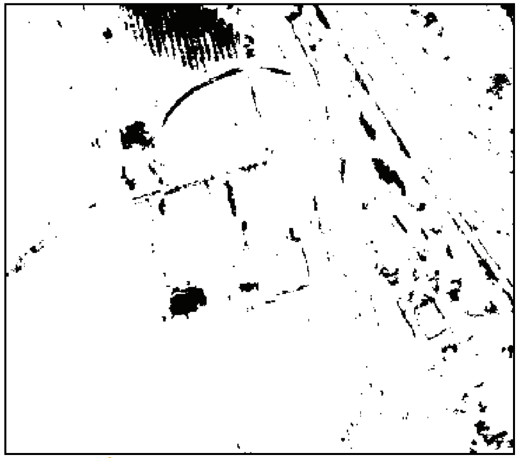
Change Detection Map
CVA Parcel Based

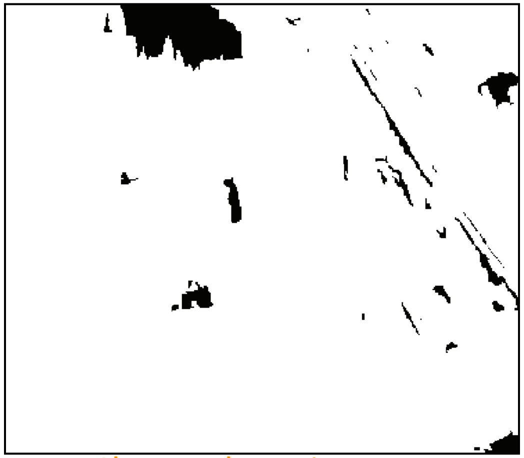
Change detection Map
Top-down Architecture

Example: Quantitative Results

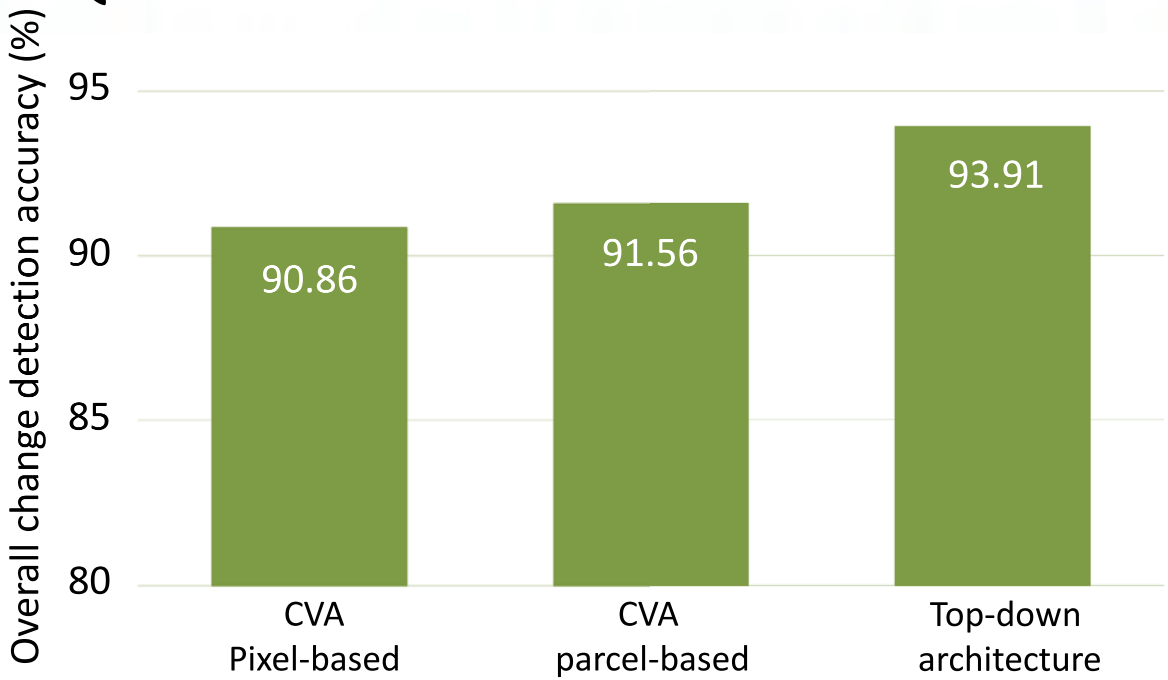

Technique	False Alarms	Missed Alarms	Total Errors	Overall accuracy (%)
CVA pixel-based	5005	9924	14929	90.86
CVA parcel-based	3537	10261	13798	91.56
Top-down architecture	1470	8480	9950	93.91

4. Change Detection in Very High Resolution SAR Images

SAR Satellite Missions

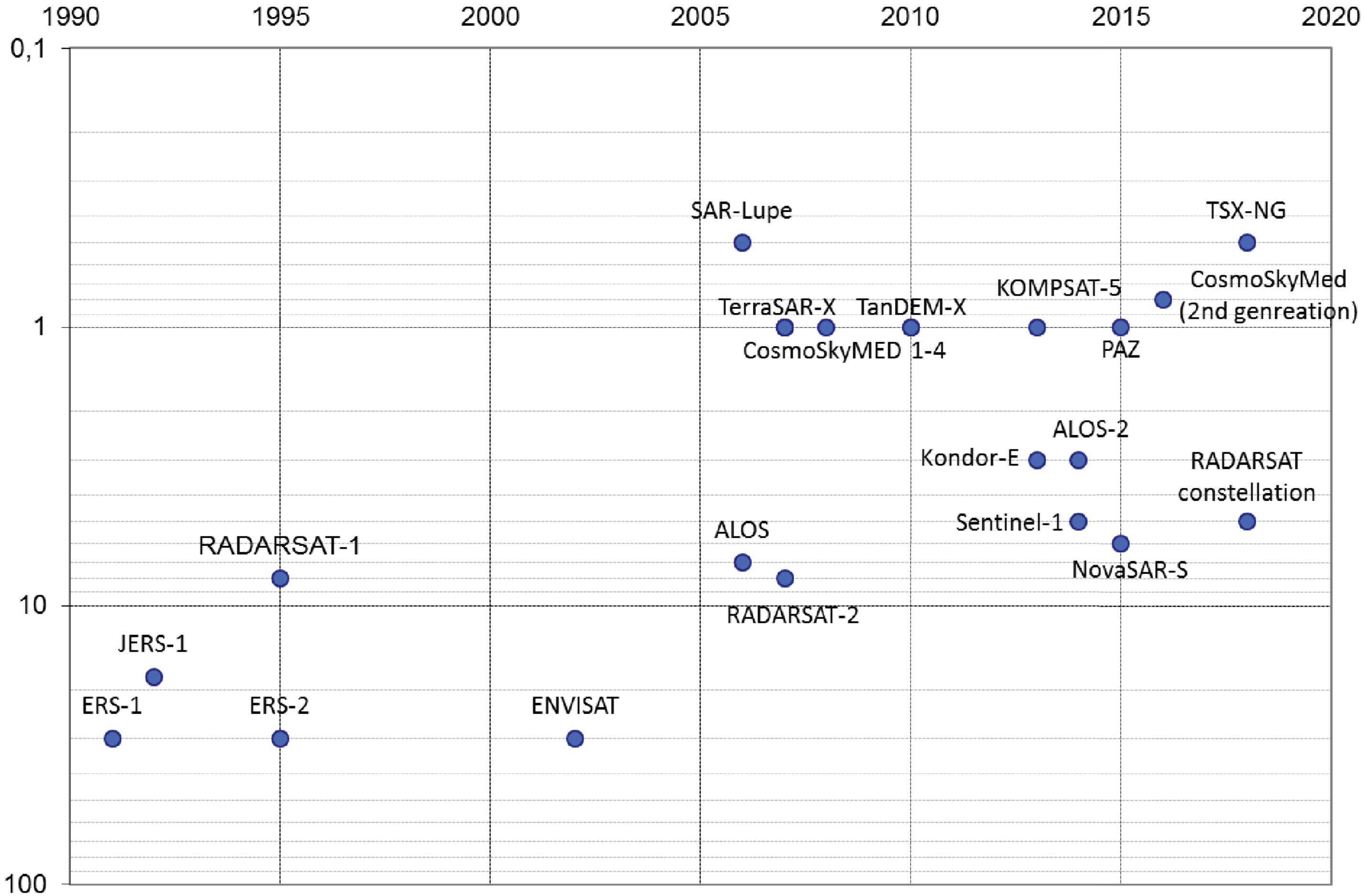

Multitemporal SAR Images: New challenges

April 2009

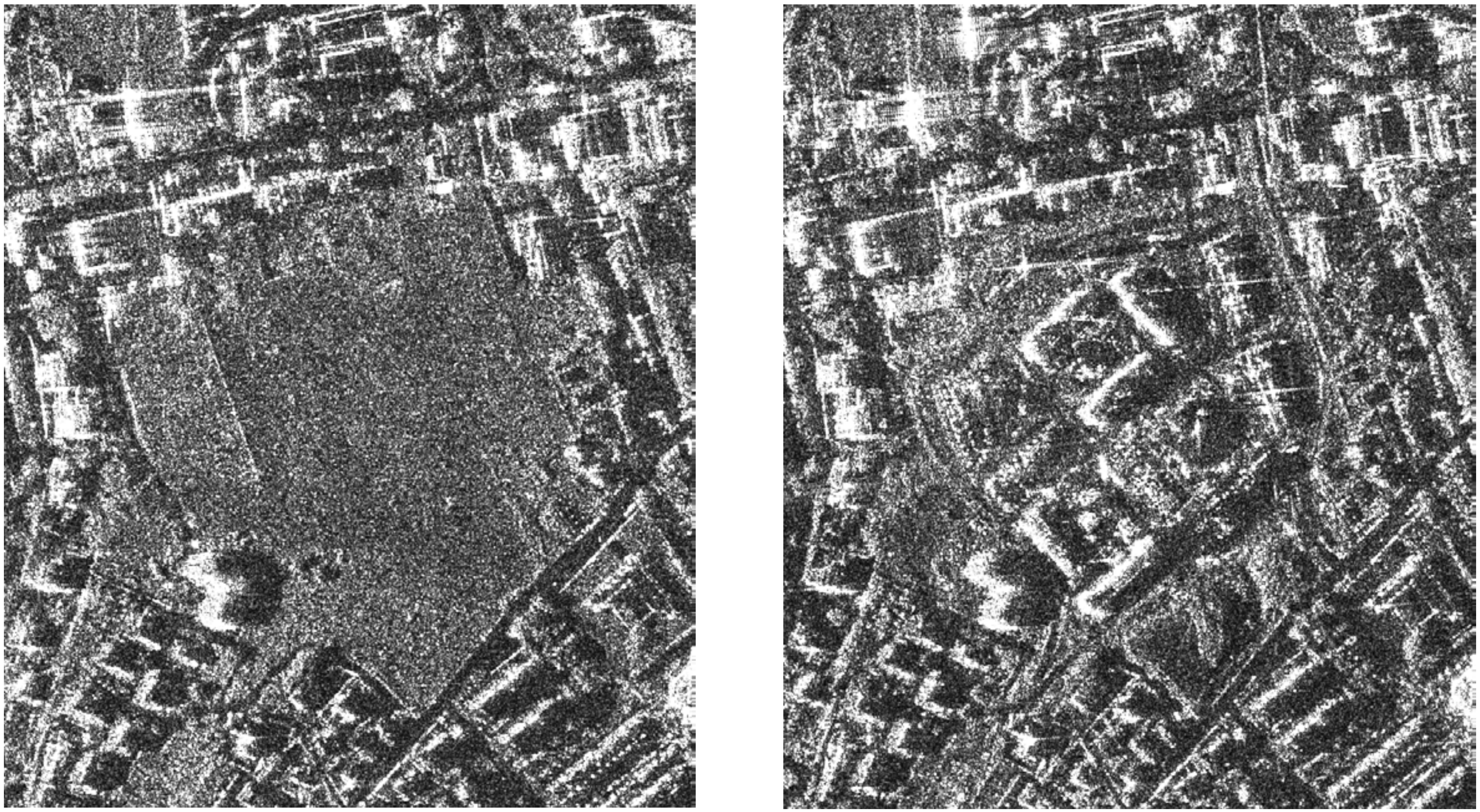

September 2009

Comso-Skymed SAR Images of the Earthquake of L'Aquila, Italy

CD in VHR SAR images

✓ In multitemporal SAR VHR images we have many sources of backscattering changes.

✓ Often backscattering changes associated with different sources exhibit characteristics similar to each other. They can be separated only by explicitly modeling the EM behavior of complex objects.

✓ To this end it is necessary to bridge the semantic gap between low level features and semantic information:

- Modelling the interaction between the EM waves and the imaged objects;
- Extracting the different object components with proper detectors;
- Combining object components for identifying the objects and the possible changes in their state.

Example: Building Detection in VHR SAR Images

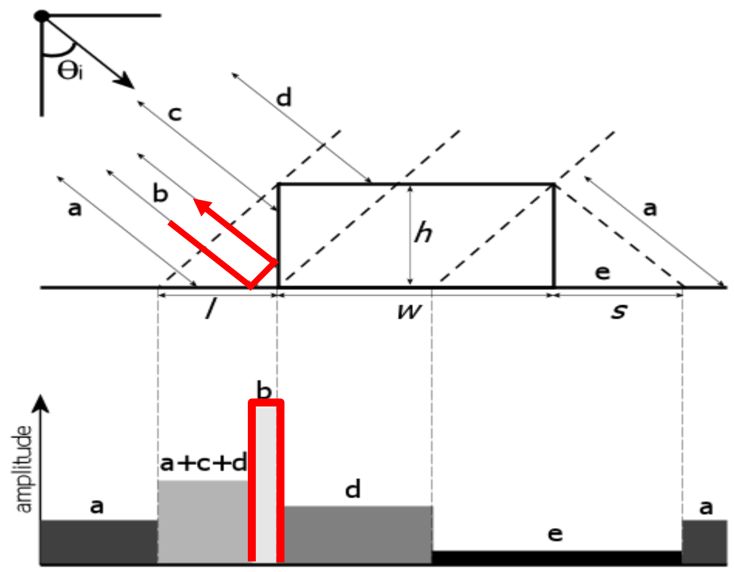

Building EM model

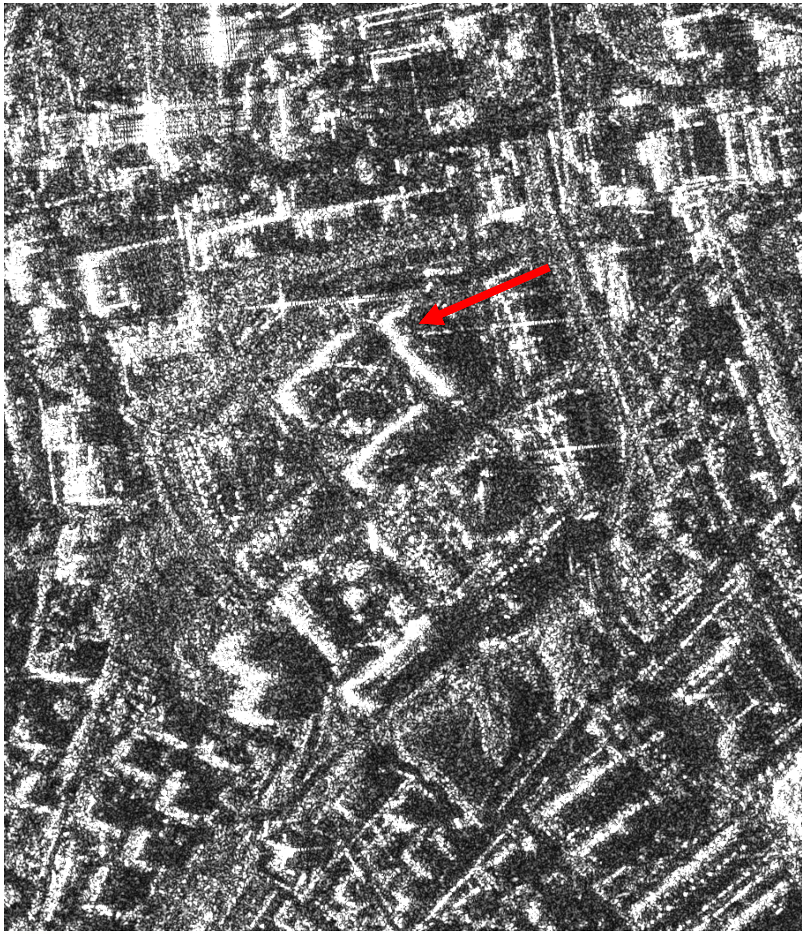

VHR satellite SAR image

Building Detection: Primitives and Semantic

Despeckled image

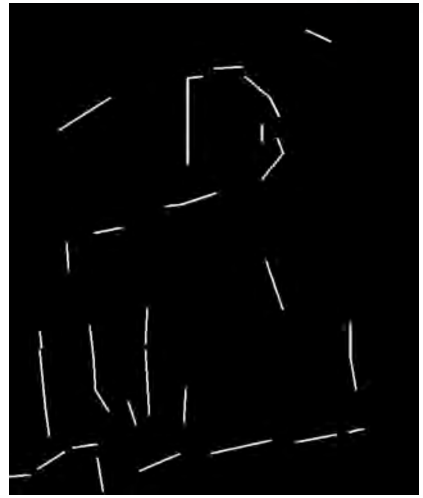

Detected lines

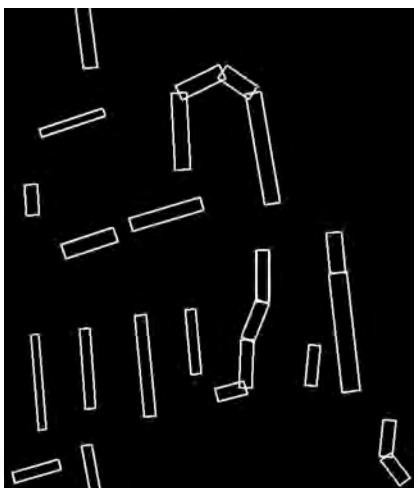

Detected bright areas

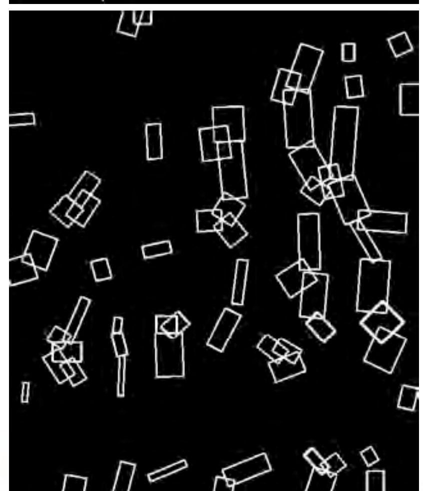

Detected shadow areas

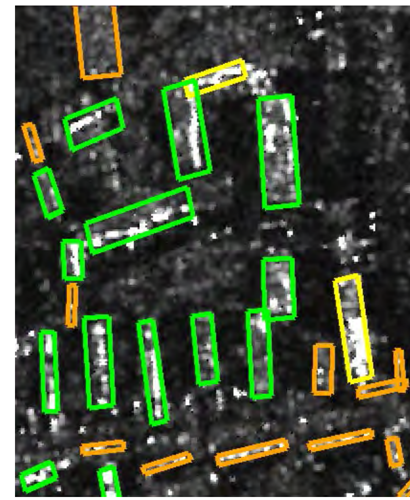

Detected building fooprints

[10] A. Ferro, D. Brunner, L. Bruzzone, “Automatic Detection and Reconstruction of Building Radar Footprints from Single VHR SAR Images”, *IEEE Trans. on Geoscience and Remote Sensing*, 2012

Change Detection in VHR SAR Images

✓ Moving from object detection in single images to object change detection in multitemporal images increases the complexity of the information extraction.

✓ In order to define an effective general approach to change detection for VHR SAR images we have to:

- Decompose the general complex problem in simpler hierarchical problems.
- Exploit the intrinsic multiscale nature of objects present in VHR images.
- Model the specific properties of expected changes for extracting the semantic meaning of backscattering changes.
- Exploit the available prior information on the considered scenario.

Example: Building Change Detection

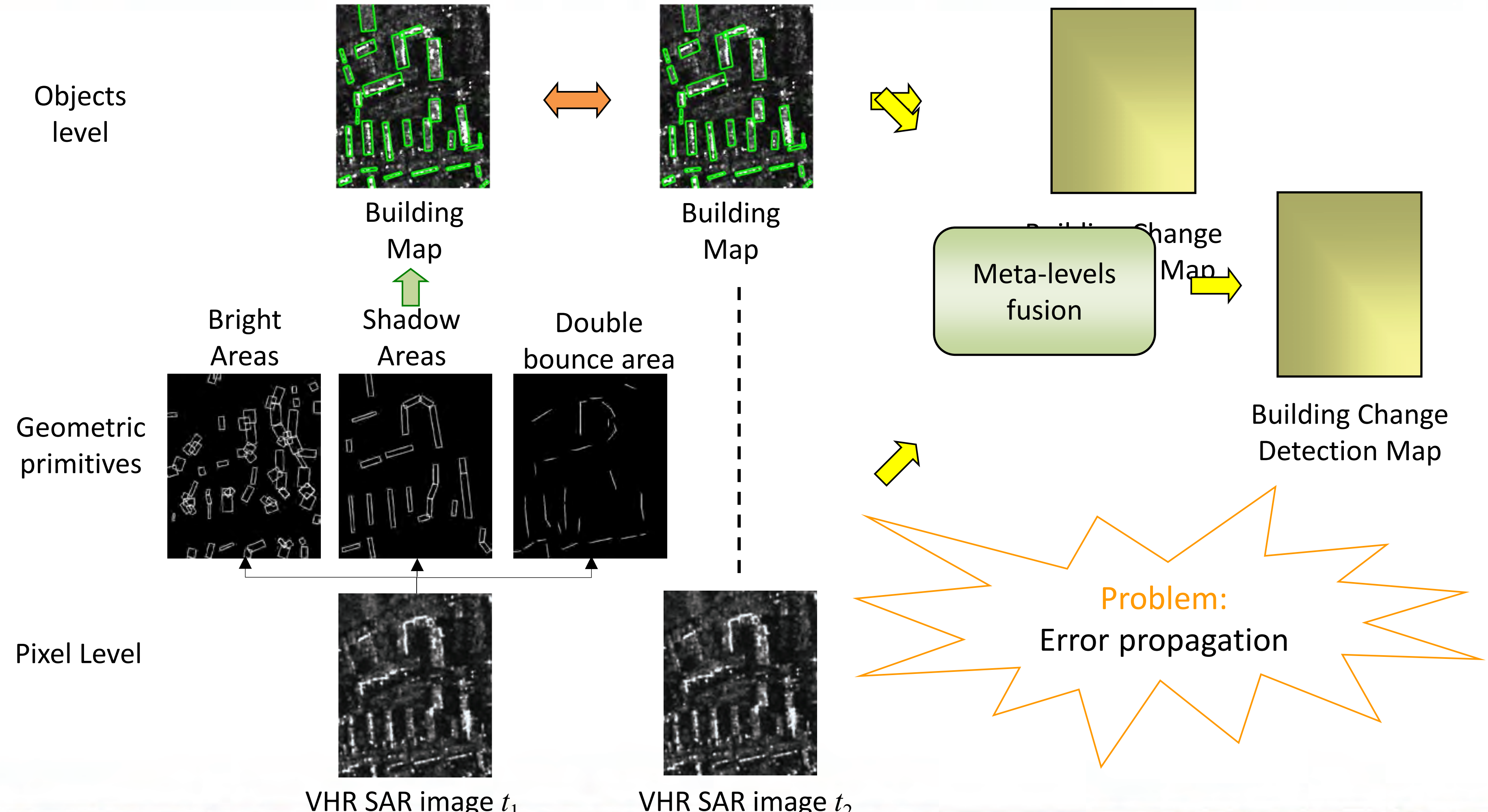

Architecture for Building Change Detection

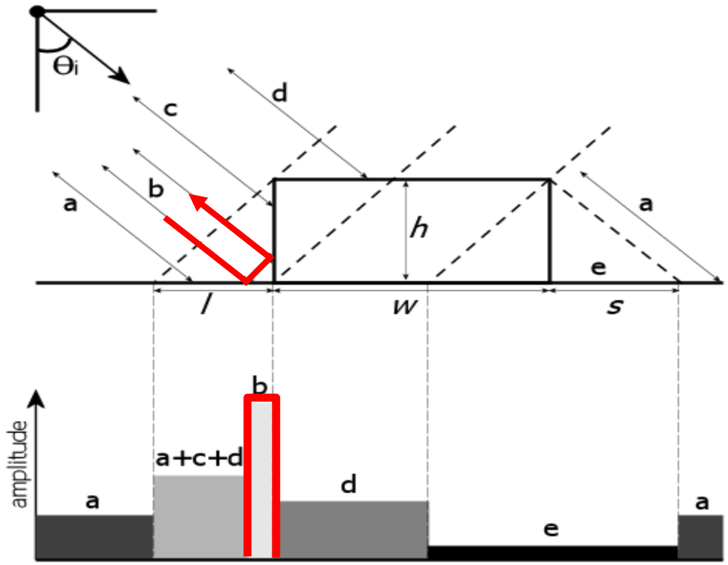

Building EM model

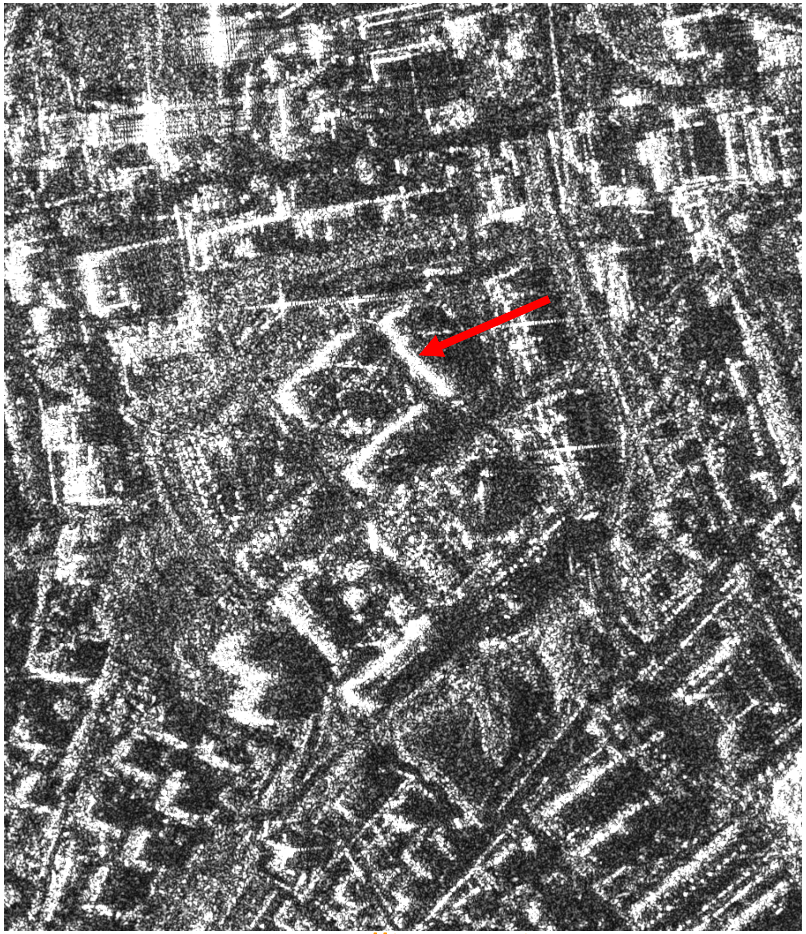

VHR satellite SAR image

Architecture for Building Change Detection

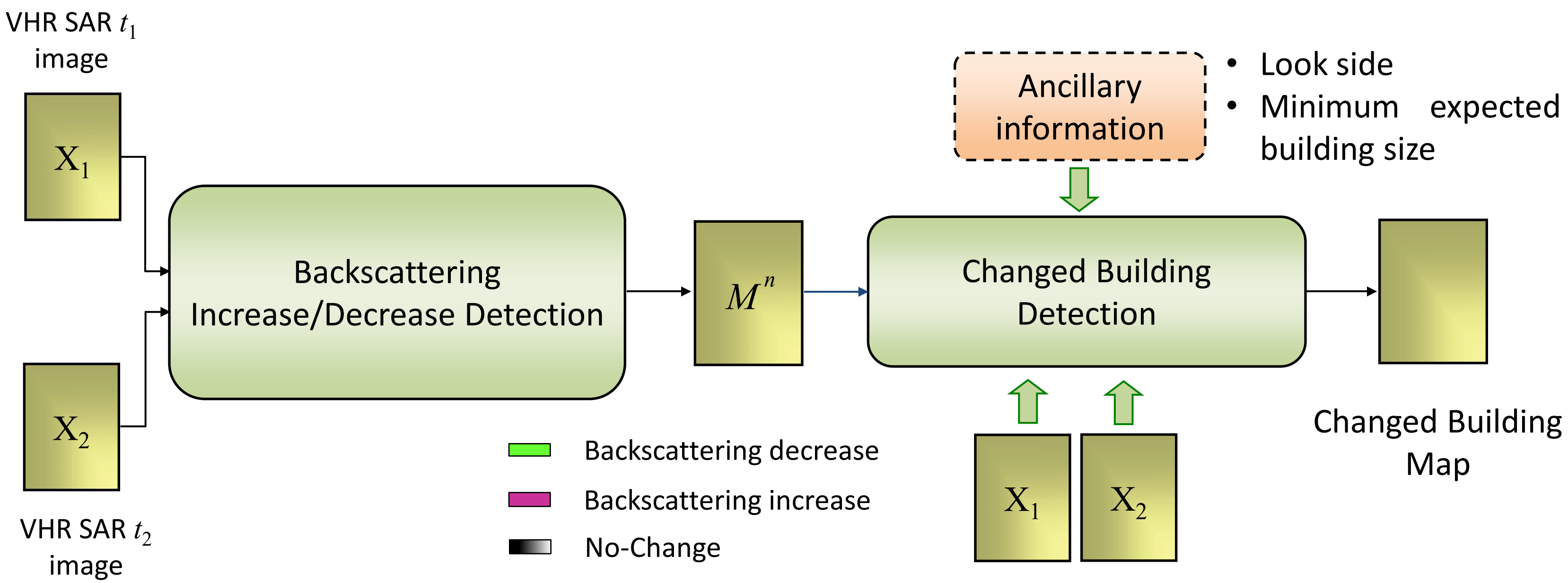

[11] C. Marin, F. Bovolo, L. Bruzzone, Building Change Detection in Multitemporal Very High Resolution SAR Images, IEEE Transactions on Geoscience and Remote Sensing, Vol. 53, 2015, pp. 2664–2682.

[12] F. Bovolo, C. Marin, L. Bruzzone, "A Hierarchical Approach to Change Detection in Very High Resolution SAR Images for Surveillance Applications," IEEE Transactions on Geoscience and Remote Sensing, Vol.51, pp. 2042-2054, 2013.

Architecture for Building Change Detection

Goal: detect changes associated with increase and decrease in backscattering.

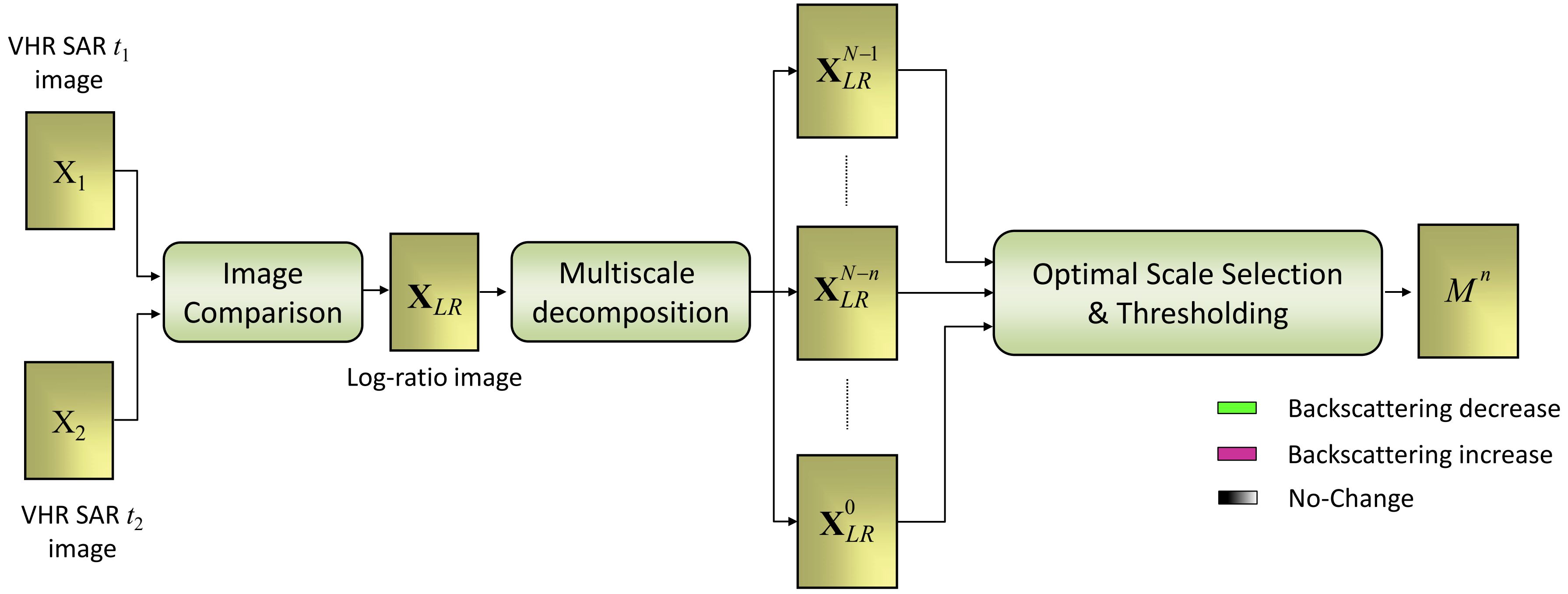

[13] F. Bovolo, L. Bruzzone, "A Detail-Preserving Scale-Driven Approach to Unsupervised Change Detection in Multitemporal SAR Images", IEEE Transactions on Geoscience and Remote Sensing, 2005, Vol.43, No. 12, pp. 2963-2972, December 2005.

Architecture for Building Change Detection

Goal: detect new/destroyed buildings.

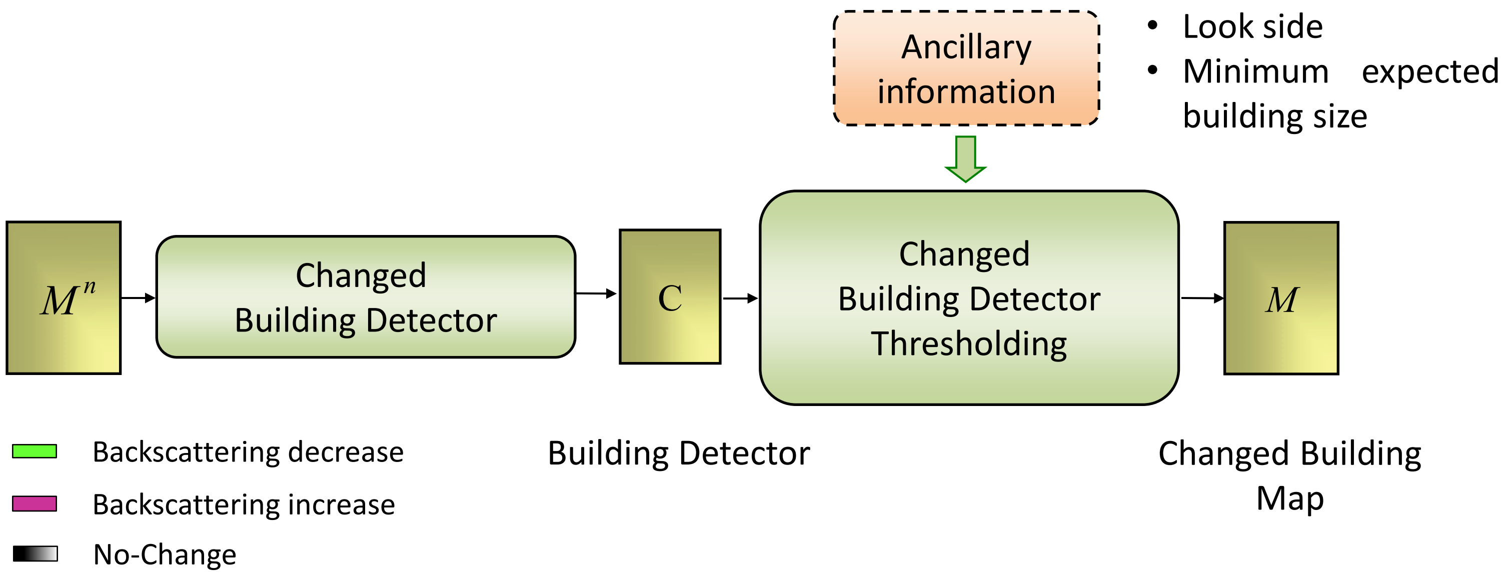

Architecture for Building Change Detection

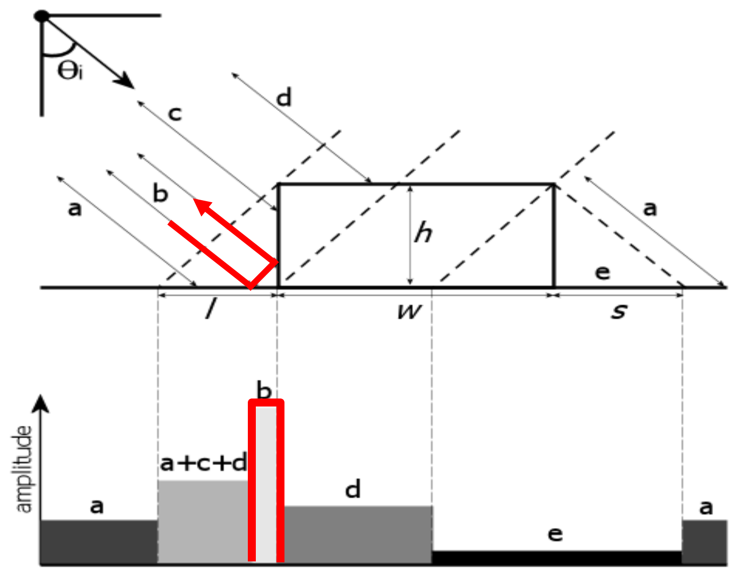

Building EM model

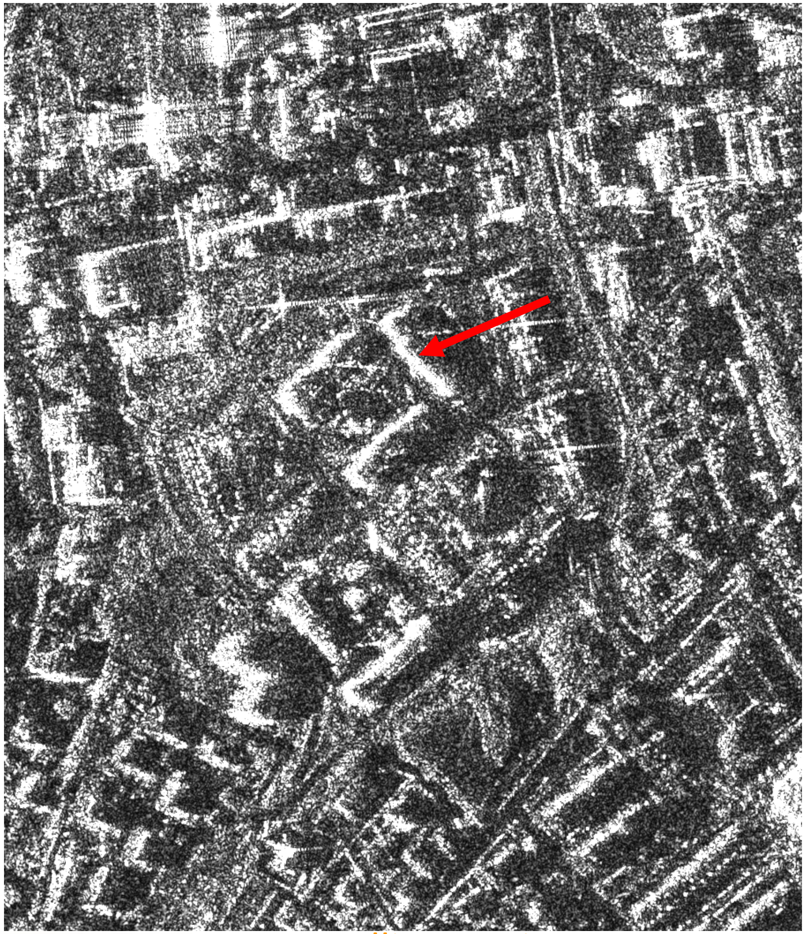

VHR satellite SAR image

Architecture for Building Change Detection

- ✓ Changes in VHR SAR images implies increase or decrease of backscattering values.

- ✓ Changes in buildings (i.e., new/destroyed buildings) implies simultaneous increase and decrease of backscattering.

⇩

Search for pairs of increase/decrease backscattering pattern.

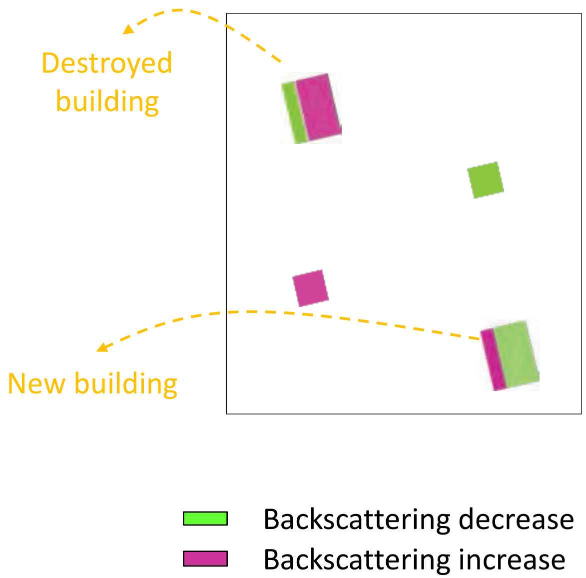

Example: Damage Assessment

New satellite SAR systems COSMO-SkyMed, TerraSAR-X and TanDEM-X can regularly acquire data on the Earth with complementary acquisition modes:

- StripMap (SM): large swath, high to medium geometrical resolution;
- SpotLight (SL): very high geometrical resolution, smaller swath.

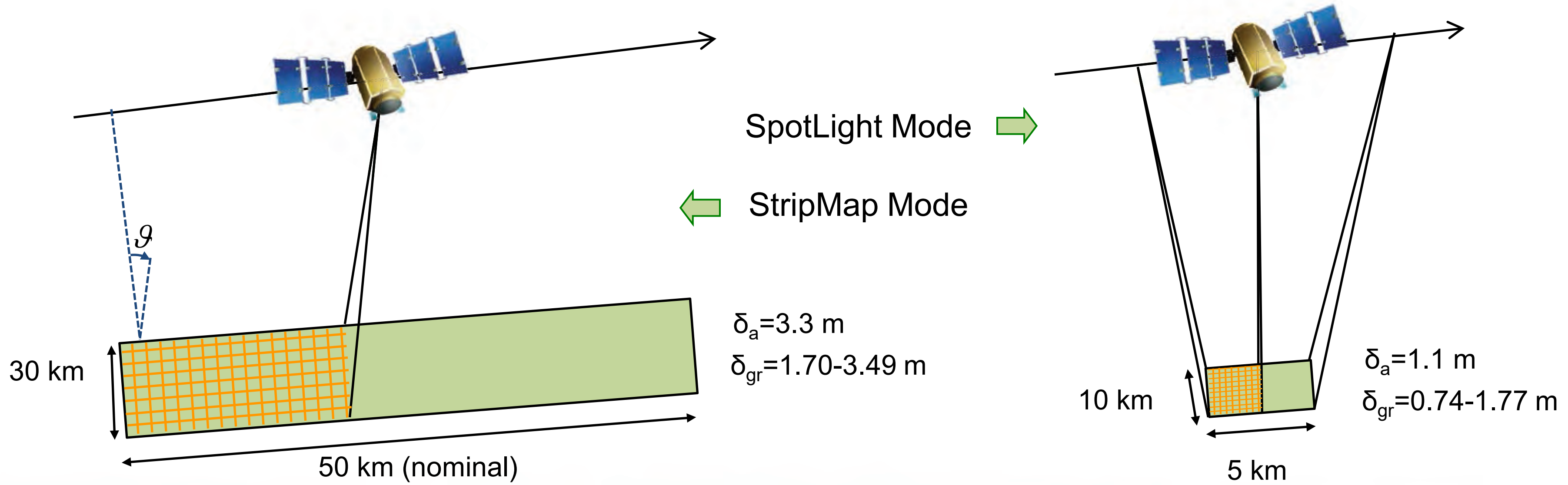

Data referred to TerraSAR-X imaging modes.

Example: Damage Assessment

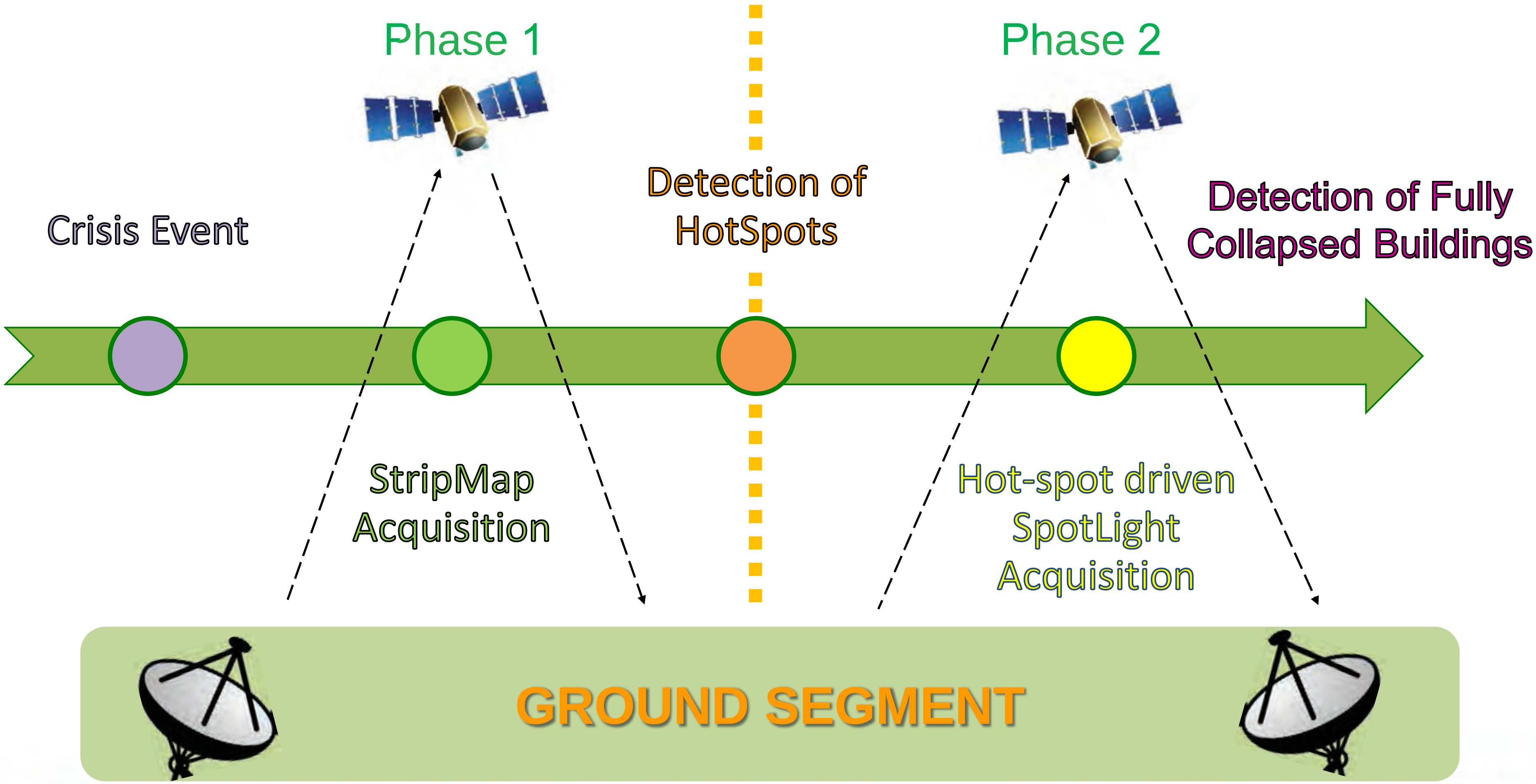

Example: L'Aquila Earthquake (Italy, April 6th, 2009)

Data set: Simulated StripMap (CSK®) images acquired 5th April 2009 and 21st April 2009.

Optical image GeoEye, Tele Atlas 2011
Google ©
April 05, 2009

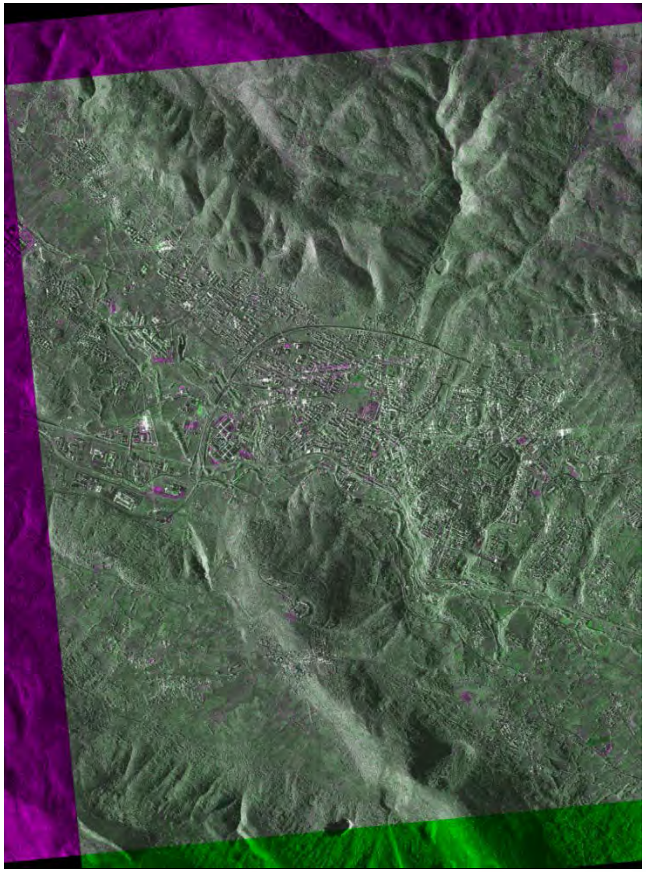

RGB multitemporal composition
(R:04/21/2009, G:04/05/2009, B:04/21/2009)
April 21, 2009

- 5m×5m resolution (Simulated)
- X-band
- 1-look
- Amplitude
- HH-polarization
- 57-58 degree incidence angle
- Ascending orbit
- Right look
- CSKS1
- Calibrated
- Co-registered
- Geo-referred

Backscattering decrease
Backscattering increase
Unchanged areas

Example: L'Aquila Earthquake (Italy, April 6th, 2009)

Wavelet Denoising performed at the 5th level, and split-based thresholding (splits 64x64 pixels).

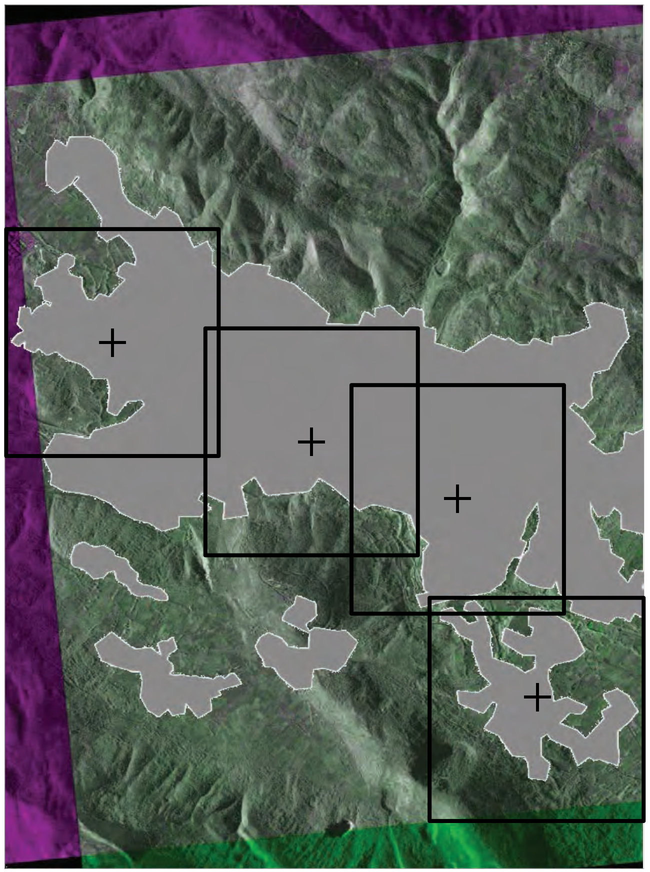

RGB multitemporal composition
(R:04/21/2009, G:04/05/2009, B:21/04/2009)

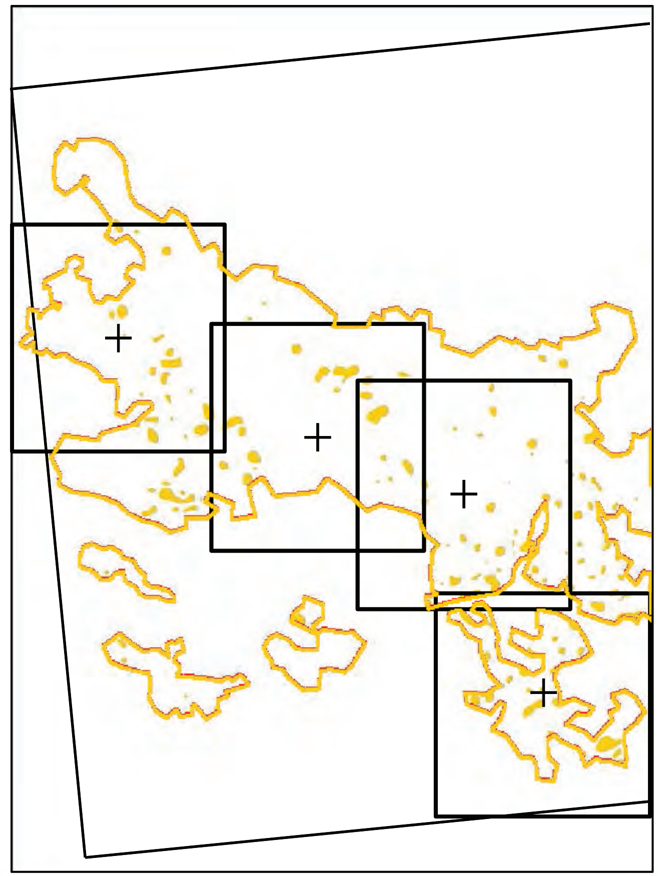

M_{RSM}^{fil}

- 5m×5m resolution (Simulated)
- X-band
- 1-look
- Amplitude
- HH-polarization
- 57-58 degree incidence angle
- Ascending orbit
- Right look
- CSKS1
- Calibrated
- Co-registered
- Geo-referred

Backscattering decrease
Backscattering increase
Unchanged areas
Hot-spots

Example: L'Aquila Earthquake (Italy, April 6th, 2009)

Detection of relevant areas and acquisition of SpotLight images.

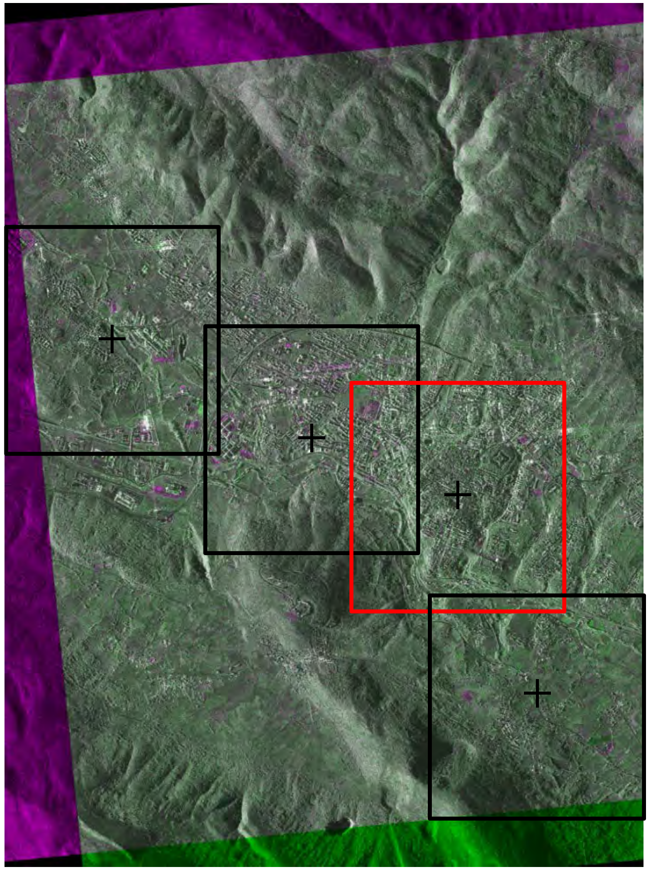

RGB multitemporal composition
(R:04/21/2009, G:04/05/2009, B:21/04/2009)

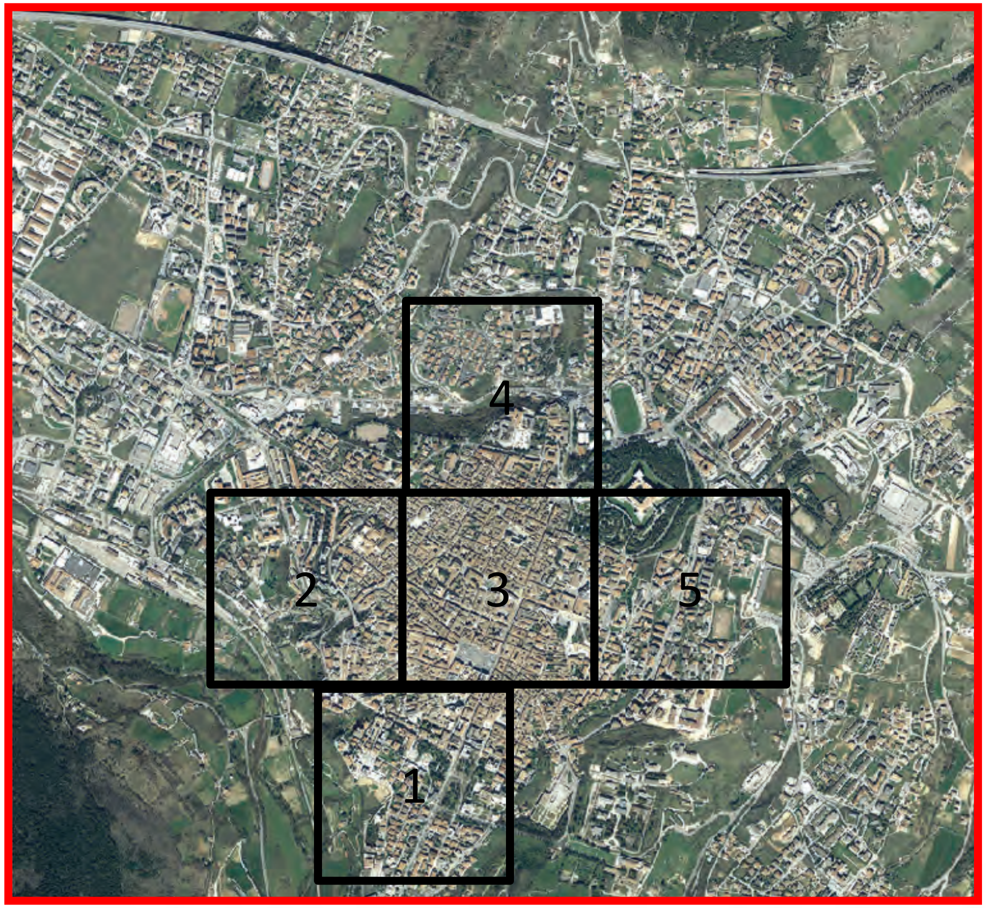

Backscattering decrease Backscattering increase Unchanged areas

Example: L'Aquila Earthquake (Italy, April 6th, 2009)

Multitemporal data set: section (1024×1024 pixels) of two spotlight (CSK®) images acquired before (5th April 2009) and after (12th September 2009) the earthquake of L'Aquila (Italy, 6th April 2009).

Optical image GeoEye, Tele Atlas 2011
Google ©
5th April 2009

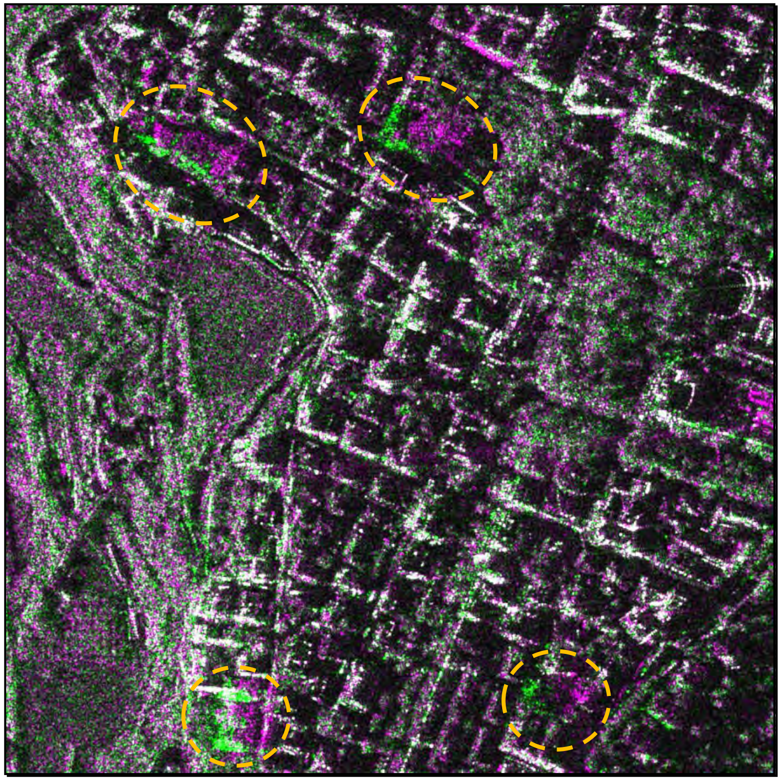

RGB multitemporal composition
(R:09/12/2009, G:04/05/2009, B:09/12/2009)
12th September 2009

- 1m×1m resolution
- X-band
- 1-look
- Amplitude
- HH-polarization
- 57-58 degree incidence angle
- Ascending orbit
- Right look
- CSKS1
- Calibrated
- Co-registered
- Geo-referred

Backscattering decrease | Backscattering increase | Unchanged areas

Example: L'Aquila Earthquake (Italy, April 6th, 2009)

Increase and decrease of backscattering performed automatically after Curvelet denoising.

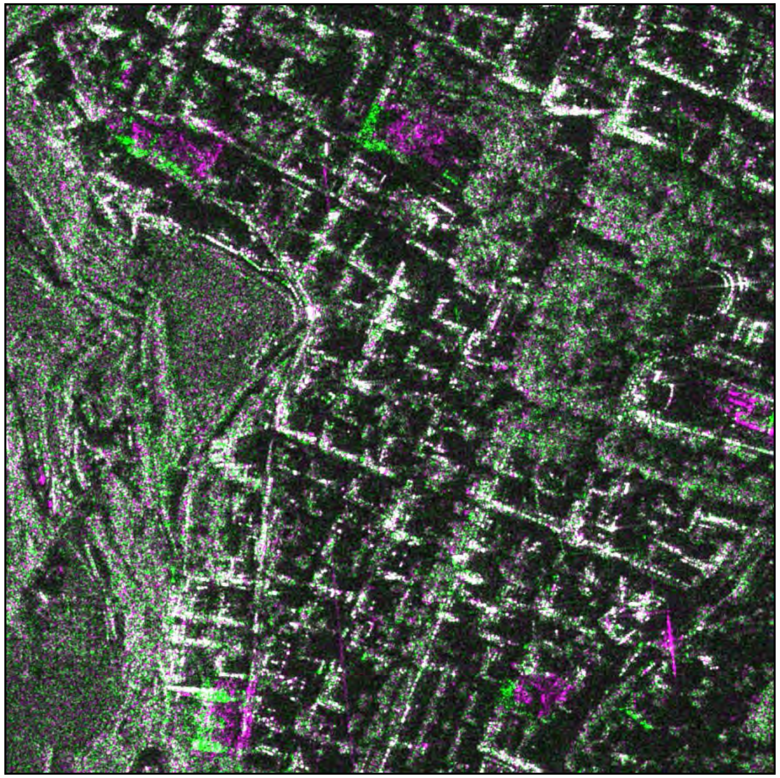

RGB multitemporal composition
(R:09/12/2009, G:04/05/2009, B:09/12/2009)

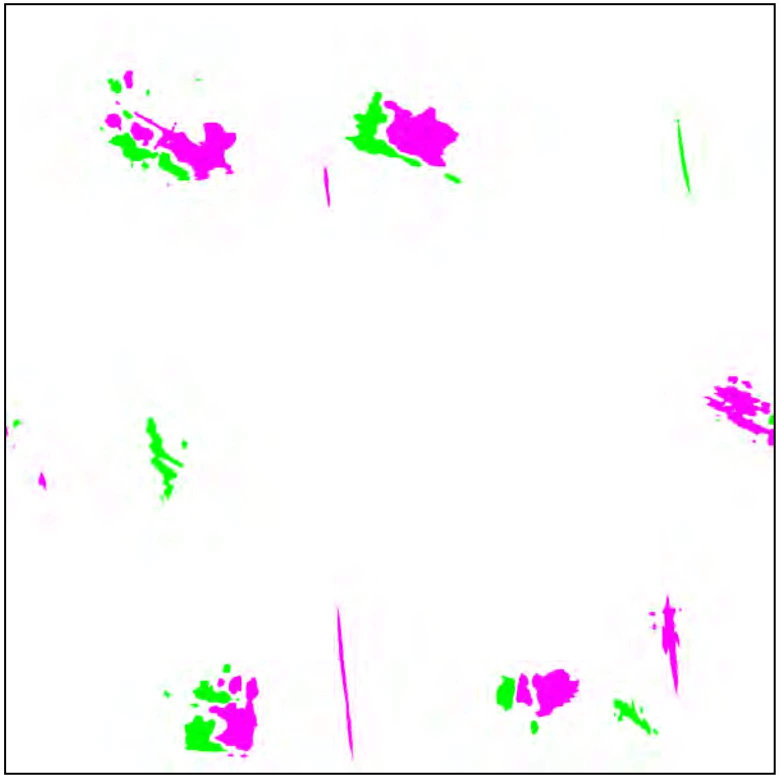

M_{SL}

- 1m×1m resolution
- X-band
- 1-look
- Amplitude
- HH-polarization
- 57-58 degree incidence angle
- Ascending orbit
- Right look
- CSKS1
- Calibrated
- Co-registered
- Geo-referred

Backscattering decrease   Backscattering increase   Unchanged areas

Example: L'Aquila Earthquake (Italy, April 6th, 2009)

Generation of the VHR building change detection map according to the output of fuzzy rules.

Optical image GeoEye, Tele Atlas 2011
Google ©

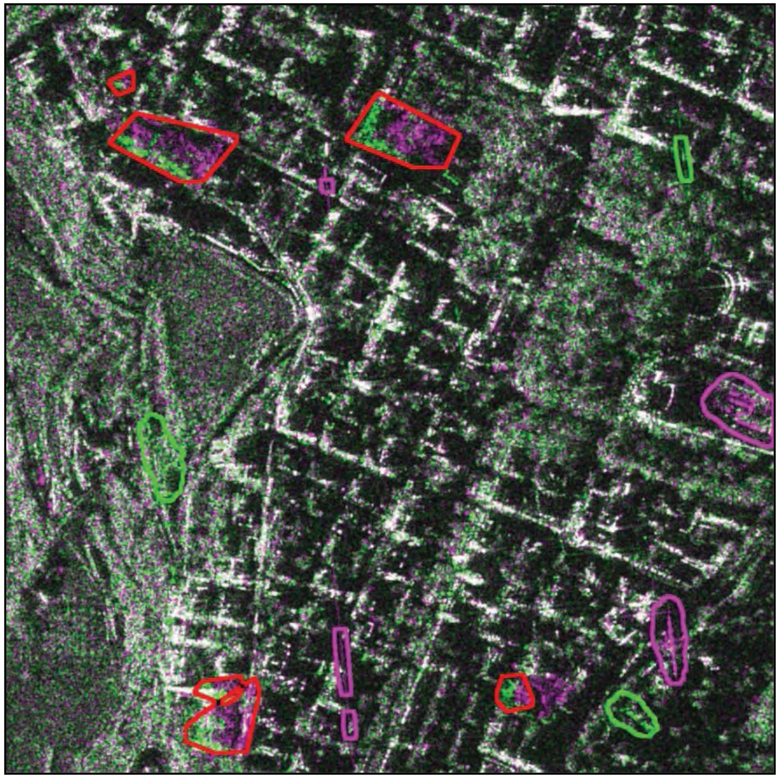

Overlay between RGB and the final buildings change detection map

- 1m×1m resolution
- X-band
- 1-look
- Amplitude
- HH-polarization
- 57-58 degree incidence angle
- Ascending orbit
- Right look
- CSKS1
- Calibrated
- Co-registered
- Geo-referred

Backscattering decrease | Backscattering increase | Collapsed buildings

Example: L'Aquila Earthquake

Pre-Crisis Reference Image

Post-Crisis Reference Image

Optical image Pictometry International Corp © Microsoft Corporation ©

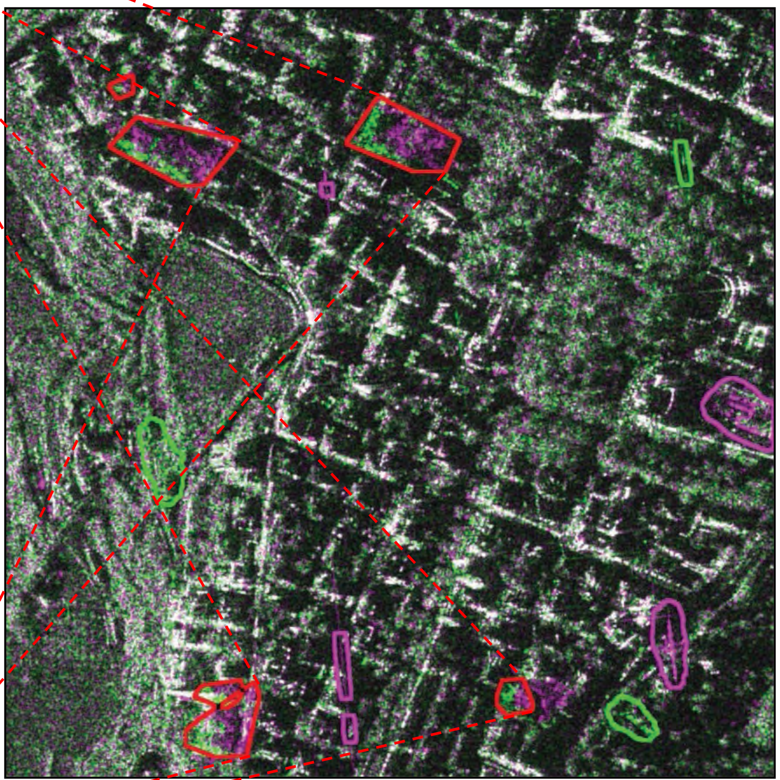

Overlay between RGB and the final buildings change detection map

- 1m×1m resolution
- X-band
- 1-look
- Amplitude
- HH-polarization
- 57-58 degree incidence angle
- Ascending orbit
- Right look
- CSKS1
- Calibrated
- Co-registered
- Geo-referred

Backscattering decrease   Backscattering increase   Collapsed buildings

Example: L'Aquila Earthquake (Italy, April 6th, 2009)

Area	Total # of buildings	Actually destroyed	Missed	False
1	200	7	0	0
2	200	6	2	0
3	400	2	1	1
4	400	0	0	1
5	200	0	0	0
Total	1400	15	3	2

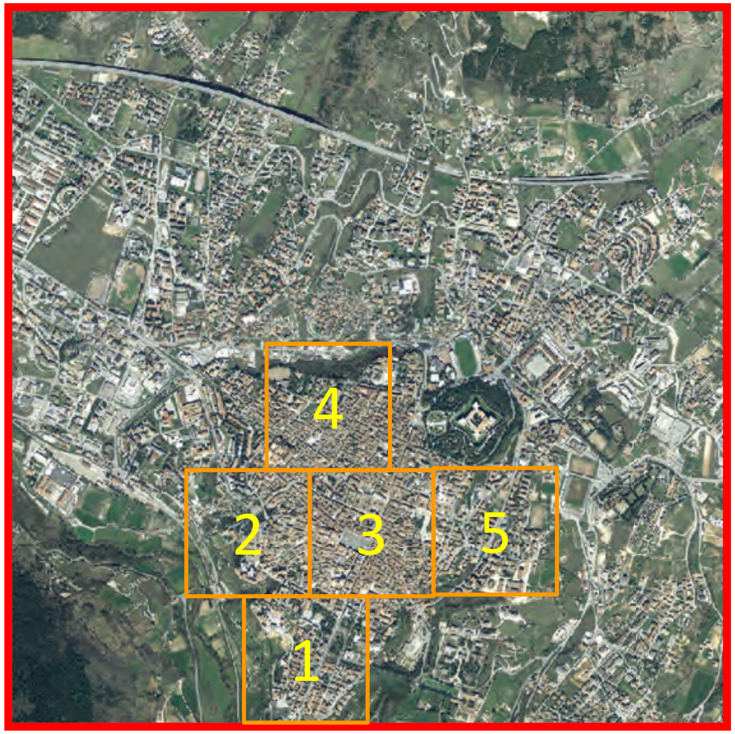

Reference about collapsed buildings derived from airborne orthophotos acquired after the earthquake available at www.regione.abruzzo.it/xcartografia/.

Example: Commercial Port Surveillance (Livorno, Italy)

Data set: section (1920×2880) of 2 spotlight Cosmo-SkyMed (CSK®) images acquired 23rd & 24th April 2010.

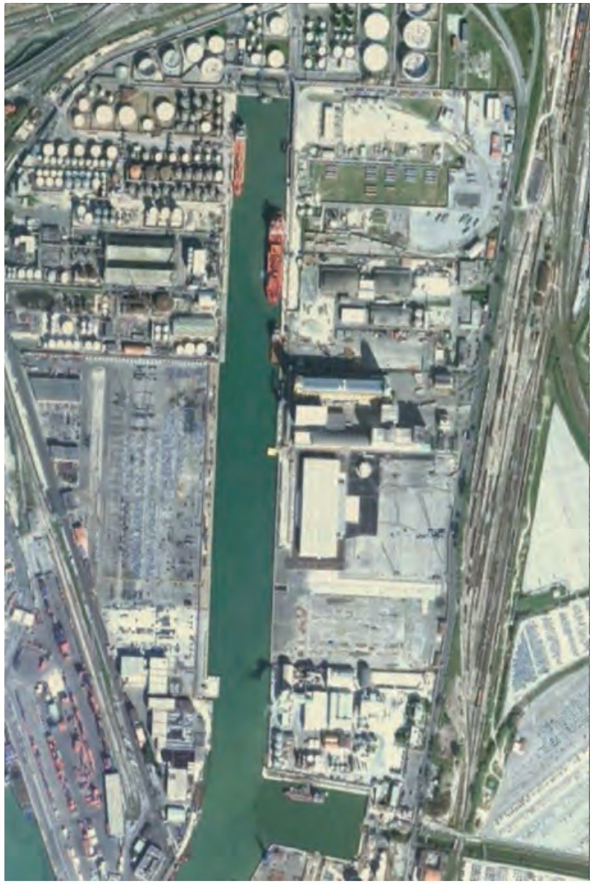

Optical image GeoEye, Tele Atlas 2011 Google ©

23rd April 2010

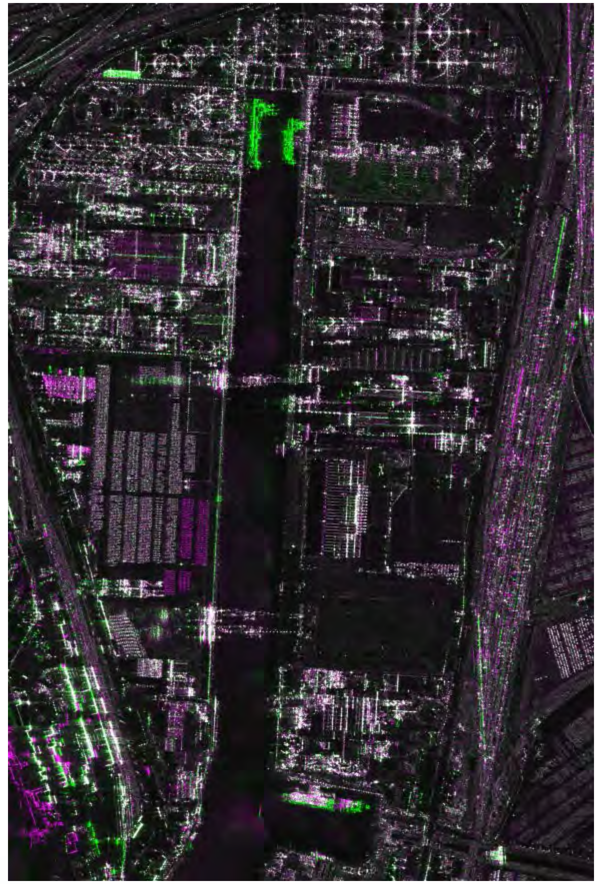

RGB multitemporal composition (R:04/24/2010, G:04/23/2010, B:04/24/2010)

24th April 2010

- 1m×1m resolution
- X-band
- 1-look
- Amplitude
- VV-polarization
- 25-26 degree incidence angle
- Descending orbit
- Right look
- CSKS2 & S3
- Calibrated
- Co-registered

Backscattering decrease

Backscattering increase

Unchanged areas

Example: Commercial Port Surveillance (Livorno, Italy)

Data set: section (1920×2880) of 2 spotlight Cosmo-SkyMed (CSK®) images acquired 23rd & 24th April 2010.

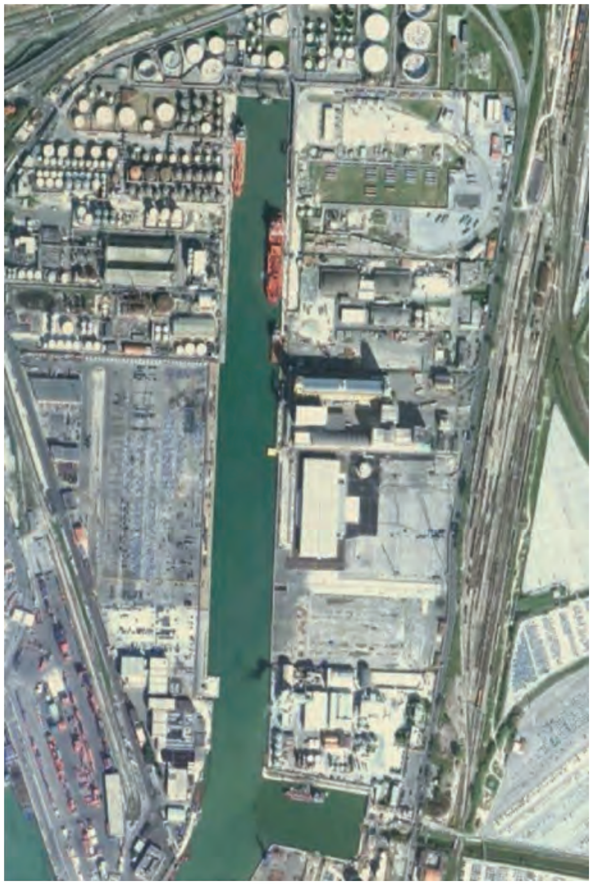

Optical image GeoEye, Tele Atlas 2011
Google ©

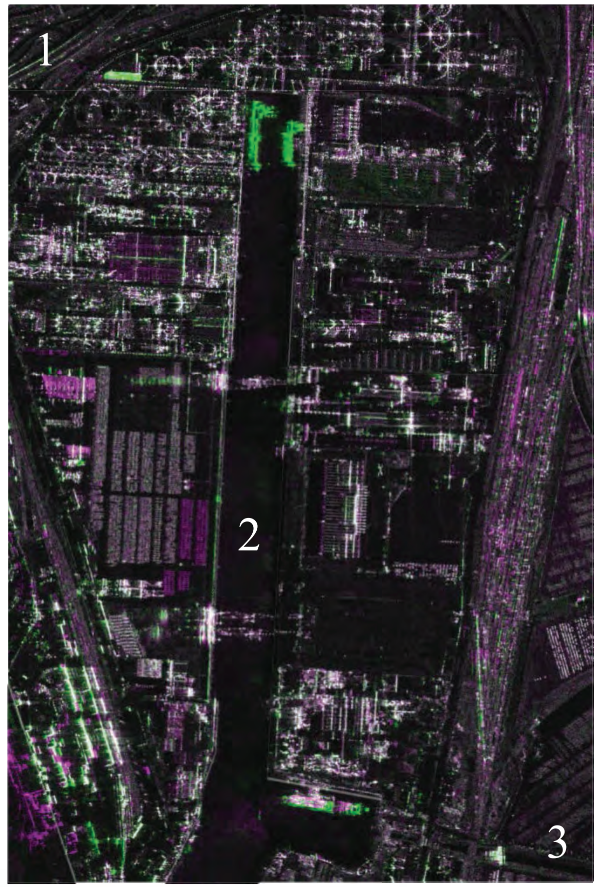

RGB multitemporal composition
(R:04/24/2010, G:04/23/2010, B:04/24/2010)

Prior knowledge on the scene

Areas of interest:

1 Chemical Terminal

2 Wet Dock

3 Cargo Terminal

- Backscattering decrease
- Backscattering increase
- Unchanged areas

Example: Commercial Port Surveillance (Livorno, Italy)

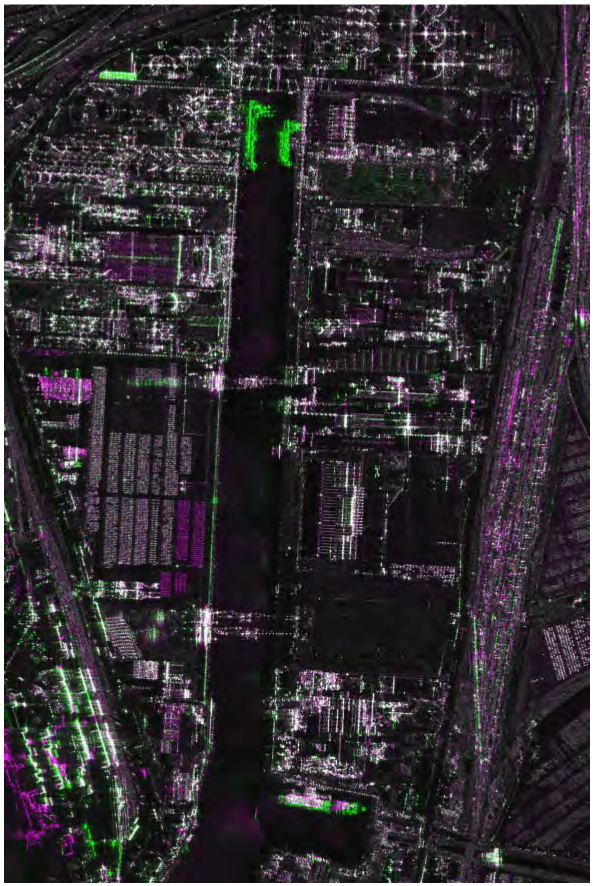

RGB multitemporal composition
(R:04/24/2010, G:04/23/2010, B:04/24/2010)

$C_h^4 \quad h=1,\ldots,H_4,\ H_4=166$

Multiscale decomposition of $\mathbf{X}_{LR}$ has been obtained by:

- ✓ 2D-SWT and 2D-ISWT with an 8-length *Daubechies* filter;
- ✓ N = 5 resolution levels.

Backscattering decrease
Backscattering increase
Unchanged areas
Changed areas

Example: Results on Cargo Terminal

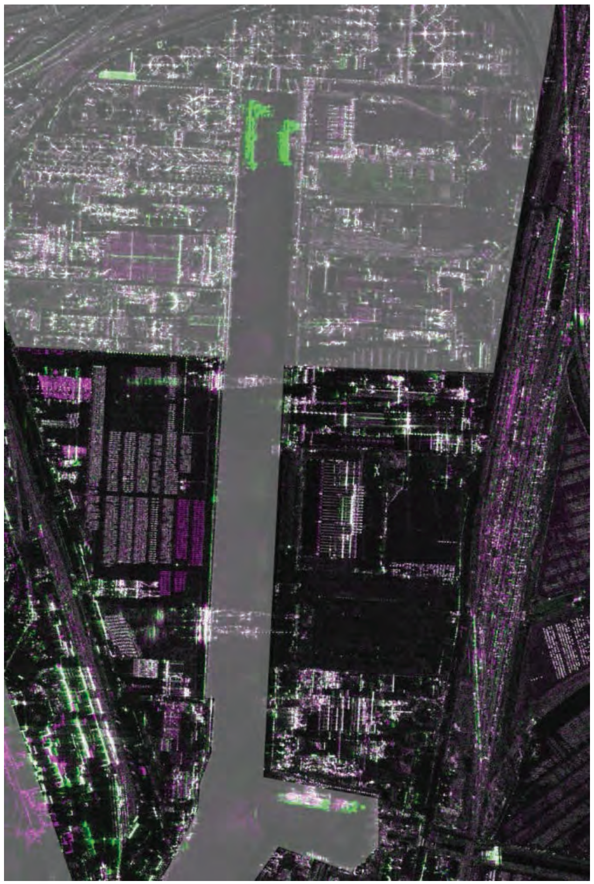

RGB multitemporal composition
(R:04/24/2010, G:04/23/2010, B:04/24/2010)

Changes of interest

- ✓ Movements of vehicles on duty in the terminal (e.g., truck, cars);
- ✓ Movements of containers.

Detector considered for car

- ✓ Build an isolated scatterers map for $\mathbf{X}_1$ and $\mathbf{X}_2$ using [15].

$$r_{PT} = 1 - \min\left(\frac{\mu_1}{\mu_2}, \frac{\mu_2}{\mu_1}\right)$$

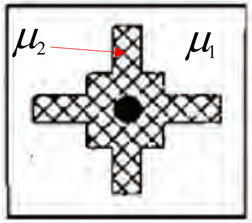

- ✓ Compare the 2 maps according to the logical operator XOR.

[15] A. Lopes, E. Nezry, R. Touzi, and H. Laur, "Structure detection and statistical adaptive speckle filtering in SAR images," *Int. J. Remote Sens.*, vol. 14, pp. 1735–1758, 1993.

Example: Results on Car Movements in Cargo Terminal

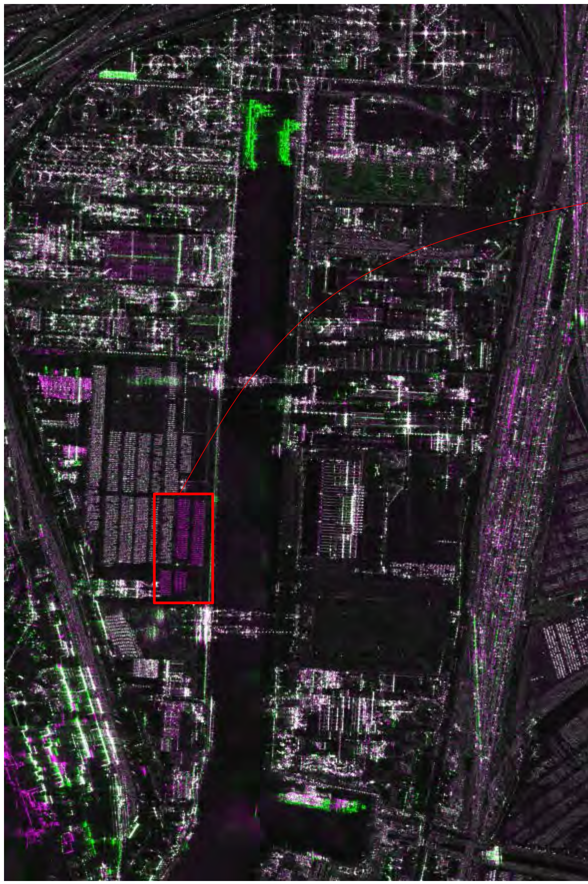

RGB multitemporal composition
(R:04/24/2010, G:04/23/2010, B:04/24/2010)

RGB multitemporal Composition

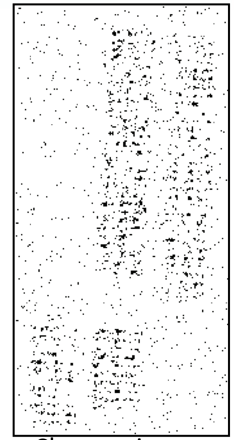

Changes in cars (standard pixel based)

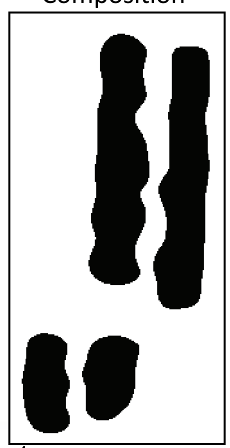

$C_{h^*}^4$ Map of changes

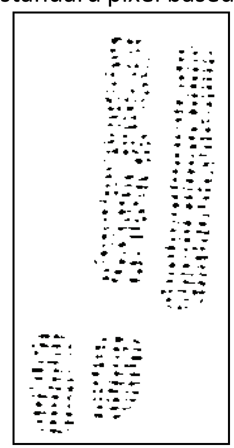

Changes in cars (proposed method)

Number of Changed Cars	
Estimated	284
Reference	249

Example: Results on Wet Dock

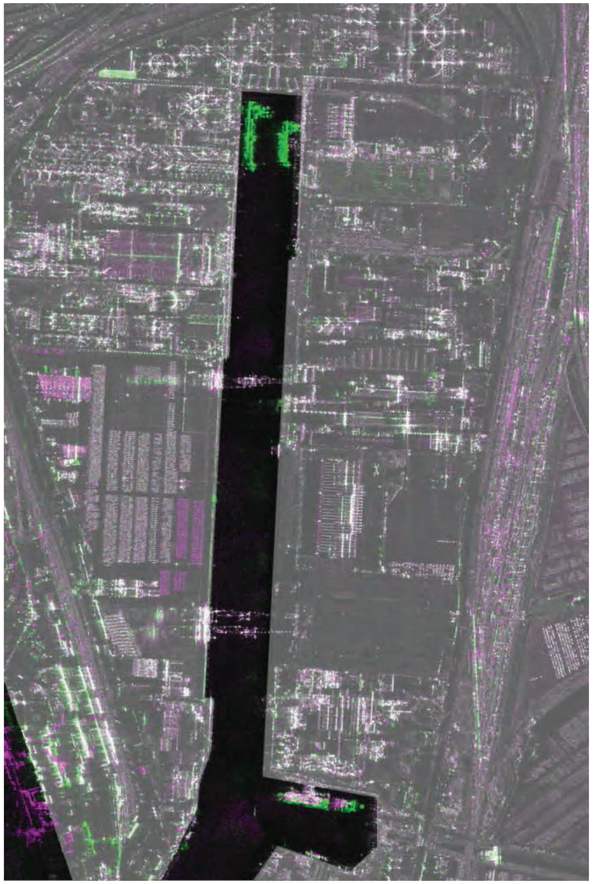

RGB multitemporal composition
(R:04/24/2010, G:04/23/2010, B:04/24/2010)

Changes of interest

- ✓ Movements of cargo ships.

Detector considered

- ✓ Due to the expected size of cargo ships, only thresholding of the log-ratio image at the lowest resolution level $\mathbf{X}_{LR}^{4}$ is performed.

Example: Cargo Ship Movement in the Wet Dock

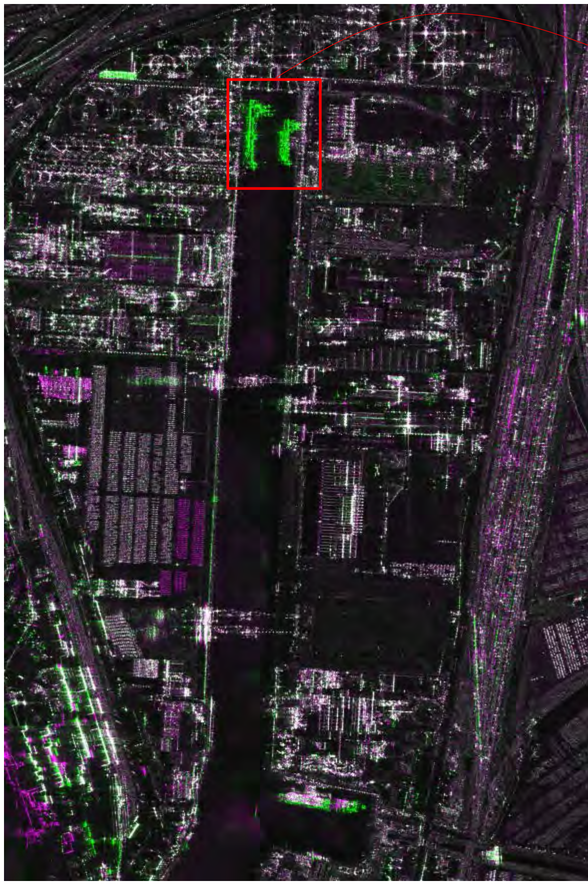

RGB multitemporal composition
(R:04/24/2010, G:04/23/2010, B:04/24/2010)

RGB multitemporal
Composition

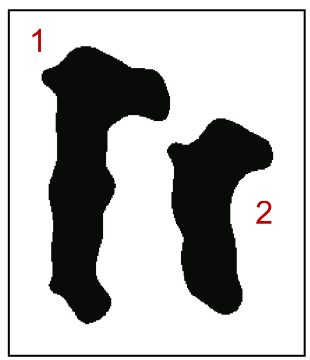

Changes in cargo ships
(Proposed method)

Aspect angle: 6 degrees

Ships	Estimated Length	Reference Length
1	117 m	115 m
2	85 m	83 m

5. Change Detection in Hyperspectral Images

Change Detection in Hyperspectral Images

- ✓ A new generation of Earth observation satellites will be available soon that acquire multitemporal images with high spectral resolution.
- ✓ Differently from the traditional multispectral sensors, hyperspectral sensors measure the solar reflected radiation in a wide wavelength spectrum (e.g., 400-2500nm) at narrow spectral intervals (e.g., 10nm).

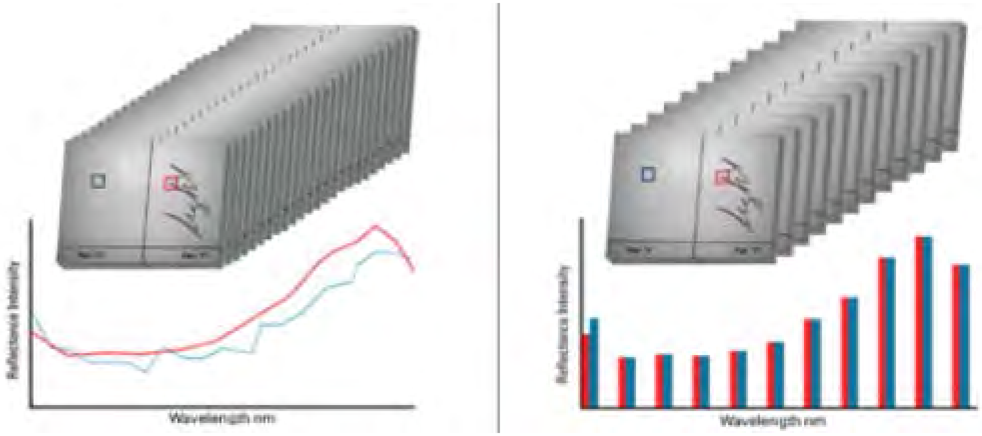

- ✓ Multitemporal hyperspectral data are highly sensitive to detailed variations of the spectral signatures of land covers when multitemporal images are considered, allowing the detection of subtle changes.

Change Detection in Hyperspectral Images

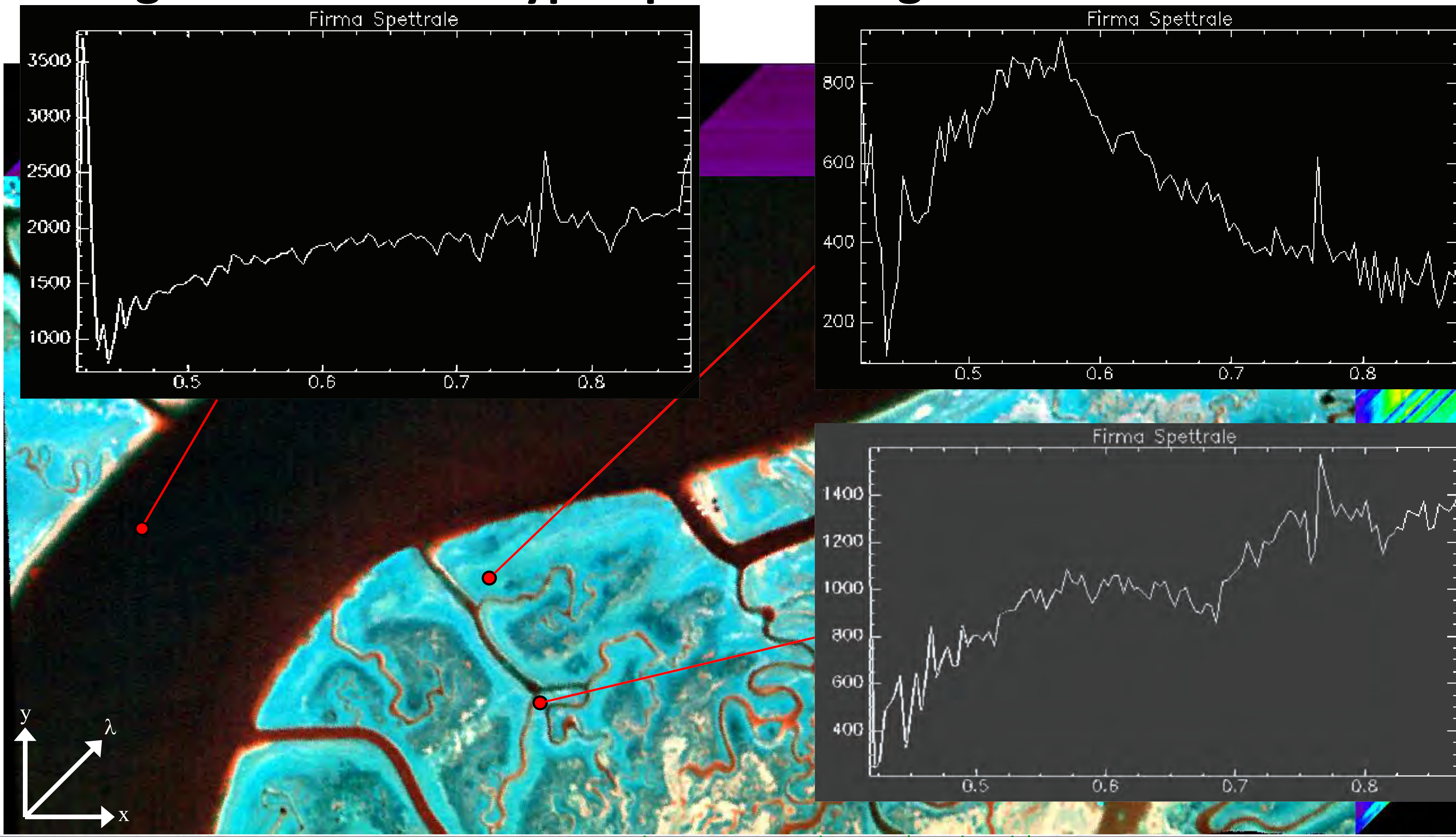

Venice Lagoon, Italy, Hyperspectral Image (115 bands)

Hyperspectral Satellite Missions

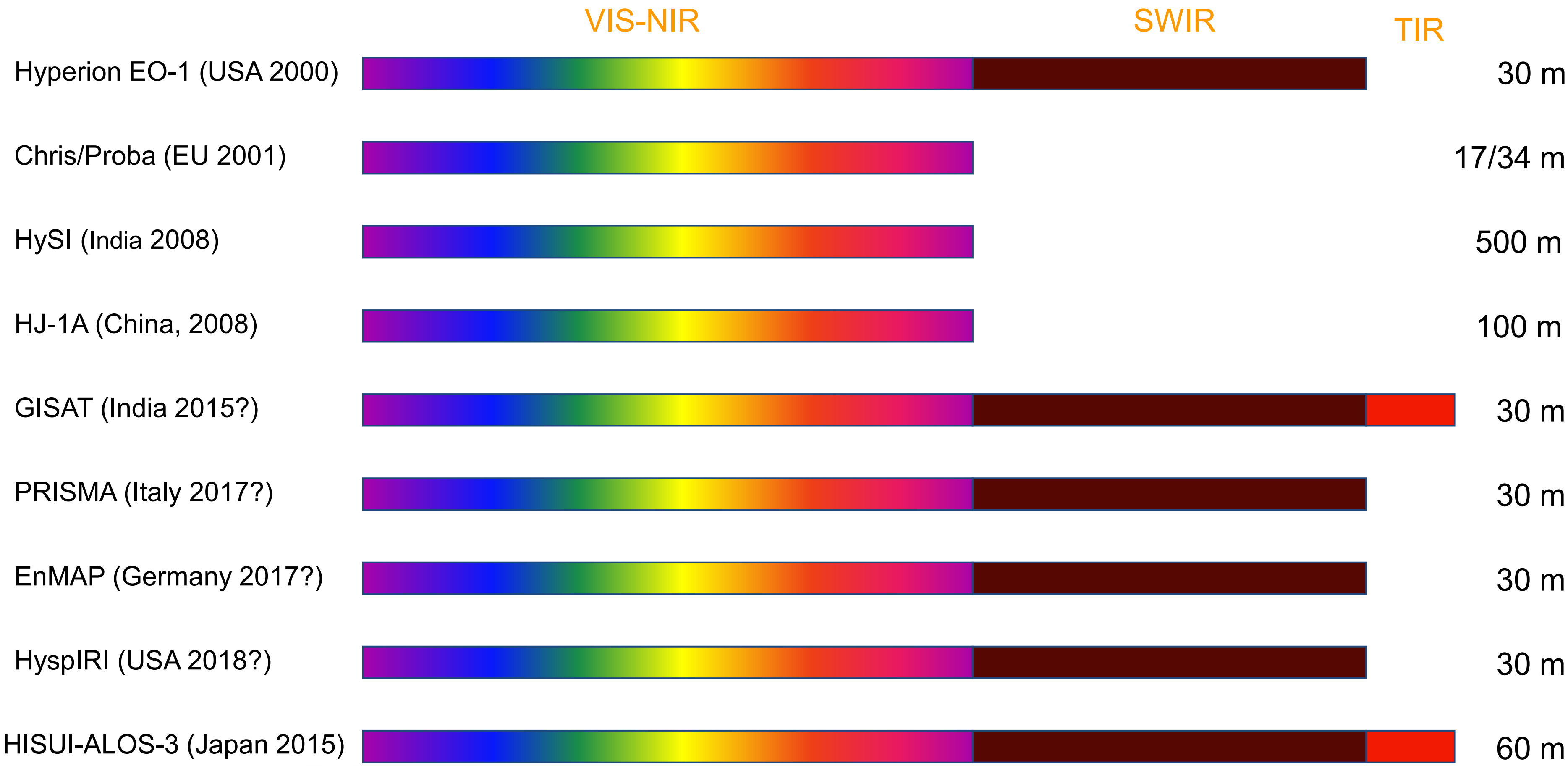

Source of data: IEEE GRSS ISIS Technical Committee

Change Detection in Hyperspectral Images

- ✓ What is a change in multitemporal hyperspectral images?
- ✓ Many atmospheric and ground phenomena may affect the spectral signature in hyperspectral images. A large number of changes may affect the spectral signatures of multitemporal hyperspectral images.
- ✓ They can be classified according to their behaviors in [16]:
  - Major changes: separated by a large spectral difference;
  - Subtle changes: associated with a given major change and showing a small but significant spectral difference among them.
- ✓ Given a specific application, only a part of these changes may be relevant.

[16] S. Liu, L. Bruzzone, F. Bovolo, P. Du, "Hierarchical Unsupervised Change Detection in Multitemporal Hyperspectral Images," IEEE Transactions on Geoscience and Remote Sensing, Vol. 53, pp. 244 - 260, 2015.

Change Detection in Hyperspectral Images

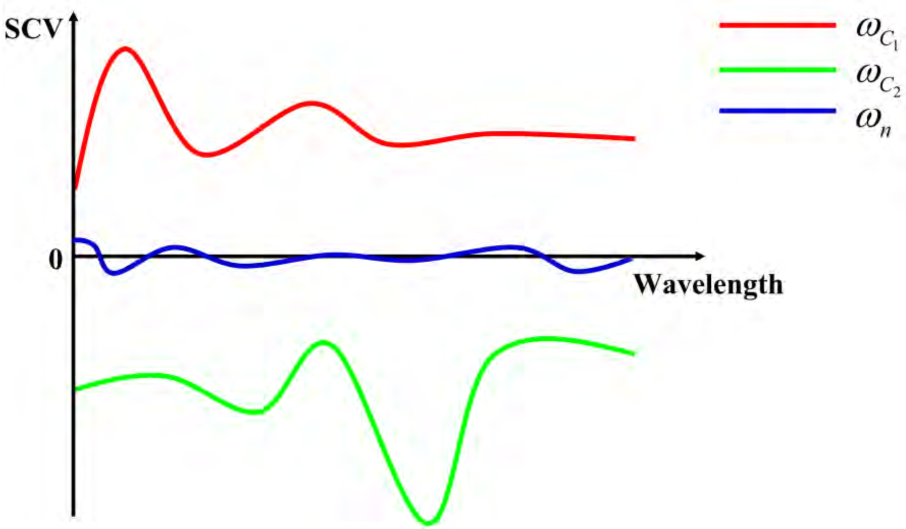

Major changes

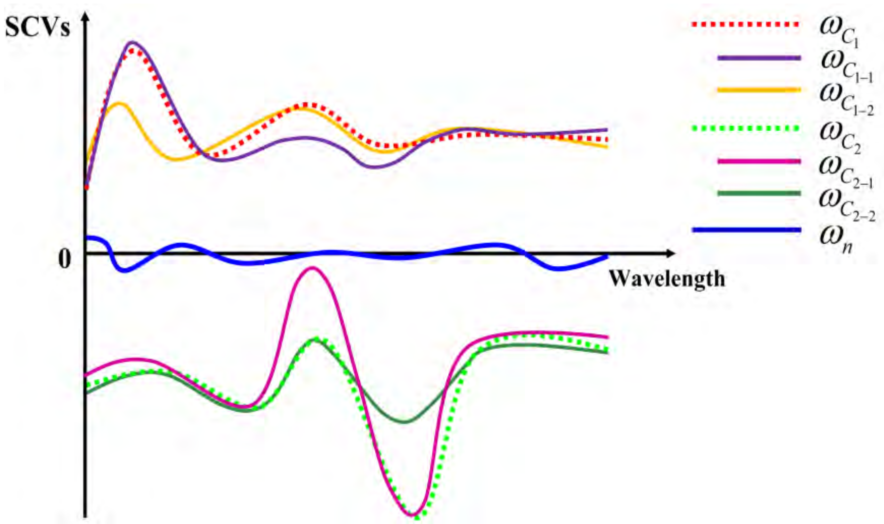

Subtle changes

Change Detection in Hyperspectral Images

- ✓ Unsupervised change detection techniques in hyperspectral images should be able to identify both major and subtle changes.
- ✓ This can be addressed by using hierarchical techniques that:
  - take advantage of the high spectral resolution;
  - identify different kinds of major change;
  - separate subtle changes within the major change class.
- ✓ Few techniques are available in the literature that address this very challenging problem. Examples of recent techniques are given in [17], [18], [19]

[17] S. Liu, L. Bruzzone, F. Bovolo, P. Du, "Hierarchical Unsupervised Change Detection in Multitemporal Hyperspectral Images," *IEEE Transactions on Geoscience and Remote Sensing*, Vol. 53, pp. 244 – 260, 2015.

[18] S. Liu, L. Bruzzone, F. Bovolo, M. Zanetti, P. Du, "Sequential Spectral Change Vector Analysis for Iteratively Discovering and Detecting Multiple Changes in Hyperspectral Images," IEEE Transactions on Geoscience and Remote Sensing, Vol. 53, pp. 4363-4378, 2015.

[19] S. Liu, L. Bruzzone, F. Bovolo, P. Du, "Multitemporal Spectral Unmixing for Change Detection in Hyperspectral Images," IEEE 2014 Int. Geoscience and Remote Sensing Symposium, (IGARSS '15), Milan, Italy, 26-31 July 2015.

Example: CD in Hyperspectral Images

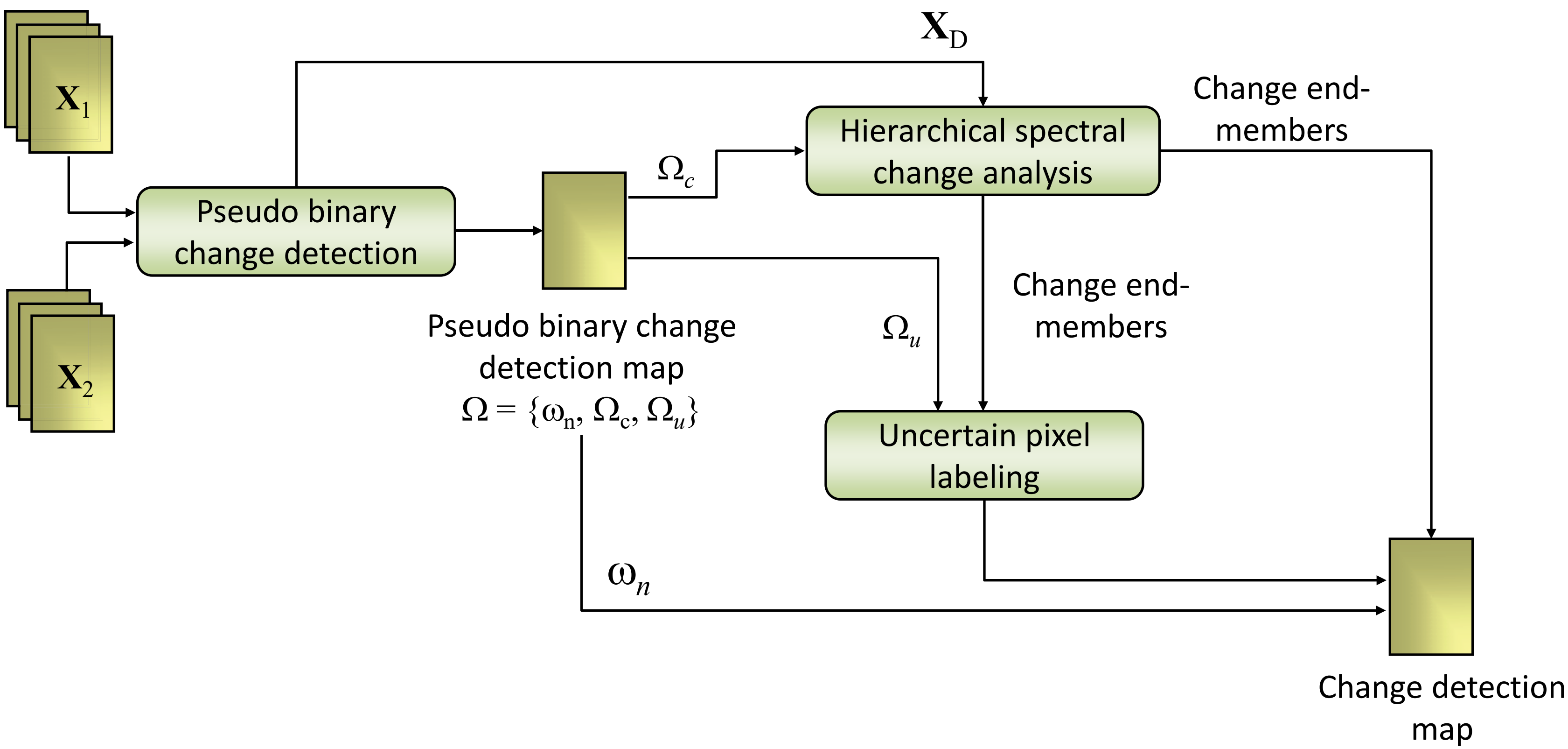

[20] S. Liu, L. Bruzzone, F. Bovolo, P. Du, "Hierarchical Unsupervised Change Detection in Multitemporal Hyperspectral Images," *IEEE Transactions on Geoscience and Remote Sensing, Vol. 53, pp. 244 – 260, 2015.*

Example: CD in Hyperspectral Images

An hierarchical tree that drives the unsupervised change detection can be constructed according to an iterative change analysis procedure.

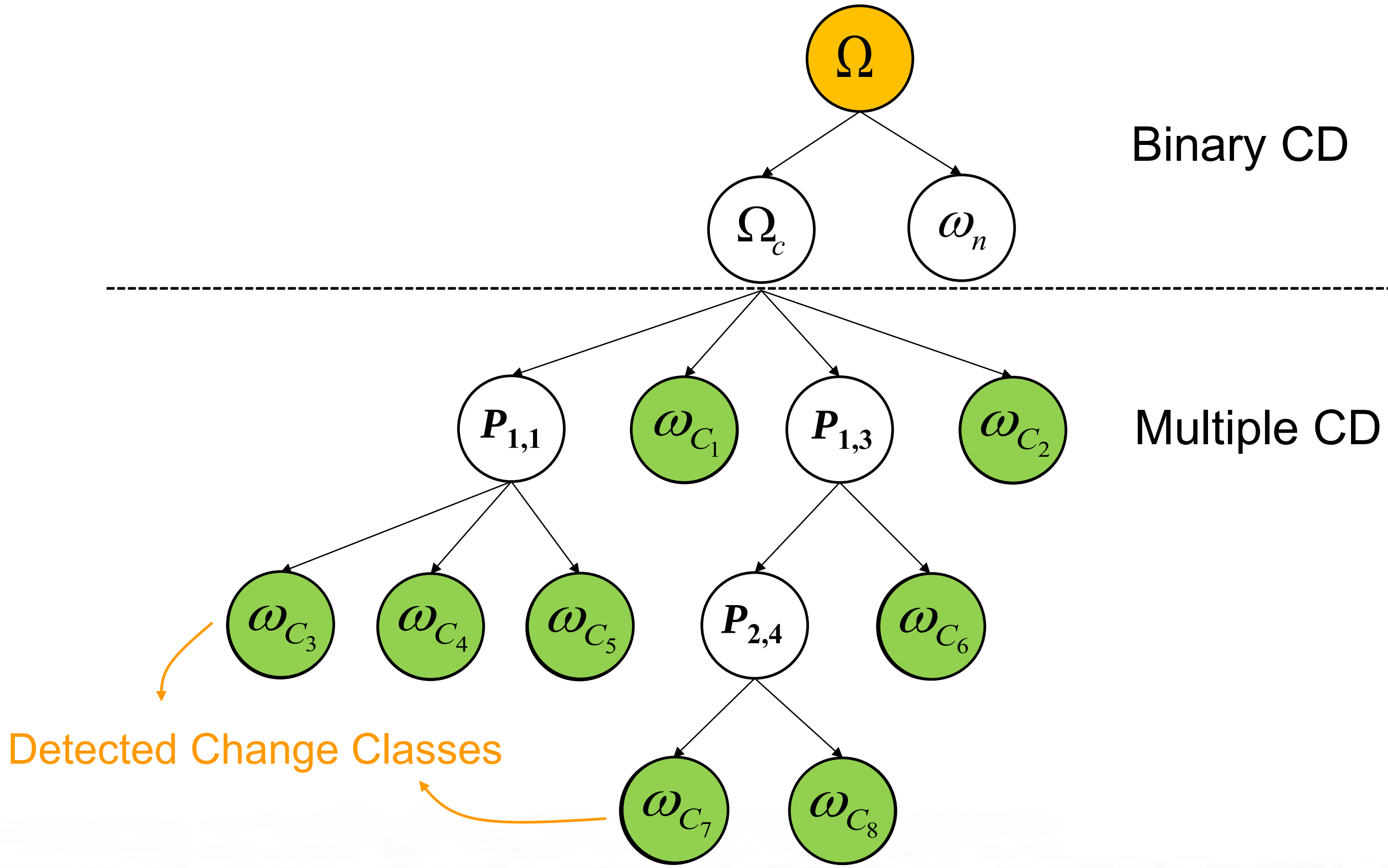

6. Change Detection in Multisensor/Multisource Images

New challenges: Data Fusion

Quickbird image before earthquake

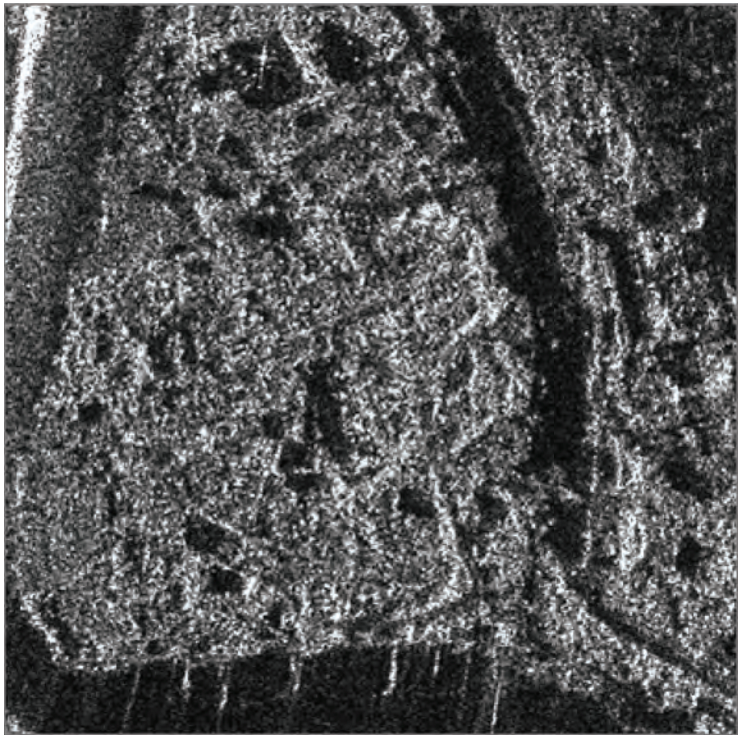

COSMO-Skymed image after earthquake

Earthquake of Sichuan province, China, May, 2008

Top-Down/Bottom-Up Approaches

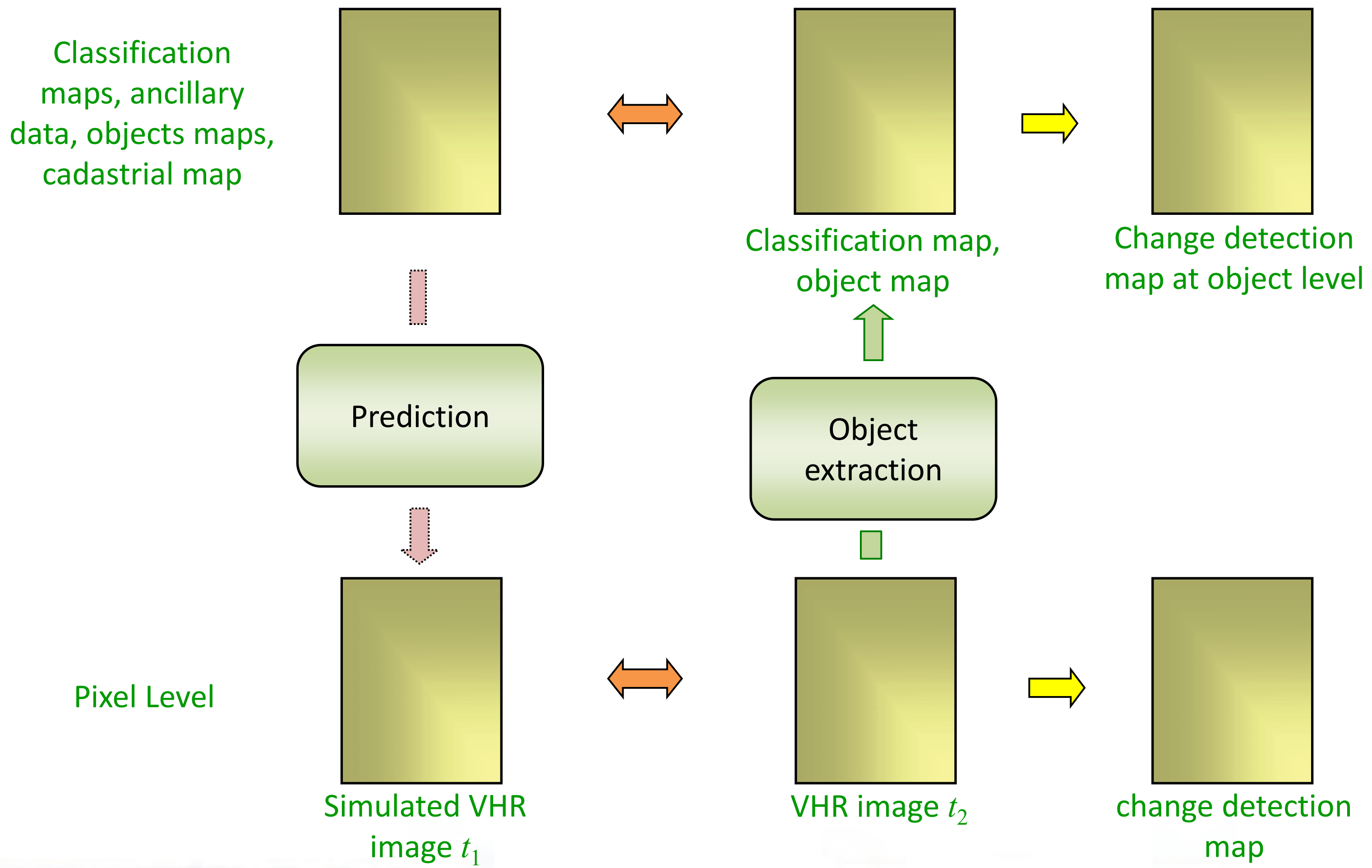

CD in Multisource Data: Example

Bulding Map at t_1

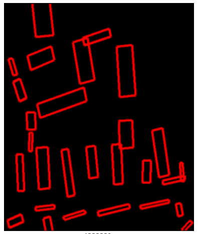

[21] D. Brunner, G. Lemoine, L. Bruzzone, “Earthquake damage assessment of buildings using VHR optical and SAR imagery”, IEEE Transactions on Geoscience and Remote Sensing, Vol. 48, No. 5, pp.2403-2420, 2010.

t_2 SAR incidence angle

Model of the building

Simulation of SAR Building Footprint

Simulated Building footprint at t_1

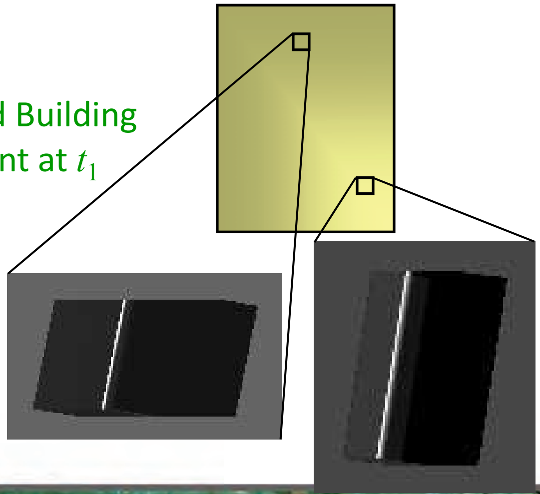

VHR SAR image t_2

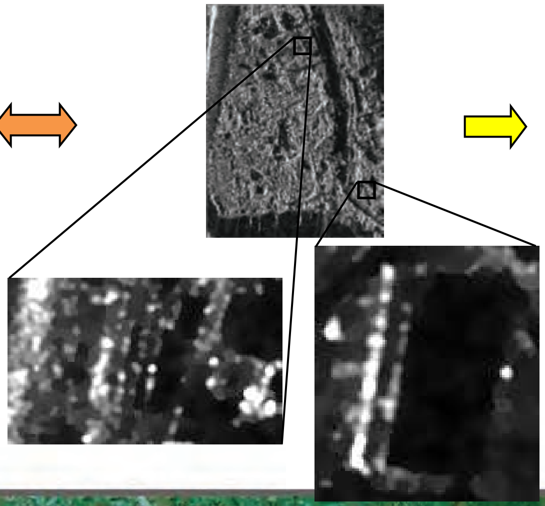

Change Detection Map of Buildings

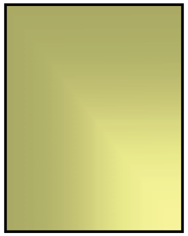

7. Conclusion

Conclusion

✓ Analysis and exploitation of time series and multitemporal images is a very important topic both from the methodological and the application perspective.

✓ Many methodological challenges are related to the properties of new satellite data that require the development of a new generation of processing techniques for the analysis of:

- VHR multispectral and SAR images.
- Hyperspectral images.
- Long time series (data mining).

✓ These properties open the possibility to develop also new applications that exploit either the very high geometrical (e.g. analysis of single buildings) or spectral (e.g. detection of subtle changes) resolution and the increased revisit time (e.g. monitoring and surveillance application).

References: General Change Detection

- A. Singh, “Digital change detection techniques using remotely-sensed data,” *Int. J. Rem. Sens.*, vol. 10, no. 6, pp. 989-1003, 1989.
- J.A. Richards, ”Thematic mapping from multitemporal image data using principal components transformation,” *Rem. Sens. Environ.*, vol. 16, pp. 35-46, 1984.
- T. Fung, “An assessment of TM imagery for land-cover change detection,” *IEEE Trans. Geosci. Rem. Sens.*, vol. 28, no. 12, 681-684, 1990.
- F. Bovolo, L. Bruzzone, “The Time Variable in Data Fusion: A Change Detection Perspective,” IEEE Geoscience and Remote Sensing Magazine, Vol. 3, No. 3, in press.
- Proceeding of Multitemp 2001, Eds: L. Bruzzone and P.C. Smits, World Scientific Publishing Co.: Singapore, ISBN: 981-02-4955-1, Book Code: 4997 hc, pp. 440, 2002.
- Proceeding of Multitemp 2003, Eds: P.C. Smits and L. Bruzzone, World Scientific Publishing Co.: Singapore, ISBN: 981-238-915-6, Book Code: 5582 hc, pp. 387, 2004.
- Proceeding of Multitemp 2005, Eds: R. King, IEEE Press, 2006.
- Proceeding of Multitemp 2007, Eds: P. Coppin, IEEE Press, 2007.
- Proceeding of Multitemp 2009, Eds: D.L. Civco, Curran Associates, Inc. 2009.
- Proceeding of Multitemp 2011, Eds: F. Bovolo, L. Bruzzone, R. King, IEEE Press, 2011.
- Proceeding of Multitemp 2013, IEEE Press, 2013.

References: General Change Detection

- “Special issue on the Analysis of Multitemporal Remote Sensing Images”, IEEE Trans. Geosci. Rem. Sens., November 2003.
- «Special issue on analysis of multitemporal remote sensing data”, *IEEE Transactions on Geoscience and Remote Sensing*, Vol. 51, pp. 1867 - 1869, 2013.
- L. Bruzzone, F. Bovolo, “Unsupervised change detection in multitemporal SAR images” in Signal and Image Processing for Remote Sensing, Ed. C.H. Chen, Taylor & Francis / CRC Press, New York, NY USA, 2007.
- P.R. Coppin, M.E. Bauer, “Digital change detection in forest ecosystems with remote sensing imagery,” Remote Sensing Reviews, vol. 13, 207-234, 1996.
- S.B. Serpico, L. Bruzzone, “Change detection”, in Information Processing for Remote Sensing, Eds: C.H. Chen, World Scientific Publishing Co.: Singapore, Chapter 15, 1999, pp. 319-336.
- D. Lu, P. Mausel, E. Brondízio and E. Moran, “Change detection techniques,” Int. J. Rem. Sens., vol. 25, no. 12, pp. 2365-2407, Jun. 2004.
- R.J. Radke, S. Andra, O. Al-Kofahi and B. Roysam, “ Image Change Detection Algorithms: A Systematic Survey,” IEEE Trans. Image Proc., vol. 14, no. 3, pp. 294 - 307, Mar. 2005.
- L. Bruzzone, F. Bovolo, “A Novel Framework for the Design of Change-Detection Systems for Very-High-Resolution Remote Sensing Images,” *Proceedings of the IEEE*, Vol. 101, pp. 609-630, 2013.

References: Binary Change Detection

- L. Castellana, A. D'Addabbo, G. Pasquariello, "A composed supervised/unsupervised approach to improve change detection from remote sensing," *Pattern Recogn. Lett.,* vol.28, no.4, pp.405-413, 2007.
- T. Fung and E. Le Drew, "The determination of optimal threshold levels for change detection using various accuracy indices," Photogram. Eng. Rem. Sens., vol. 54, no. 10, pp. 1449-1454, 1988.
- J.B. Collins and C.E. Woodcock, "Change detection using the Gram-Schmidt transformation applied to mapping forest mortality," Rem. Sens. Environ., vol. 50, pp. 267-279, 1994.
- L. Bruzzone, D. Fernández Prieto, "An adaptive parcel-based technique for unsupervised change detection", Int. J. Rem. Sens., Vol. 21, No. 4, 10 March 2000, pp. 817-822.
- L. Bruzzone, D. Fernández Prieto, "Automatic analysis of the difference image for unsupervised change detection", IEEE Trans. Geosci. Rem. Sens., Vol. 38, No.3, May 2000, pp. 1171-1182.
- A.A. Nielsen, K. Conradsen, and J.J. Simpson, "Multivariate Alteration Detection (MAD) and MAF Postprocessing in Multispectral, Bitemporal Image Data: New Approaches to Change Detection Studies," Rem. Sens. Environ., vol. 64, pp. 1-19, 1998.
- F. Bovolo, L. Bruzzone, "A Detail-Preserving Scale-Driven Approach to Unsupervised Change Detection in Multitemporal SAR Images", IEEE Trans. Geosci. Rem. Sens., 2005, Vol.43, No. 12, Dec. 2005.
- J. Inglada and G. Mercier, "A new statistical similarity measure for change detection in multitemporal SAR images and its extension to multiscale change analysis," IEEE Trans. Geosci. Rem. Sens., vol. 45, pp. 1432-1445, 2007.

References: Binary Change Detection

- P.L. Rosin and E. Ioannidis, “Evaluation of global image thresholding for change detection,” Pattern Recog. Lett., Vol. 24, pp. 2345-2356, 2003.
- D.M. Muchoney and B.N. Haack, “Change detection for monitoring forest defoliation,” Photogram. Eng. Rem. Sens., Vol. 60, pp. 1243–1251, 1994
- Y. Bazi, L. Bruzzone, F. Melgani, “An unsupervised approach based on the generalized Gaussian model to automatic change detection in multitemporal SAR images,” IEEE Trans. Geosci. Rem. Sens., vol. 43, No. 4, pp. 874-887, 2005.
- J. Inglada, and G. Mercier, “A New Statistical Similarity Measure for Change Detection in Multitemporal SAR Images and Its Extension to Multiscale Change Analysis,” IEEE Trans. Geosci. Rem. Sens, vol. 45, no. 5, pp. 1432-1445, 2007.
- Y. Bazi, L. Bruzzone, F. Melgani, “Automatic Identification of the Number and Values of Decision Thresholds in the Log-ratio Image for Change Detection in SAR Images,” IEEE Geosci. Rem. Sens. Lett., Vol. 3, No. 3, pp. 349- 353, 2006.
- L. Bruzzone, D. Fernández Prieto, “A minimum-cost thresholding technique for unsupervised change detection”, Int. J. Rem. Sens., Vol. 21, No. 18, pp. 3539-3544, 2000.

References: Binary Change Detection

- S. Ghosh, L. Bruzzone, S. Patra, F. Bovolo e A. Ghosh, “A Context-Sensitive Technique for Unsupervised Change Detection based on Hopfield Type Neural Networks,” IEEE Trans. Geosci. Rem. Sens., Vol. 45, No. 3, pp. 778-789, March 2007.
- F. Bovolo, L. Bruzzone, “A Split-Based Approach to Unsupervised Change Detection in Large-Size Multitemporal Images: Application to Tsunami Damage Assessment,” IEEE Trans. Geosci. Rem. Sens., Vol. 45, No. 6, pp. 1658-1670, June 2007.
- F. Bovolo, L. Bruzzone, M. Marconcini, “A Novel Approach to Unsupervised Change Detection Based on a Semisupervised SVM and a Similarity Measure,” IEEE Trans. Geosci. Rem. Sens., Vol. 46, No. 7, pp. 2070-2082, July 2008.
- M. Dalla Mura, J.A. Benediktsson, F. Bovolo, L. Bruzzone, “An Unsupervised Technique Based on Morphological Filters for Change Detection in Very High Resolution Images,” IEEE Geosci. Rem. Sens. Lett., Vol. 5, No. 3, pp. 433-437, July 2008.
- F. Bovolo, “A Multilevel Parcel-Based Approach to Change Detection in Very High Resolution Multitemporal Images,” IEEE Geosci. Rem. Sens. Lett., Vol. 6, No. 1, pp. 33-37, 2009.
- L. Bruzzone, D. Fernández Prieto, “An adaptive semi-parametric and context-based approach to unsupervised change detection in multitemporal remote sensing images”, IEEE Trans. Image Proc., Vol. 11, No. 4, pp. 452-466, April 2002.

References: Binary Change Detection

- N. Falco, M. Dalla Mura, F. Bovolo, J.A. Benediktsson, L. Bruzzone, “Change Detection in VHR Images Based on Morphological Attribute Profiles,” IEEE Geoscience and Remote Sensing Letters, Vol. 10, pp. 636-640, 2013.

- E. Rignot and J. van Zyl, “Change detection techniques for ERS-1 SAR data,” IEEE Trans. Geosci. Remote Sens., vol. 31, no. 4, pp. 896-906, jul 1993.

- P.S. Chavez, Jr and D. J. Mackinnon, “Automatic detection of vegetation changes in the southwestern United States using remotely sensed images,” Photogramm. Eng. Remote Sensing, vol. 60, no. 5, pp. 1285-1294, May 1994.

- J. Cihlar, T. J. Pultz, and A.L. Gray, “Change detection with synthetic aperture radar,” Int. J. Remote Sensing, vol. 13, no. 3, pp. 401-414, 1992.

- T. Hame, I. Heiler and J. San Miguel-Ayanz, “An unsupervised change detection and recognition system for forestry,” Int. J. Remote Sensing, vol. 19, no. 6, pp. 1079-1099, Apr. 1998.

- F. Bovolo, G. Camps-Valls, L. Bruzzone, “An Unsupervised Support Vector Method for Change Detection,” SPIE 2007, SPIE Conference on Image and Signal Processing for Remote Sensing XII, Ed. L. Bruzzone, Vol. 6748, pp. 674809.1-674809.10.

References: Binary Change Detection

- F. Bovolo, L. Bruzzone, L. Capobianco, S. Marchesi, F. Nencini, A. Garzelli, “Analysis of the Effects of Pansharpening in Change Detection on VHR Images,” IEEE Geoscience and Remote Sensing Letters, Vol. 7, No. 1, pp.53-57, 2010.

- F. Bovolo, G. Camps-Valls, L. Bruzzone, “A Support Vector Domain Method for Change Detection in Multitemporal Images,” *Pattern Recognition Letters*, Vol. 31, No. 10, pp. 1148-1154, 2010.

- F. Bovolo, S. Marchesi, L. Bruzzone, “A Framework for Automatic and Unsupervised Detection of Multiple Changes in Multitemporal Images”, *IEEE Transactions on Geoscience and Remote Sensing*, Vol. 50, No. 6, pp. 2196-2212, 2011.

- L. Bruzzone, F. Bovolo, “A Novel Framework for the Design of Change-Detection Systems for Very-High-Resolution Remote Sensing Images,” *Proceedings of the IEEE*, Vol. 101, pp. 609-630, 2013.

- N. Falco, M. Dalla Mura, F. Bovolo, J.A. Benediktsson, L. Bruzzone, “Change Detection in VHR Images Based on Morphological Attribute Profiles,” IEEE Geoscience and Remote Sensing Letters, Vol. 10, pp. 636-640, 2013.

- F. Bovolo, C. Marin, L. Bruzzone, “A Hierarchical Approach to Change Detection in Very High Resolution SAR Images for Surveillance Applications,” *IEEE Transactions on Geoscience and Remote Sensing*, Vol.51, pp.2042-2054,2013.

References: Binary Change Detection

- C. Marin, L. Bruzzone, F. Bovolo, “Building change detection in Multitemporal very high resolution SAR images,” IEEE Transactions on Geoscience and Remote Sensing, Vol. 53, pp. 2664 – 2682, 2015.
- D. Capella Zanotta, L. Bruzzone, F. Bovolo, Y.E. Shimabukuro, “An Adaptive Semi-Supervised Approach to the Detection of User-Defined Recurrent Changes in Image Time Series,” IEEE Transactions on Geoscience and Remote Sensing, Vol. 53, pp. 3707 - 3719, 2015.

References: Registration Noise

- P. Gong, E.F. Ledrew, and J.R.Miller, "Registration-noise reduction in difference images for change detection," Int. J. Rem. Sens., vol. 13, no. 4, pp773-779, 1992.
- L. Bruzzone and S.B. Serpico, "Detection of changes in remotely-sensed images by the selective use of multi-spectral information," Int. J. Rem. Sens., vol. 18, no. 18, pp 3883-3888, 1997.
- D. Stow, "Reducing misregistration effects for pixel-level analysis of land-cover change," Int. J. Rem. Sens., vol. 20, pp 2477-2483, 1999.
- D. Stow, D. Chen, L. Coulter, "Detection of pixel-level land-cover changes with multi-temporal imagery: theory and examples with imagery of 1 meter and 1 kilometer spatial resolutions," in Analysis of Multi-Temporal Remote Sensing Images, Eds: L. Bruzzone, P. Smits, Singapore: World Scientific, 2002, pp. 59-66.
- L. Bruzzone and R.Cossu, "An Adaptive Approach to Reducing Registration Noise Effects in Unsupervised Change Detection ," IEEE Trans. .Geosci. and Rem. Sens., vol. 4, November 2003.
- F. Bovolo, L. Bruzzone, S. Marchesi, "Analysis and Adaptive Estimation of the Registration Noise Distribution in Multitemporal VHR Images," *IEEE Transactions on Geoscience and Remote Sensing,* Vol. 47, No. 8, pp. 2658-2671, 2009.
- S. Marchesi, F. Bovolo, L. Bruzzone, "A Context-Sensitive Technique Robust to Registration Noise for Change Detection in VHR Multispectral Images," *IEEE Transactions on Image Processing*, Vol. 19, No. 7, pp. 1877 - 1889, 2010.

References: Multiclass Change Detection

- W.A. Malila, “Change vector analysis: an approach for detecting forest changes with Landsat”, *Proc. LARS Machine Processing of Remotely Sensed Data Symposium*, W. Lafayette, IN: Laboratory for the Application of Remote Sensing, pp. 326-336, 1980.

- P.H. Swain, “Bayesian classification in time varying environment,” IEEE Trans. Sys., Man, and Cyber., vol. SMC-8, 1978, 879-883.

- F. Bovolo and L. Bruzzone, “A Theoretical Framework for Unsupervised Change Detection Based on Change Vector Analysis in Polar Domain”, IEEE Trans. Geosci. Rem. Sens., Vol. 45, No. 1, pp. 218-236, 2007.

- L. Bruzzone and S. B. Serpico, “An iterative technique for the detection of land-cover transitions in multitemporal remote-sensing images,” IEEE Trans. Geosci. Rem. Sens., vol. 35, no. 4, pp. 858-867, 1997.

- L. Bruzzone, D. Fernández Prieto, S.B. Serpico, “A neural-statistical approach to multitemporal and multisource remote-sensing image classification”, IEEE Trans. Geosci. Rem. Sens., Vol. 37, No. 3, pp. 1350-1359.

- L. Bruzzone, R. Cossu, G. Vernazza, “Detection of land-cover transitions by combining multidate classifiers”, Pattern Recog. Lett., Vol. 25, No. 13, 1 October 2004, pp. 1491-1500.

- L. Bruzzone, R. Cossu, “A multiple cascade-classifier system for a robust a partially unsupervised updating of land-cover maps”, IEEE Trans. Geosci. Rem. Sens., Vol. 40, No. 9, Settembre 2002, pp. 1984-1996.

References: Multiclass Change Detection

- L. Bruzzone, M. Marconcini, U. Wegmuller, A. Wiesmann, “An advanced system for the automatic classification of multitemporal SAR images”, IEEE Trans. Geosci. Rem. Sens., Vol. 42, No. 6, June 2004, pp. 1321-1334
- E.F. Lambin and Strahler, “Change vector analysis in multi-temporal space: a tool to detect and categorize land-cover change processes using high temporal-resolution satellite data,” Rem. Sens. Environ. 48, 231-244, 1994.
- L. Andres, W.A. Salas and D. Skole, “Fourier analysis of multi-temporal AVHRR data applied to a land cover classification,”. Int. J. Rem. Sens., Vol.15, pp. 1115-1121, 1994.
- A. Azzali and M. Menenti, “Mapping vegetation-soil complexes in southern Africa using temporal fourier analysis of NOAA AVHRR NDVI data,” Int. J. Remote Sens., vol. 21, pp. 973–996, 2000.
- A. Anyambe and J. R. Eastman, “Interannual variability of NDVI over Africa and its relation to El Ninõ—southern oscillation,” Int. J. Remote Sens., vol. 17, pp. 2533–2548, 1996.
- Z. Li and M. Kafatos, “Interannual variability of vegetation in the United States and its relation to El Ninõ—southern oscillation,” Rem. Sens. Environ., vol. 71, pp. 239–247, 2000.
- F. Bovolo, S. Marchesi, L. Bruzzone, “A Framework for Automatic and Unsupervised Detection of Multiple Changes in Multitemporal Images,” IEEE Transactions on Geoscience and Remote Sensing, Vol. 50, No. 6, pp. 2196-2212, 2012.

References: Multiclass Change Detection

- F. Bovolo, C. Marin, L. Bruzzone, “A Novel Approach to Building Change Detection in VHR SAR Images,” Proceedings of the SPIE Conference on Image and Signal Processing for Remote Sensing, Edinburg, UK, September 2012.
- F. Bovolo, C. Marin, L. Bruzzone, “A Hierarchical Approach to Change Detection in Very High Resolution SAR Images for Surveillance Applications,” IEEE Transactions on Geoscience and Remote Sensing, Vol.51, pp. 2042-2054, 2013.
- B. Narayan Subudhi, F. Bovolo, A. Ghosh, L. Bruzzone, “Spatio-contextual Fuzzy Clustering with Markov Random Field Model for Change Detection in Remotely Sensed Images,” Optics & Laser Technology, Vol. 57, pp. 284-292, 2014.
- S. Liu, L. Bruzzone, F. Bovolo, M. Zanetti, P. Du, “Sequential Spectral Change Vector Analysis for Change Detection in Multitemporal Hyperspectral Images,” IEEE Transactions on Geoscience and Remote Sensing, Vol. 53, pp. 4363 – 4378, 2015.
- S. Liu, L. Bruzzone, F. Bovolo, P. Du, “Hierarchical unsupervised change detection in multitemporal hyperspectral images,” IEEE Transactions on Geoscience and Remote Sensing, Vol. 53, pp. 244 - 260, 2015.
- M. Frank, M. Canty, “Unsupervised Change Detection for Hyperspectral Images,” *In 12th JPL Airborne Earth Science Workshop*, pp.63-72, 2003.

References: Multiclass Change Detection

- M. J. Canty, A. A. Nielsen, "Visualization and unsupervised classification of changes in multispectral satellite imagery," Int. J. Remote Sens., vol.27, no.18, pp.3961-3975, 2006.
- A. Schaum, A. Stocker, "Hyperspectral change detection and supervised matched filtering based on covariance equalization," Proc. SPIE, 5425, pp.77-90, 2004.
- A. Schaum, A. Stocker, "Long-interval chronochrome target detection," Int. Symp. Spectral Sens. Res. 1997.
- A.A. Nielsen, "The Regularized Iteratively Reweighted MAD Method for Change Detection in Multi- and Hyperspectral Data," IEEE Trans. on Image Proc., vol.16, no.2, pp.463-478, 2007.
- V. Ortiz-Rivera, M. Vélez-Reyes, B. Roysam, "Change detection in hyperspectral imagery using temporal principal components," Proc. SPIE, Algorithms and Technologies for Multispectral, Hyperspectral, and Ultraspectral Imagery XII. vol. 6233, 2006.
- Q. Du, N. Younan, R. King, "Change Analysis for Hyperspectral Imagery," Int. Workshop on MultiTemp, 1-4, 18-20 July, 2007.
- J. Meola, M.T. Eismann, R.L. Moses, J.N. Ash, "Detecting Changes in Hyperspectral Imagery Using a Model-Based Approach," IEEE Trans. Geosci. Rem. Sens., vol.49, no.7, pp. 2647-2661, 2011.
- M. T. Eismann, J. Meola, A. Stocker, S. Beaven, A. Schaum, "Hyperspectral change detection in the presence of diurnal and seasonal variations," IEEE Trans. Geosci. Remote Sens., vol.46, no.1, 237-249, 2008.

References: Others

- J.R. Eastman and M. Fulk, “Long sequence time series evaluation using standardized principal components,” Photogram. Eng. Rem. Sens., Vol. 59, pp. 991-996, 1993.
- R.S. DeFries, M.C. Hansen, M. Steininger, R. Dubayah, R.S. Sohlberg and J.R.G. Townshend, “Subpixel forest cover in Central Africa from multisensor, multi-temporal data,” Rem. Sens. Environ., 60, 228-246, 1997.
- D.J. Hayes, S.A. Sader, “Comparison of change-detection techniques for monitoring tropical forest clearing and vegetation regrowth in a time series,” Photogram. Eng. Rem. Sens., Vol. 67, pp. 1067-1075, 2001.
- E.H. Wilson, S.A. Sader, “Detection of forest harvest type using multiple dates of Landsat TM imagery,” Rem. Sens. Environ., Vol. 80, pp. 385-396, 2002.
- R.R. Nemani, C.D. Keeling, H.Hashimoto, W.M. Jolly, S.C. Piper, C.J. Tucker, R.B. Myneni, D.O. Fuller, “Trends in NDVI time series and their relation to rangeland and crop production in Senegal, 1987-1993,” Int. J. Rem. Sens., Vol. 19, pp. 2013-2018, 1998.
- J. P. Jenkins, B. H. Braswell, S. E. Frolking, and J. D. Aber, “Detecting and predicting spatial and interannual patterns of temperate forest springtime phenology in the eastern US,” Geophys. Res. Lett., vol. 29, no. 2201, 2002.
- F. Pacifici, N. Longbotham, W.J. Emery, “The Importance of Physical Quantities for the Analysis of Multitemporal and Multiangular Optical Very High Spatial Resolution Images,” IEEE Transactions on Geoscience and Remote Sensing, Vol. 52, pp. 6241 – 6256, 2014.

References: Others

- T. Jiaojiao, A.A. Nielsen, P. Reinartz, P., “Improving Change Detection in Forest Areas Based on Stereo Panchromatic Imagery Using Kernel MNF,” IEEE Transactions on Geoscience and Remote Sensing, Vol. 52, pp. 7130 – 7139, 2014.
- G. Quin, B. Pinel-Puyssegur, J.-M. Nicolas, P. Loreaux, “MIMOSA: An Automatic Change Detection Method for SAR Time Series,” IEEE Transactions on Geoscience and Remote Sensing, Vol. 52, pp. 5349 – 5363, 2014.
- F. Baselice, G. Ferraioli, V. Pascazio, “Markovian Change Detection of Urban Areas Using Very High Resolution Complex SAR Images,” IEEE Geoscience and Remote Sensing Letters, Vol. 5, pp. 995 – 999, 2014.
- Thu Trang Le, A.M. Atto, E. Trouvé, J.-M. Nicolas, “ Adaptive Multitemporal SAR Image Filtering Based on the Change Detection Matrix, ” IEEE Geoscience and Remote Sensing Letters, Vol. 11, pp. 1826 – 1830, 2014.
- A. Marino, I Hajnsek, “A Change Detector Based on an Optimization With Polarimetric SAR Imagery,” IEEE Transactions on Geoscience and Remote Sensing, Vol. 52 , pp. 4781 – 4798, 2014.
- A.J. Lingg, E. Zelnio, F. Garber, B.D. Rigling, “A Sequential Framework for Image Change Detection,” IEEE Transactions on Image Processing, Vol. 23, pp. 2405 – 2413, 2014.